

DELFT UNIVERSITY OF TECHNOLOGY

MULTI DISCIPLINARY PROJECT

**Site specific investigation and anchor
mooring design for a floating OTEC system
offshore of Barranquilla, Colombia**

Authors:

Onne VAN DER GRAAF
Jeroen VAN DER DOES DE
WILLEBOIS
Huub HILLEN
Kris FRANKEN

Supervisors:

Prof. Dr. Riaan VAN 'T VEER
Dr. Jeremy BRICKER
Ir. Diego ACEVEDO
Ir. Berend Jan KLEUTE

MP237

Faculty of Mechanical, Maritime and Materials Engineering (3mE)
Faculty of Civil Engineering and Geosciences (CEG)

May 7, 2018

Executive Summary

The main goal of this project is to determine the optimal location for an OTEC installation with a minimum lifespan of 30 years off the coast of Barranquilla and to make an anchor mooring design for the floater on which this installation is located. For this purpose an analysis of the local environmental conditions has been performed. This analysis will also be used for the determination of the lengths of the seawater intake- and return pipes. These are not only dependent on temperature but also on the density of the water mixture returned to the sea and the depth of the euphotic layer. This report will also give an advice on the marine traffic interaction. This advice will be based on local bathymetry and soil conditions. Bluerise has identified an area near the coast of Barranquilla for which OTEC can be applied. This area is situated within Colombia's territorial waters (within 12 nautical miles, or 22.2 kilometers), where two locations have been identified by Bluerise: Location 1: 11.2028 latitude, -75.0003 longitude, Location 2: 11.2772 latitude, -74.9208 longitude.

Environmental conditions

The daily wind direction is NE-ENE. There is no clear extreme wind direction. The daily waves have a dominant Northeast direction while the extreme waves have a dominant Northern direction. The extreme waves are generated far north of Barranquilla by very high wind speeds which explains the relatively high extreme significant wave heights in the area and the relatively low extreme wind speeds. The yearly average (nautical) surface current direction at the two possible floater locations is predominantly south or southeast. The top 20 strongest current speeds in the past few decades have come from the west or southwest however and therefore these are the normative current directions. The environmental conditions are equal for both possible floater locations. A temperature difference of 20°C is reached at warm water intake and cold water intake depths of 30 and 763 meters, respectively. The depths at which a temperature difference of 22°C is reached are 36 and 1023 meters (with temperatures of 27 and 5 degrees, respectively). The influence of the Magdalena river and upwelling is concluded to be negligible.

Marine traffic

The two locations with safety zones are located in a traffic dense area. The area is getting more traffic intense in the upcoming years. However, it will not pose an immediate treat to the operation. Around 100 vessels per year pass through or near the safety zone, this means approximately $100/365 \approx 0.27$ vessels per day (or one vessel every three days). The state of Colombia is responsible for the distribution of information and protection of the safety zones. Therefore, as there is no responsibility for Bluerise, both locations are equally attractive. As location 2 has slightly less traffic, it would be preferable from a safety point of view.

Seawater intake- and return pipes

Assuming a cold seawater intake temperature of 5°C and a warm seawater intake temperature of 27°C, the intake pipe lengths become 1023 and 36 meters, respectively. Based on the equation of state, the mixed water return flow pipe length becomes 130 m. At this depth, the effects of a difference in density between the surrounding seawater and the mixed returned water are

minimized. Also, the depth is outside of the euphotic zone which minimizes algae growth. If the intake water is higher than 27 degrees, the discharge temperature will have a higher temperature. Calculations with the Equation of State reveal that the warmer the discharge temperature, the lower the density of the discharge water is. Whenever the discharge temperature is higher than the output temperatures, less depth is needed in order for the discharge water to be naturally buoyant. As the intake temperature fluctuates throughout the year, it is therefore advised to design the length of the discharge pipe at 120 meters. If, however, it is preferred to make the pipe as short as possible, it's possible to make the pipe around 100 meters in length. As long as the discharge is below the euphotic layer, no severe environmental consequences are expected. At 100 meters depth the density of the discharge water is heavier than the density of the surrounding water, and thus it will sink to the depth where it is naturally buoyant.

Anchor mooring design

The proposed anchor mooring design consists of a spread-moored 4x3 taut mooring system. The lines are composed of three parts: a 50 meter chain connected to the ship, a 1290 meter fibre line part and another 150 meter chain at the end that is connected to the anchor. The floater is positioned in a 58,05° angle with respect to the north in a northeast direction. This ensures comfortable operation during daily conditions and will reduce fatigue build up. The hurricane conditions were found to be governing. The design complies with the basis of design stated in section 5.3 and with the DNV-OS-E301 code and the API Recommended Practice 2SK.

Contractors/Suppliers analysis

Colombia does not have a shipyard that meets the requirement of converting a second-hand cargo ship to an OTEC-floater so the conversion of the ship must be carried out outside of Colombia. The modification of the floater will include the installation of mooring equipment on deck, such as chain stoppers, fairleads and gearboxes. Various international companies are suitable for carrying out such conversion. One example is SBM Offshore. In Colombia there are no contractors that have experience with the installation of large offshore floaters. Outside of Colombia, there are numerous contractors that have experience with the installation of offshore floaters and specifically FPSO's. Because of the similarities between the installation of an FPSO and the proposed OTEC floater discussed in this report these contractors are competent for the job. Typical contractors with these capabilities are Van Oord, SBM Offshore and Boskalis. The different types of line parts are commonly provided by different specialized suppliers. There are many different suppliers of offshore anchors for application in a taut leg mooring system which can handle the maximum design loads of our design. Vryhof is a possible supplier.

Acknowledgements

A special thanks goes out to Riaan van 't Veer, Jeremy Bricker, Berend Jan Kleute and Diego Acevedo, who supervised our work and helped us with many issues during the project.

We are also very grateful for the offices at the Universidad Simón Bolívar which we could use for free thanks to Poala Amar Sepúlveda and Juan Manuel Palacio.

We were very lucky to get help from Ricardo Morales, former captain of the Colombian navy and former director of CIOH, who introduced us to CIOH and who helped us with acquiring the data we needed. Thank you very much for this.

Our gratitude goes out to the Mercator Ocean Service Desk for being so involved and for helping us so well with all our issues and questions. The same can be said for Peter Groenewoud from BMT Argoss for offering his expertise to our project and even doing a free site-specific analysis for us. This help has been essential to the success of our project.

Next to our Professor there are several parties that helped us with regards to the anchor mooring design. First of all we were very lucky that Bureau Veritas provided us with their mooring design software. And special thanks to Guillaume de Hauteclocque which helped us with all our questions regarding HydroSTAR and Ariane8. Then we would also like to thank Job Pinkster and Jort Braun from respectively SBM Offshore and Bluewater for thinking along and sharing their expertise with us. Their guidance made it possible for us to complete the design in the given tight time schedule.

Finally, thank you Diana for taking us on trips, showing us around, teaching us Spanish and for the lovely Colombian Christmas dinner!

Contents

Executive Summary	i
Acknowledgements	iii
1 Introduction	1
1.1 Our vision	1
1.2 OTEC technology	1
1.3 Barranquilla, Atlantico	2
1.4 Reading guide	3
2 Research setup	4
2.1 Project mission and scope	4
2.2 Deliverables	4
2.3 Methodology	4
2.4 Project resources	5
3 Environmental conditions	6
3.1 Bathymetry	6
3.2 Wind conditions	7
3.3 Wave conditions	8
3.4 Current	11
3.5 Ocean temperature	13
3.6 Conclusion	15
4 Marine traffic	16
4.1 Safety regulations regarding offshore floaters	16
4.2 Marine traffic interaction	17
4.3 Conclusion	20
5 Anchor mooring design	21
5.1 Location	21
5.2 Floater	21
5.3 Basis of design	22
5.4 Mooring system	22
5.5 HydroSTAR	24
5.6 Ariane8	27
5.7 Conclusion	31
6 Seawater intake- and return pipes	32
6.1 Warm water intake pipe	32
6.2 Cold water intake pipe	32
6.3 Mixed water return pipe	32
6.4 Conclusion	35

7	Contractors/Suppliers Analysis	37
7.1	Modification of the floater	37
7.2	Installation of the anchor mooring system	37
7.3	Lines	38
7.4	Anchors	38
8	Conclusion and discussion	39
8.1	Conclusion	39
8.2	Discussion	39
8.3	Recommendations	39
A	Wind and wave data	41
B	Temperature profiles	46
C	Current maps	53
D	Marine traffic	55
E	HydroSTAR	60
E.1	Input	60
E.2	Output	65
F	Input Ariane8	70
G	Tensions and offset for extreme environmental conditions	71
H	Calibration	79
I	Maximum Offset Analysis	85
J	Intake- and return pipes	87
	Bibliography	91

List of Figures

1.1	Possible floater locations	2
3.1	Contour plot of the bathymetry near Barranquilla	6
3.2	Daily wind climate around Barranquilla (nautical convention)	7
3.3	Storm tracks (1946-2015)	8
3.4	Wave climate around Barranquilla	9
3.5	Overview of wind and swell waves	10
3.6	Directional spreading of extreme H_s per return period (Groenewoud, 2017)	10
3.7	Caribbean surface current (Joanna Gyory, 2013)	11
3.8	Surface currents near Barranquilla (averaged over the period 2013-2017).	11
3.9	Directional current rose near Barranquilla	12
3.10	Temperature over depth profile (June)	13
3.11	Temperature difference for different depths over time	14
3.12	Temperature for different depths over time	14
3.13	Sea temperature map of the Caribbean Sea	15
4.1	Average density of ships per year near Barranquilla	17
4.2	Average density of ships per year near the two locations per vessel size (2016)	18
4.3	Average density of ships per vessel type per year near Barranquilla	19
5.1	Taut Mooring System (ABCMoorings, 2014)	23
5.2	Catenary Mooring System (ABCMoorings, 2014)	23
5.3	Mesh made with the HydroSTAR AMG	25
5.4	Mooring Lay-out	28
5.5	Tension in line 6	28
5.6	Horizontal offset in east direction	29
5.7	Horizontal offset in north direction	29
5.8	Horizontal offset in Z-direction	30
5.9	Tension in line 6 with single line damage of line 5	30
5.10	Average density of ships per year near Barranquilla	31
6.1	Euphotic layer depths and Chlorophyll concentration at the surface	35
A.1	Distribution of mean wave period of the daily wave conditions	41
A.2	Tropical storm tracks per month	44
B.1	Temperature profiles for 5 different locations with different depths off the coast of Barranquilla	46
C.1	Seasonal maps of the Caribbean surface current	53
C.2	Subsurface currents near Barranquilla (averaged over the period 2013-2017)	54
D.1	Density of marine traffic (2016)	55

D.2 Density of marine traffic (2015)	58
E.1 HydroSTAR screenshot HSlec command	60
E.2 HydroSTAR screenshot HSchk command	61
E.3 HydroSTAR screenshot HSinf -g command	61
E.4 HydroSTAR screenshot HStat command	62
E.5 HydroSTAR screenshot HSrdf command	63
E.6 HydroSTAR screenshot HSmcn command	63
E.7 HydroSTAR screenshot HSdft command	64
E.8 HydroSTAR screenshot HSrao command	65
E.9 RAO - Surge	65
E.10 RAO - Sway	66
E.11 RAO - Heave	66
E.12 RAO - Roll	67
E.13 RAO - Pitch	67
E.14 RAO - yaw	68
E.15 Drift load - Fx	68
E.16 Drift load - Fy	69
E.17 Drift load - Mz	69
G.1 Tension over time: line 1	71
G.2 Tension over time: line 2	71
G.3 Tension over time: line 3	72
G.4 Tension over time: line 4	72
G.5 Tension over time: line 5	73
G.6 Tension over time: line 6	73
G.7 Tension over time: line 7	74
G.8 Tension over time: line 8	74
G.9 Tension over time: line 9	75
G.10 Tension over time: line 10	75
G.11 Tension over time: line 11	76
G.12 Tension over time: line 12	76
G.13 Maximum horizontal offset in east direction	77
G.14 Maximum horizontal offset in north direction	77
G.15 Maximum horizontal offset in Z-direction	78
H.1 Situation 1: tension in line 1	79
H.2 Situation 1: tension in line 2	79
H.3 Situation 1: tension in line 3	79
H.4 Situation 1: tension in line 4	80
H.5 Situation 1: tension in line 5	80
H.6 Situation 1: tension in line 6	80
H.7 Situation 1: tension in line 7	80
H.8 Situation 1: tension in line 8	80
H.9 Situation 1: tension in line 9	81
H.10 Situation 1: tension in line 10	81
H.11 Situation 1: tension in line 11	81
H.12 Situation 1: tension in line 12	81
H.13 Situation 2: tension in line 1	81
H.14 Situation 2: tension in line 2	82
H.15 Situation 2: tension in line 3	82
H.16 Situation 2: tension in line 4	82
H.17 Situation 2: tension in line 5	82
H.18 Situation 2: tension in line 6	82
H.19 Situation 2: tension in line 7	83
H.20 Situation 2: tension in line 8	83
H.21 Situation 2: tension in line 9	83
H.22 Situation 2: tension in line 10	83

H.23 Situation 2: tension in line 11	83
H.24 Situation 2: tension in line 12	84
I.1 Maximum offset analysis: line 4	85
I.2 Maximum offset analysis: line 5	85
I.3 Maximum offset analysis: line 6	85
I.4 Maximum offset analysis: line 10	85
I.5 Maximum offset analysis: line 11	86
I.6 Maximum offset analysis: line 12	86
J.1 Average salinity in PSU at different depths (2000-2009)	87
J.2 Average density in $kg/m^3 - 1000$ at different depths (2000-2009)	88
J.3 Short MatLab code description	89
J.4 Global seasonal distribution of Case-1 and Case-2 waters	90

List of Tables

3.1	Number of storms off the coast of Barranquilla (1946-2015)	8
3.2	Top 20 surface current velocities for data (2007-2016)	12
3.3	Depths of optimum temperatures for warm and cold water intake pipes	14
4.1	Legenda marine traffic analysis	17
4.2	Forecast on number of vessels for the Port of Barranquilla	19
4.3	Percentage of growth for number of vessels	20
5.1	Main dimensions Protefs bulk carrier	21
A.1	Number of wind events per velocity and direction	42
A.2	Percentage of occurrence of combinations of wind velocity and direction	43
A.3	All storm events off the coast of Barranquilla (1946-2015)	43
B.1	Sea temperatures and temperature differences over depth (2007-2016)	52
D.1	Color coding of marine traffic density maps	55
F.1	Environment data	70
F.2	Vessel coordinates	70
F.3	Anchor coordinates	70
H.1	Displacements	79

1

Introduction

This report documents the results of a multidisciplinary research project performed by group MP237 from Delft University of Technology for Bluerise BV. The background to this project is given in this chapter. In section 1.1, the motivation for this project is explained. In section 1.2, the concept of OTEC technology is introduced. Consequently, in section 1.3 the considerations for the research location are explained. Finally, the reading guide is given in section 1.4.

1.1 Our vision

As students of Delft University of Technology, enrolled in master programmes of the faculty Civil and Geotechnical Engineering we were given the opportunity to do a multidisciplinary project. The topic of such a project can be anything as long as it requires different insights and thus people with different backgrounds. Accordingly, the multidisciplinary project is the perfect occasion to work together with people from different disciplines to achieve a common goal. As young engineers, we think renewable energy will and has to play a major role in meeting future energy demands. Therefore, we are very eager to make a contribution to this field. Bluerise offers a unique way of working with renewable energy and is developing solutions with a technology called ‘Ocean Thermal Energy Conversion’, or OTEC. The topics that Bluerise encounters in the design of an OTEC system are very well suited for our fields of interest and we believe that both our hydraulic and offshore engineering backgrounds will be of value in bringing OTEC technology to a higher level.

1.2 OTEC technology

Ocean Thermal Energy Conversion is a renewable energy technology that can generate electricity and drinking water and can provide cooling for greenhouses and buildings. The difference in temperature between the sun heated ocean surface and the cold deep sea drives the system to produce energy. But what defines OTEC systems from other renewable energy sources? Wind and solar energy both cannot produce a constant energy supply and hydropower is often accompanied by resettlement issues and social unrest. The unique selling point of OTEC systems thus lies in its stability and relatively undisturbing character. The different ocean temperatures are very stable which leads to a constant source of energy, available all year, both day and night. Utilizing only a small portion of the ocean’s energy could potentially cover the global energy need. The hindrance from OTEC installations is minimal, as it is only visible a few meters above waterlevel, while located miles offshore. To produce energy efficiently the temperature difference between the intake depths of the warm and cold water should be at least 20 degrees Celsius. This temperature difference is only present in (sub-)tropic regions.

1.3 Barranquilla, Atlantico

Producing energy with OTEC technology is possible in tropical waters, defined as the equatorial region between 20°N and 20°S. In this region, large parts of the ocean fulfill the requirement of having a minimum temperature difference of 20°C throughout the year (Acevado et al., 2017). Through public records, Bluerise has identified that an area near the coast of Barranquilla, Colombia has the potential to produce energy with OTEC technology. This area is situated within Colombia's territorial waters (within 12 nautical miles, or 22.2 kilometers). This area is shown in figure 1.1. A feasibility study has been conducted by Bluerise for this area, which concluded with a promising outcome for a potential 10 MW offshore OTEC powerplant. Before an OTEC installation can be installed, this preliminary conclusion has to be substantiated with a more detailed study of the local environmental conditions. This study will also lead to a more specific location for the installation. The Barranquilla location is different from other current Bluerise BV OTEC sites as it is located offshore instead of onshore. Because the seabed near Barranquilla has a relatively small angle, the water depth necessary for a 20°C temperature difference is reached far offshore. This would make the cold water intake pipe for an onshore location too long and therefore, too expensive. The installation will thus be placed on a 'floater', a floating platform which will be kept in place with an anchor mooring system.

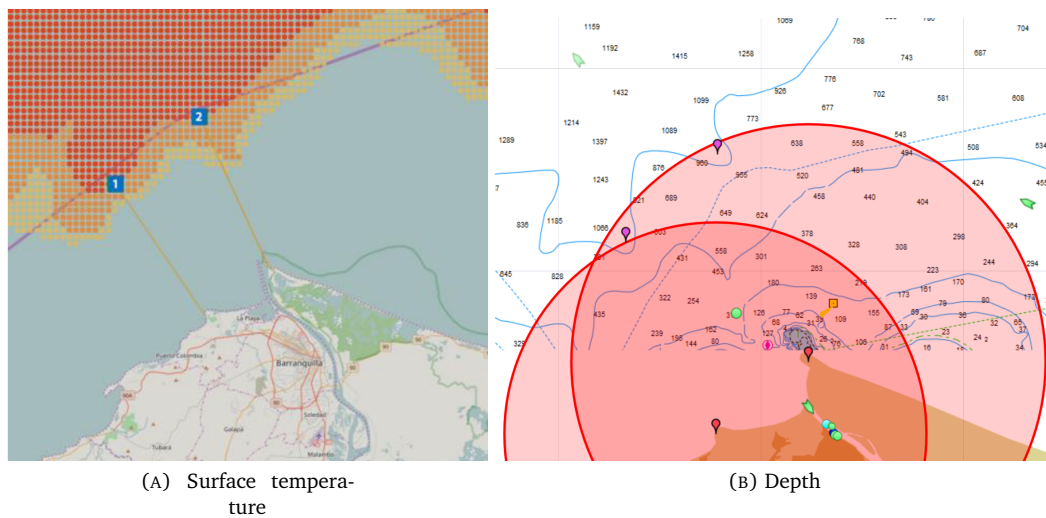


FIGURE 1.1: Possible floater locations (location 1 is located at approximately -75.00, 11.04 decimal degrees and location 2 is located at approximately -74.89, 11.30 decimal degrees)

The two locations have been determined with the 'Ocean Potential' software developed by Bluerise and with MarineTraffic¹. Location 1 is located approximately 20 kilometers from a point on the coast with latitude 11.0398254 and longitude -74.9223156. Location 2 is located approximately 22.5 kilometers from a point on the coast with latitude 11.1010100 and longitude -74.8414099 (Acevado et al., 2017). See figure 1.1 (A). The OTEC installation needs approximately 1000 meters depth for the cold water intake. In figure 1.1 (B) two radii with a radius of 20 and 22.5 kilometer have been drawn in a nautical chart. The two purple tags indicate the possible locations of the floater. They are located at:

- **Location 1: 11.2028 latitude, -75.0003 longitude**
- **Location 2: 11.2772 latitude, -74.9208 longitude**

¹<https://www.marinetraffic.com/>(Acevado et al., 2017)

1.4 Reading guide

In chapter 2 the project mission and scope are determined along with the deliverables. The methodology is elaborated on here and the project resources are discussed. In chapter 3 the environmental conditions are studied for the area of the possible floater locations. In chapter 4 the marine traffic in the area and its implications on the location of the floater is discussed. The anchor mooring design is further elaborated on in chapter 5. This includes the floater, the positioning, the anchor lines and the modelling programs Ariane8 and Hydrostar. The length of the seawater intake- and return pipes is discussed in chapter 6. In chapter 7 an analysis is done of contractors and suppliers. Finally, chapter 8 contains a discussion of the results and all relevant conclusions.

2

Research setup

2.1 Project mission and scope

The main goal of this project is to determine the optimal location for an OTEC installation with a minimum lifespan of 30 years off the coast of Barranquilla and to make an anchor mooring design for the floater on which this installation is located. For this purpose an analysis of the local environmental conditions has been performed. This analysis will also be used for the determination of the lengths of the seawater intake- and return pipes. These are not only dependent on temperature but also on the density of the water mixture returned to the sea and the depth of the euphotical layer. This report will also give an advice on the configuration of the power cable that transports the produced energy from the floater to the shore. This advice will be based on local bathymetry and soil conditions.

All these activities can be ranged under the second project development phase '*Development and Front-End Engineering*' as defined by Bluerise BV in the feasibility report for Barranquilla.

2.2 Deliverables

As discussed with Bluerise BV, this report will contain:

- A full local environmental analysis, containing:
 - Bathymetry
 - Wave climate
 - Currents
 - Wind climate
 - Temperature profiles over depth
 - Density profiles
 - A worked out anchor mooring design for the OTEC installation floater
- Marine traffic analysis regarding possible interaction between the floater and marine traffic
- An advice on the length of the seawater intake- and return flow pipes

2.3 Methodology

2.3.1 Environmental study

First, a study was done on the environmental conditions in the area of interest to determine the boundary conditions for the anchor mooring design. For the environmental study, a number of databases (elaborated on in section 2.4) were used. No on-site measurements were done.

2.3.2 Anchor Mooring design

As mentioned in section 2.2 this report will contain an anchor mooring design for the OTEC floater. To come up with this design two types of advanced modelling software have been used; HydroSTAR for Experts and Ariane 8. Both programs have been developed by the French certification agency Bureau Veritas. HydroSTAR is an advanced hydrodynamic software program which is used to perform diffraction and radiation calculations and to calculate hydrodynamic coefficients which serve as input for Ariane8. Ariane8 is an efficient static and time domain multi-body mooring software program. With this software the OTEC floater and its mooring system have been modeled.

2.4 Project resources

For the purposes of this project, a number of databases have been used. These databases are:

waveclimate.com

From waveclimate.com (a website of BMT Argoss) we extracted wind- and wave climate data from 1992 until 2016 with a time step of 3 hours. The data includes (among other parameters) wind speed and direction at 10 meters above the water surface, significant wave height and mean direction, and peak wave period. As stated on the website the datasets do not accurately portray hurricane conditions.

Copernicus Marine Environment Monitoring Service (CMEMS)

As stated on their website, "*The CMEMS provides regular and systematic core reference information on the state of the physical oceans and regional seas. The observations and forecasts produced by the service support all marine applications.*" The dataset used for this project is **GLOBAL_ANALYSIS_FORECAST_PHY_001_024-MONTHLY**. This dataset gives monthly averaged data on (among other things) temperature, salinity, surface current velocity/direction and potential sea bottom temperature. The resolution of this dataset is $1/12^\circ$ and it provides this data for 50 vertical layers (with unequal size). The output format of the dataset is **netCDF**.

Atlas de los Datos Oceanográficos de Colombia 1922-2013. Temperatura, Salinidad, Densidad, Velocidad Geostrofica

This atlas has been published by the Centro de Investigaciones Oceanograficas e Hidrograficas (CIOH) and contains salinity, temperature, density and depth data for the coastal areas of Colombia. Mainly the salinity and density data has been used for this report. Temperature data was used only to validate the CMEMS data.

3

Environmental conditions

In this chapter a full analysis of environmental conditions is presented for an area spanning both possible floater locations.

3.1 Bathymetry

The yellow contour line in figure 3.1 represents the 1000 meter depth line. This is the approximate depth of the cold water intake pipe (Acevado et al., 2017). The 1000 meter depth line is located relatively far from the shore (≈ 20 kilometers). The two possible locations of the floater determined in the feasibility study by Acevado et al. (2017) have been indicated in the figure, as well as the location of Barranquilla.

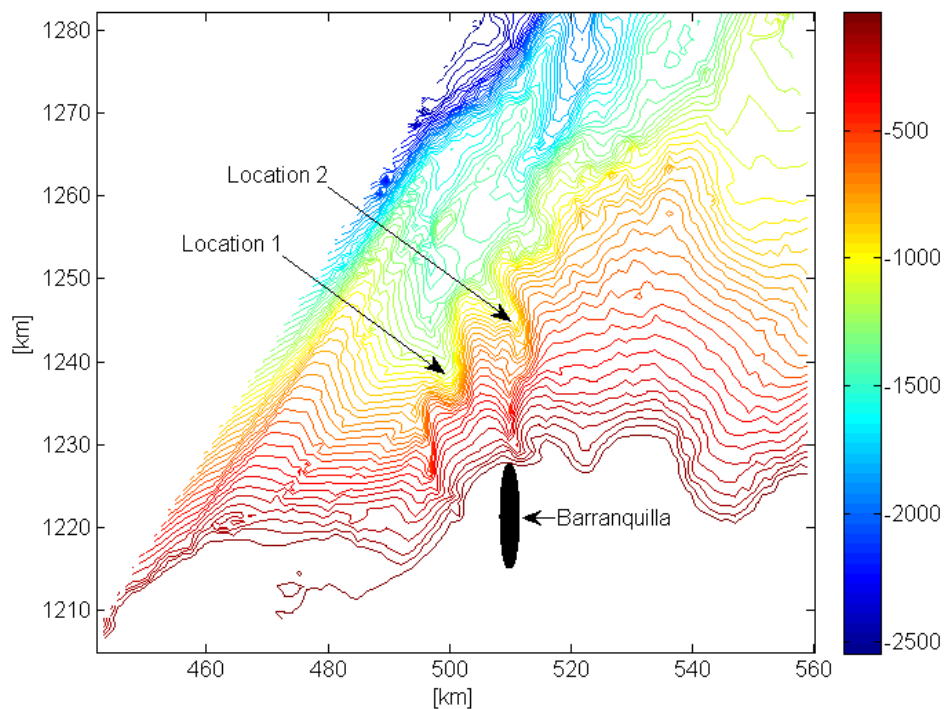


FIGURE 3.1: Contour plot of the bathymetry near Barranquilla. Location 1 and 2 indicate the two possible floater locations as determined in the feasibility study.

3.2 Wind conditions

The wind climate has been divided into two components; **daily wind speeds** (3.2.1) and **extreme wind speeds** (3.2.2). The daily wind speeds have been analyzed with a dataset from BMT Argoss (2017) containing sustained wind speed at 10 m above the surface and associated direction for a period from 1992 until 2016. This dataset does not accurately represent tropical depression, tropical storm and hurricane conditions. These are extreme wind conditions that have been analyzed separately by BMT Argoss (2017). It is thus important to be aware of the fact that the maximum wind speeds in subsection 3.2.1 are not the actual maximum wind speeds in the area of interest but only those of the daily conditions. The two conditions have been separated because daily wind conditions are important for fatigue calculations and calculations of the roll of the floater and extreme conditions are important for maximum cable tension calculations. See appendix A for more detailed tables and plots.

3.2.1 Daily wind speeds

During daily conditions the wind in the area offshore of Barranquilla almost solely enters the area from the 50°-80° range (NE-ENE) and can reach up to 18 m/s, or 65 km/h (wind force 8 on the Beaufort scale). See appendix A, figure A.2 for a wind direction vs. velocity table for the period from 1992 until 2016.

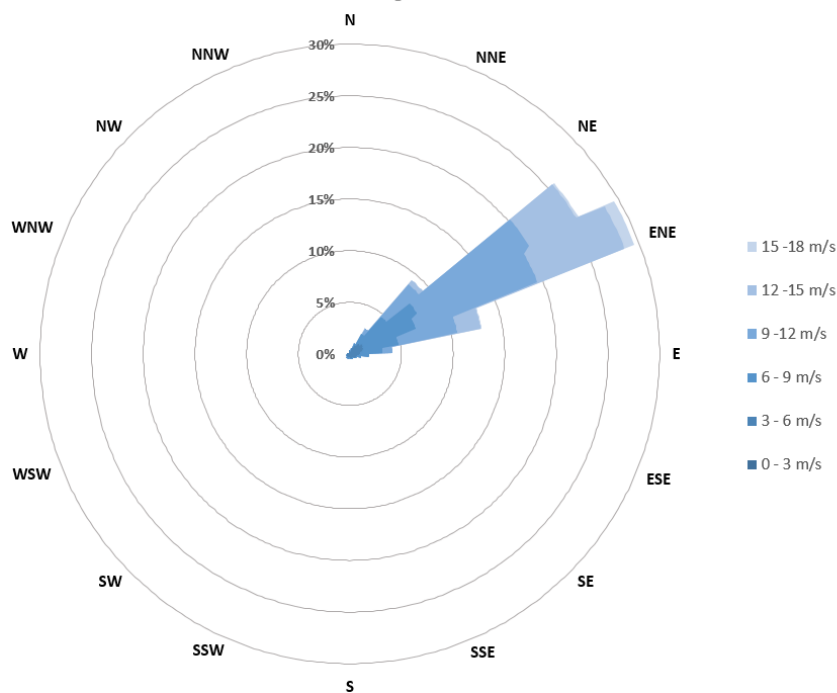


FIGURE 3.2: Daily wind climate around Barranquilla (nautical convention)

3.2.2 Extreme wind speeds

The dataset used for the analysis in section 3.2.1 does not accurately portray extremes because it does not model extreme wind data properly (BMT Argoss, 2017). To include the effects of hurricanes, tropical storms and tropical depressions, a site-specific analysis by Groenewoud (2017) has been done. The results of this analysis are elaborated on in this report but methods and/or raw data will remain confidential.

Figure 3.3 shows all storm tracks within a radius of 2000 km of the area of interest (the red square in figure 3.3) from 1946 until 2015. Table 3.1 shows the number of storm events based on the Saffir-Simpson scale. The Caribbean Sea has frequently seen storms since 1946.

However, compared to the rest of the Caribbean Sea, the area off the coast of Barranquilla has seen little severe storm-/hurricane wind speeds.

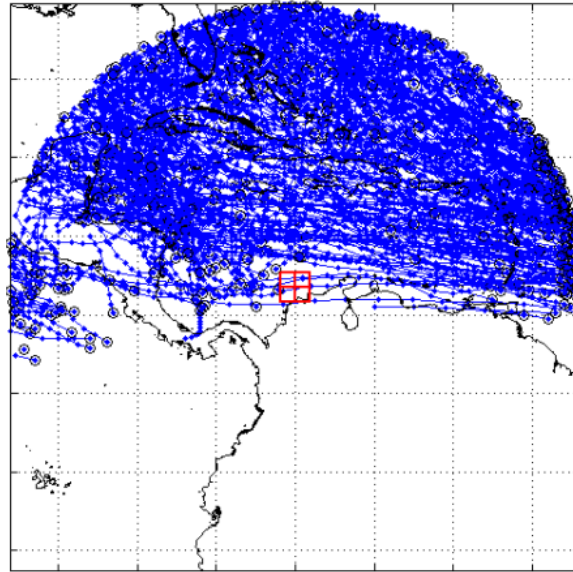


FIGURE 3.3: All storm tracks in a range of 2000 km of the area of interest (red square) from 1946 until 2015 (Groenewoud, 2017)

SS-Cat	Min [m/s]	Max [m/s]	All
HR-5	69,4		0
HR-4	58,1	69,4	0
HR-3	49,2	58,1	0
HR-2	42,5	49,2	2
HR-1	32,5	42,5	5
TS	17,2	32,5	102
TD	0,1	17,2	381
-	0,0	0,1	0
			490

TABLE 3.1: Number of storms off the coast of Barranquilla (red square in figure 3.3) with the according Saffir-Simpson hurricane wind scale (SSHWS) from 1946 until 2015 (see Appendix A, table A.3 for storms classified by month). The storm wind speeds presented in the table are given for the area of interest. They are thus not the actual maximum wind speeds of the storm itself (e.g. a HR-4 hurricane far away from the area of interest could lead to only HR-1 wind speeds in the area of interest).

3.3 Wave conditions

Wave data has also been divided into two conditions; **daily wave conditions** (3.3.1) and **extreme wave conditions** (3.3.2). The daily wave conditions are derived from the same dataset as was used for the daily wind conditions. The daily wave conditions are used for the determination of the draft of the ship (as the roll period in daily conditions is an important factor in the design). The extreme wave conditions are used to determine the position and width of the anchor lines as they are governed by extreme loading. Just as the extreme wind conditions, the extreme wave conditions have been determined from the analysis Groenewoud (2017).

3.3.1 Daily wave conditions

The significant wave height vs directional spreading graph in figure 3.4 shows the total (daily) wave climate for the area of interest.

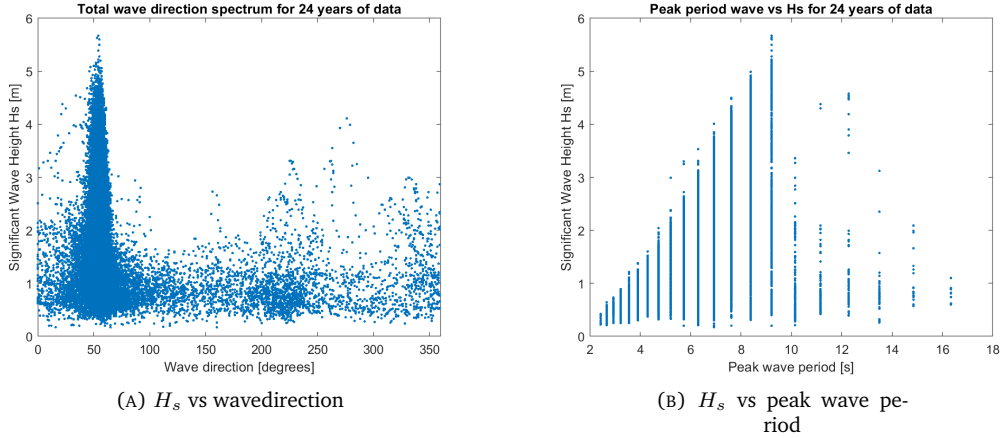


FIGURE 3.4: Wave climate around Barranquilla

The total wave climate has been divided into **Wind** (figure 3.5-A) and **Swell** waves (figure 3.5-B). The majority of the waves arrives at the location of interest from a direction of 30° (north northeast) until 70° (East northeast). The most probable mean wave period of the daily conditions is approximately ≈ 6 to 7 seconds. More details of this distribution can be found in figure A.1 in Appendix A.

A significant amount of smaller waves arrives at the location of interest from the southeast. This is counter intuitive as this means that many waves come from the direction of the shore. The most probable explanation is reflection as it would also explain why all the associated significant wave heights are much smaller than the incoming significant wave heights. This is substantiated by using the equation for wave length approximation (Fenton and McKee, 1990):

$$kd \approx \frac{\alpha + \beta^2(\cosh \beta)^{-2}}{\tanh \beta + \beta(\cosh \beta)^{-2}} \quad (3.1)$$

with

$$\alpha = \frac{\omega^2 d}{g} \quad \text{and} \quad \beta = \alpha(\tanh \alpha)^{-1/2} \quad (3.2)$$

Calculating for the wave period from the highest waves as derived from figure 3.4, ≈ 9.6 seconds, the associated wave length becomes 140 m. Where these waves enter intermediate water the bottom slope is approximately 0.07, which can be classified in between dissipative and reflective beaches with an inclination towards reflective (Bosboom and Stive, 2013).

The highest waves arrive from 50° and can be as high as 5.5 meters, as is shown in figure 3.5-A. For the swell waves, the majority of the waves come from 50° with a maximum wave height of 2.5 meters with a few outliers to 4.3 meters as is shown in figure 3.5-B.

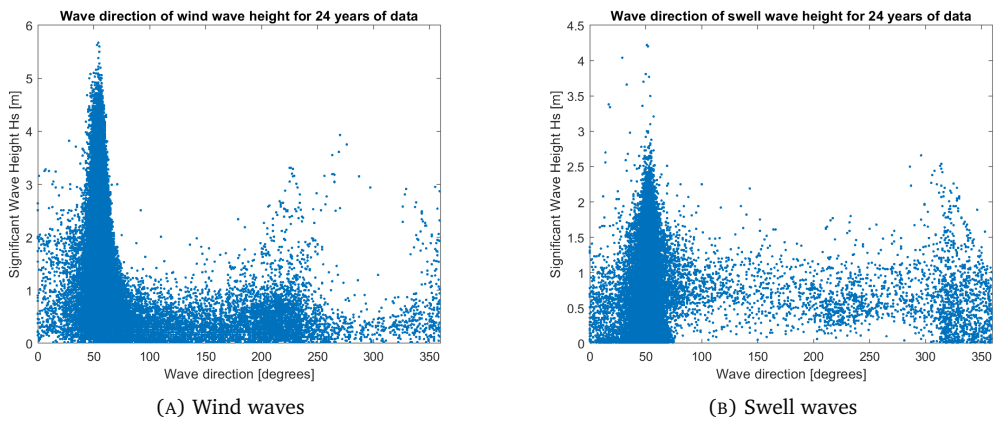


FIGURE 3.5: Overview of wind and swell waves. Please note the difference in scale between the two graphs.

3.3.2 Extreme wave conditions

The site-specific analysis by BMT Argoss has produced figure 3.6 which shows that extreme waves arrive at the area of interest mainly from the west, northwest, north and northeast. This is in line with figure 3.3 in which almost all storm tracks are situated in these directions from the location of interest. The waves coming in from the direction of the shore are again expected to be caused by reflection.

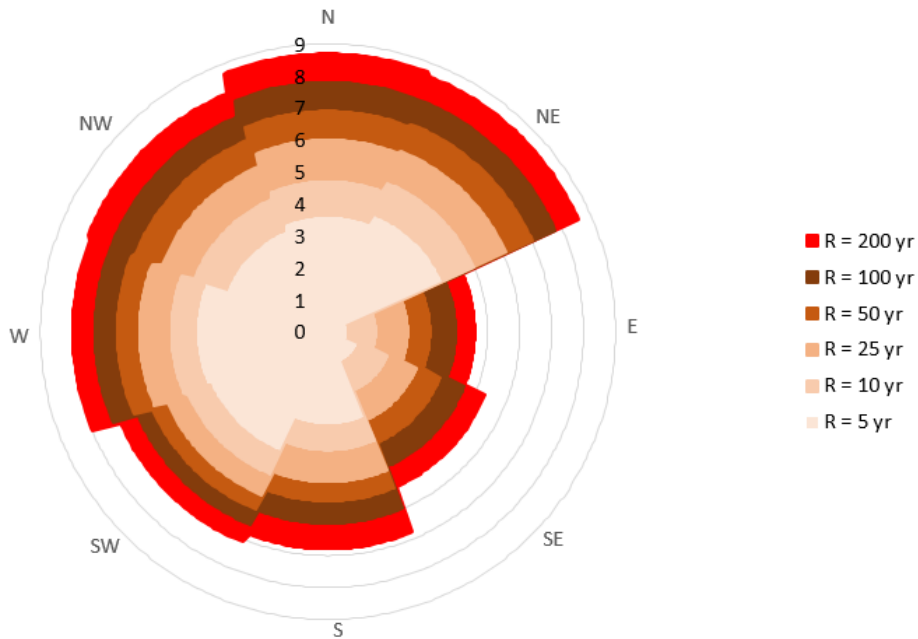


FIGURE 3.6: Directional spreading of extreme H_s per return period (Groenewoud, 2017)

3.4 Current

According to Kjerfve (1981), "analysis of tidal characteristics from 45 gauge locations indicates that the Caribbean Sea has a microtidal range, for the most part between 10 and 20 cm". It is thus safe to assume that the tides have no significant effect on the current direction and magnitude in the Caribbean Sea. The currents there exist due to the 'global conveyor belt'. Thermohaline circulation, driven by the constantly blowing southeast trade wind, produces a warm surface current flowing through the Caribbean Sea, entering through the Lesser Antilles and exiting through the strait between Mexico and Cuba (figure 3.7).

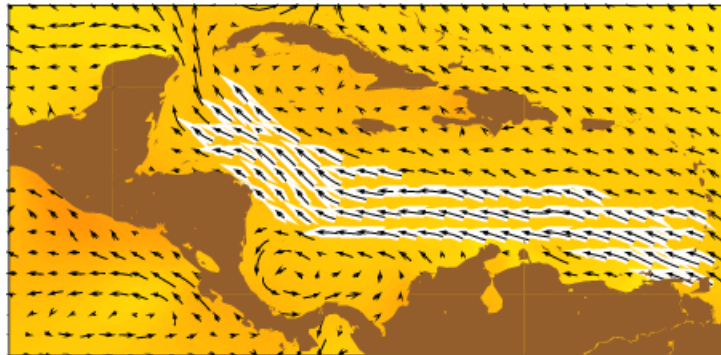


FIGURE 3.7: Caribbean surface current (Joanna Gyory, 2013). See appendix C for seasonal maps.

As can be seen in figure 3.7, this current causes a large scale eddy in the Colombian Basin. For the project location this means that surface currents are mainly directed from the southern- and southeastern direction. A more detailed look at the project location as portrayed in figure 3.8 shows the same general behaviour.

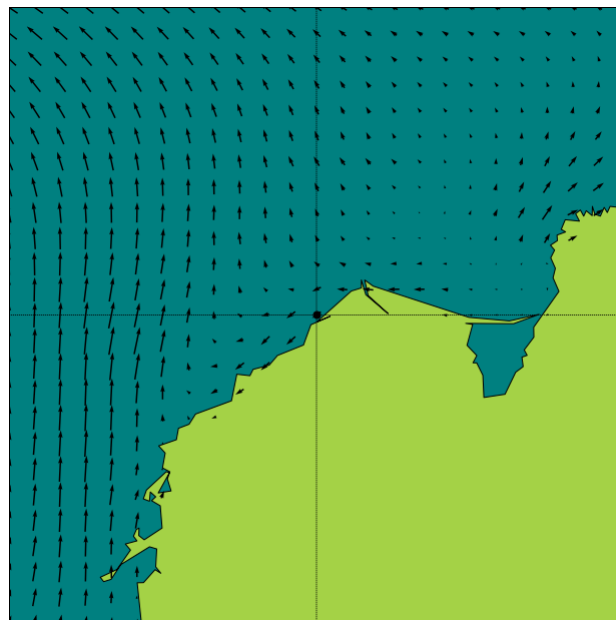


FIGURE 3.8: Surface currents near Barranquilla (averaged over the period 2013-2017).

Due to (among other factors) continuity the direction of the current varies over depth. At $z = 40m$, $z = 220m$ and $z = 1245m$, the subsurface current direction is mainly from the western- and southwestern direction while at $z = 763m$ it is mainly directed from the northeastern direction along the coast (figure C.2). Subsurface currents are determined by Copernicus with

ARGO¹ floats, GOSUD² and DBCP³ drifters

These plots have been created from a dataset spanning 2013-2017 by averaging over the entire period. Therefore, they do not include daily or seasonal variation. A further analysis of current velocities shows that since 2007 the 20 strongest surface current events have all come from the west or west southwest (240°-270°) though, so this is assumed as the normative direction.

Date	Current velocity [m/s]	Current heading (nautical) [°]
04-10-16	1,47	247
03-10-16	1,37	244
16-11-17	1,18	250
05-10-16	1,17	248
17-11-17	1,16	249
02-10-16	1,11	255
05-11-08	1,08	255
30-07-11	1,07	250
15-11-17	1,06	253
06-11-08	1,06	254
25-10-17	1,05	249
24-08-11	1,05	249
18-11-17	1,04	252
25-08-11	1,03	253
28-11-16	1,01	259
31-07-11	1,00	256
29-07-11	0,97	258
15-07-11	0,96	251
01-11-07	0,95	249

TABLE 3.2: Top 20 surface current velocities for data (2007-2016)

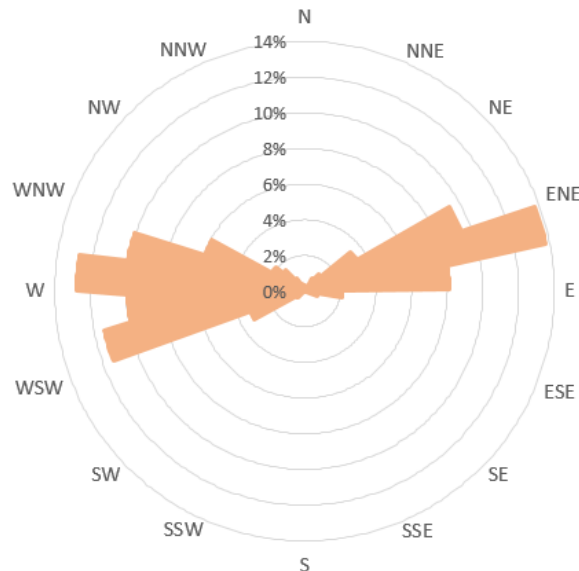


FIGURE 3.9: Directional current rose near Barranquilla (2007-2016). Note that the length of each bin indicates probability of occurrence, not magnitude of the current velocity.

¹Array for Real-Time Geostrophic Oceanography

²Global Ocean Surface Underway Data Pilot Project

³(Data Buoy Cooperation Panel)

3.5 Ocean temperature

For OTEC, the ocean's temperature is one of the most important aspects if not the most important one. In section 3.5.1 the temperature (difference) profiles are analyzed for the area of interest. In section 3.5.2 the possible occurrence of upwelling in the area of interest is discussed as well as the effects of the Magdalena river on temperature profiles.

3.5.1 Temperature profiles

An analysis of temperature data for the area shows that temperature profiles for different locations off the coast of Barranquilla (in the area of interest) are almost identical. This is especially evident from figure 3.10, in which the temperature profiles at 5 different locations with different depths off the coast of Barranquilla are plotted for January. All months show this similarity, see appendix B, figure B.1.

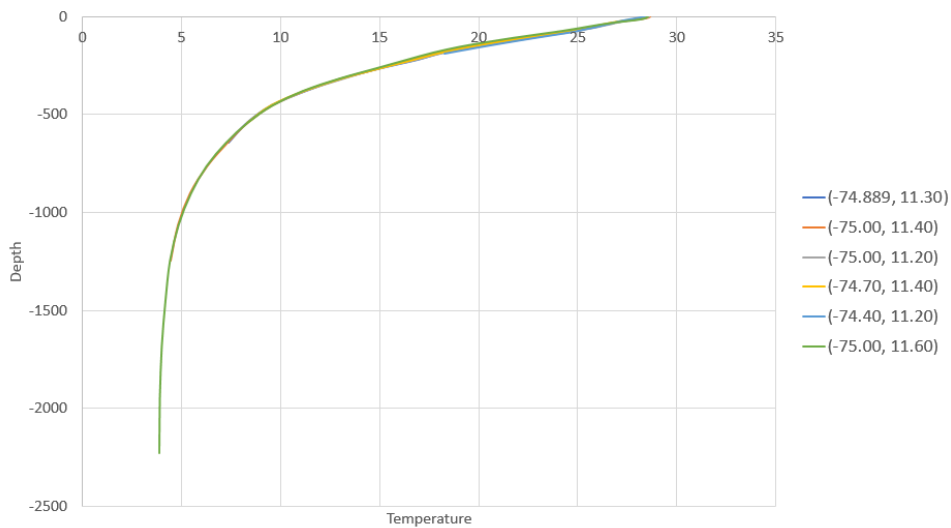


FIGURE 3.10: Temperature over depth profile at 5 locations with different depths (June)

This means that the choice of a location for the floater, temperature wise, depends only on the bathymetry at the location. As long as the depth at a location is at least 902 metres (see appendix B.1), the temperature difference with a depth of 30 metres will always be more than 20°C. Figure 3.11 shows that there is also a clear upward trend in the temperature differences between different layers off the coast of Barranquilla. Note that the temperature at deeper layers of the ocean stays practically constant (figure 3.12) meaning that the temperature difference growth is caused by temperature rise at the top layers of the ocean. The upward trend is based on a period of approximately 10 years. It can therefore not be solely explained by El Niño, which has a return period of approximately 4-5 years. Why there is an upward trend to be found is not part of the scope of this project and is thus not researched. However, the most probable cause of the upward trend is global warming.

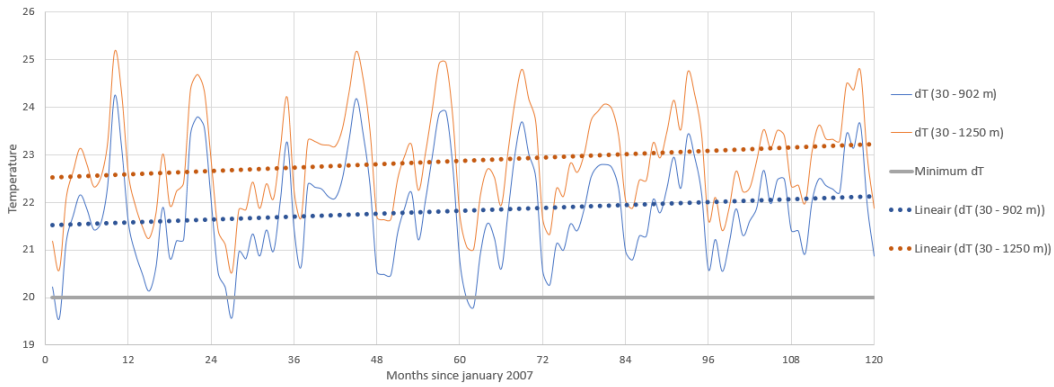


FIGURE 3.11: Temperature differences between different depths over time (valid in the entire area of interest). Data generated using E.U. Copernicus Marine Service Information.

This upward trend is especially interesting because it means that the cold water intake pipe could be approximately 763 m, which is significantly shorter than 1000 m.

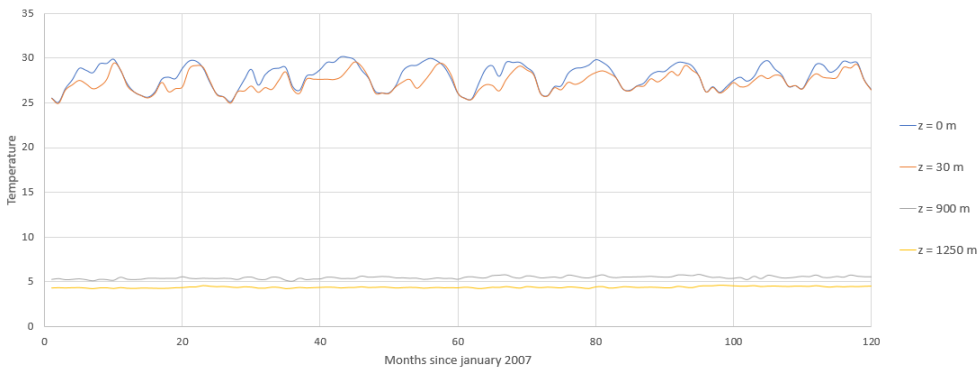


FIGURE 3.12: Temperatures at different depths over time. Data generated using E.U. Copernicus Marine Service Information.

For the OTEC technology to be efficient the temperature difference between warm and cold intake water should be as large as possible with a minimum of 20 degrees. A difference of 22 degrees is considered the maximum value in the area for which the pipes will not have to be too long. The values are taken at 5 and 27 degrees. The (average) values for which these two temperatures are reached are given in table 3.3. The temperatures per depth cannot to be fitted to a distribution (e.g. Normal, Weibull, Rayleigh) and therefore only the minimum and maximum temperatures for both depths were added to indicate a range of possible temperatures. A larger temperature difference can be reached by shortening the cold water intake pipe and/or lengthening the warm water intake pipe.

z	T_{min}	T_{avg}	T_{max}
36	24,91	27,00	30,66
1023	4,60	5,00	5,47

TABLE 3.3: Depths of optimum temperatures for warm and cold water intake pipes (Kirkenier, 2014)

Table 3.3 shows that the depths at which the temperatures of 27°C and 5°C occur are 36 and 1023 meters, respectively. These depths have been determined with linear interpolation between $z = 34, 43$ and $z = 40, 34$. Even though the profile is not linear, linear interpolation can be applied because of the small difference between the upper and lower range, meaning errors will be very small.

3.5.2 Upwelling

From the temporal analysis it has been concluded that upwelling can be found east of the location of interest but that there are no significant negative effects of upwelling at the location of interest itself (figure 3.13). Also, the discharge of the Magdalena river does not have a significant effect on the temperatures at the depths of the warm and cold water intake pipes.

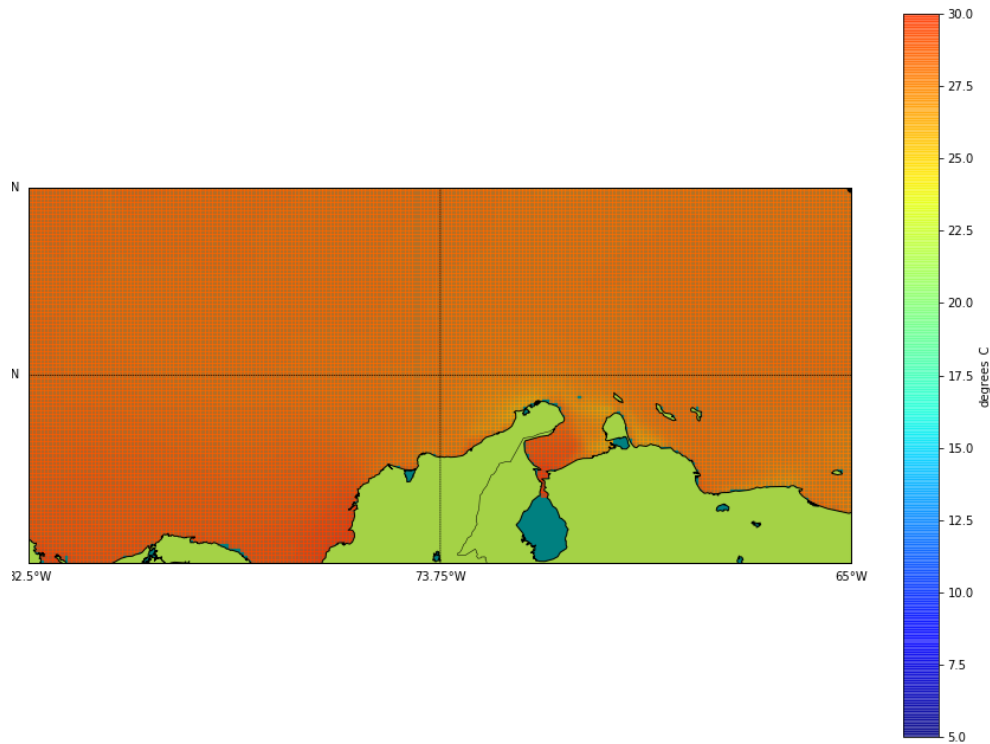


FIGURE 3.13: Sea temperature map of (part of) the Caribbean Sea showing upwelling east of the location of interest (data is averaged over time (2017))

3.6 Conclusion

The daily wind direction is NE-ENE. There is no clear extreme wind direction. The daily waves have a dominant northeast direction while the extreme waves have a dominant northern direction. The extreme waves are generated far north of Barranquilla by very high wind speeds which explains the relatively high extreme significant wave heights in the area and the relatively low extreme wind speeds. The average surface current direction at the two possible floater locations is predominantly south or southeast. Taking seasonal variation into account however, the dominant surface current direction becomes west or west southwest. The environmental conditions are equal for both possible floater locations. A temperature difference of 20°C is reached at warm water intake and cold water intake depths of 30 and 763 meters, respectively. The depths at which a temperature difference of 22°C is reached are 36 and 1023 meters (with temperatures of 27 and 5 degrees, respectively). The influence of the Magdalena river and upwelling is concluded to be negligible.

4

Marine traffic

In this section possible interaction of the two locations for the floater with ship routeing is analyzed. In section 4.1 safety regulations regarding the floater with marine traffic are discussed. In section 4.2, possible interaction of marine traffic with the floater is analyzed and discussed.

4.1 Safety regulations regarding offshore floaters

In order to minimize possible collisions with ships, regulations have been made by the International Maritime Organisation (IMO) and United Nations Conference on the Law of the Sea (UNCLOS) to prevent collisions. IMO has drafted safety regulations with regard to offshore structures and ship routeing. The International Regulations for Preventing Collisions at Sea are mandatory for all member states of IMO. Colombia is a member state of IMO.

Safety zone

Article 60(4) of UNCLOS provides that States may, when necessary, establish reasonable safety zones around artificial islands, installations and structures "in which it may take appropriate measures to ensure the safety both of navigation and of the artificial islands installation and structures". Paragraph 5 of the same article establishes that the breadth of these safety zones should be determined by the coastal State, taking into account "applicable international standards". In principle this breadth must not exceed 500 metres, except as authorized by "generally accepted international standards" or as recommended by the "competent international organization" (IMO). In accordance with article 60(6), ships must respect those safety zones and comply with "generally accepted international standards" concerning navigation in the vicinity of offshore installations and safety zones(IMO, 2014). When the floater is placed, a 500 meter safety distance should be maintained.

Ship routeing

IMO resolution A.379(X) states that the floater should not obstruct sea approaches and shipping routes. "In accordance with paragraph 7, offshore installations and safety zones around them may not be established where this may cause interference in the use of recognized sea lanes essential to international navigation"(IMO, 2014). Also, the pattern of shipping traffic should be assessed for potential interference early on. In section 4.2, the pattern of shipping traffic is analyzed.

Distribution of information

Marine traffic should be warned when they are nearing a 500 meter safety zone of an offshore structure. IMO resolution A.341(IX) states that the coastal state is responsible for the distribution of information concerning the location of offshore installations or structures and the

breadth of safety zones around them. The distribution of information should take the form of Notices to Mariners (preliminary, permanent and temporary), radio warnings, lights and sound signals. Permanent installations, structures or safety zones should be shown on all appropriate navigational charts (IMO, 1975). When Bluerise acquires the permit to deploy an OTEC platform offshore Barranquilla, the state of Colombia will be responsible for the distribution of information regarding its location and safety zone after installation.





4.2 Marine traffic interaction

The two locations identified in chapter 1 are considered in a full marine traffic analysis. In this analysis, the 500 meter safety zone is included as identified in section 4.1. The analysis covers 2015 and 2016 to get reliable results.

Marine traffic analysis

The marine traffic data is obtained from MarineTraffic (MarineTraffic, 2017). The total data for 2016 is shown in density maps. The maps have a colour coding "based on a rather compound algorithm. An approximate estimation on the numeric values of the corresponding colours follows - the numbers refer to distinct vessels on a daily basis and count positions per square km" (MarineTraffic, 2017).

TABLE 4.1: Legenda marine traffic analysis

Legenda	Color	Number of vessels
	Blue	Less than 30
	Green	30 to 70
	Yellow	70 to 140
	Red	more than 140

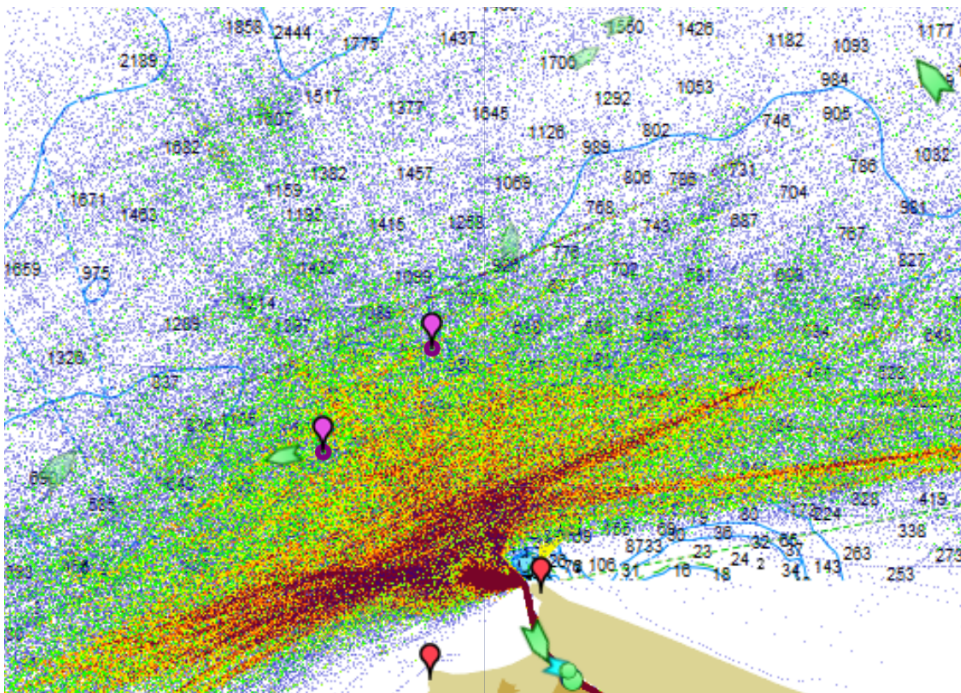


FIGURE 4.1: Average density of ships per year near Barranquilla

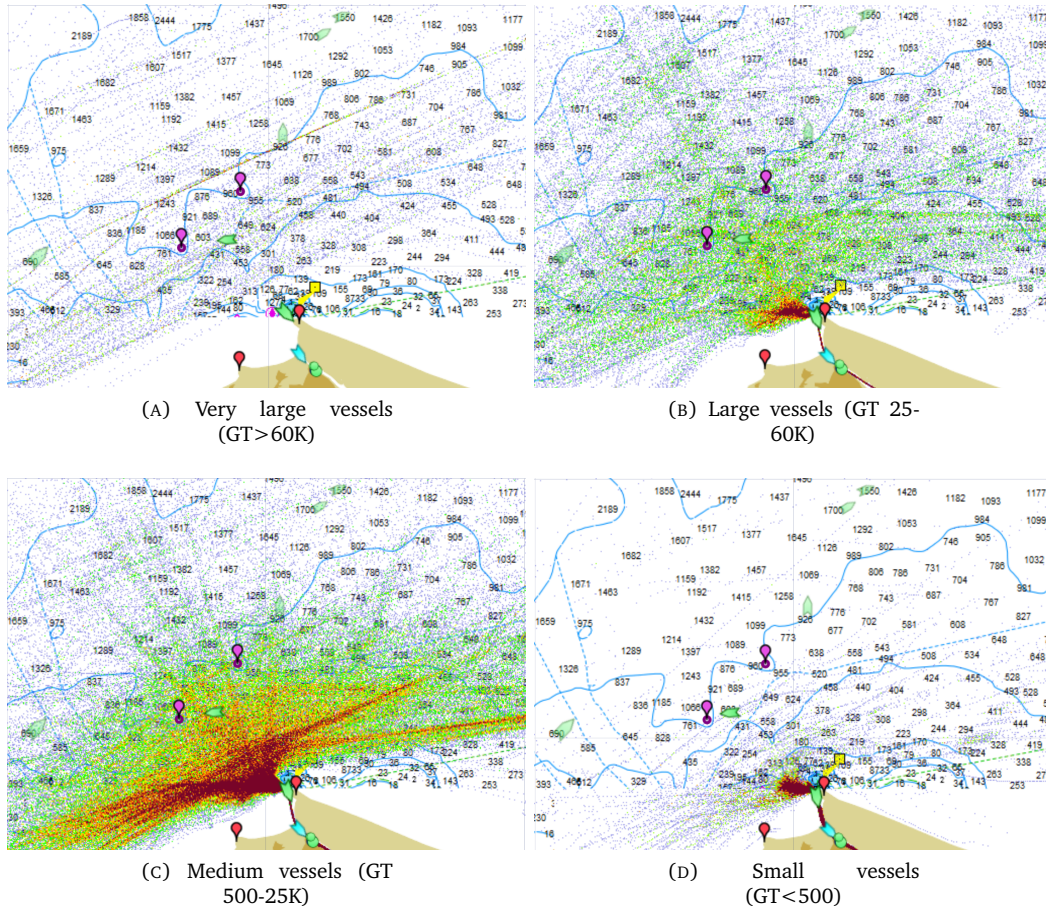


FIGURE 4.2: Average density of ships per year near the two locations per vessel size (2016)

The total ship movements per year are shown in figure I.6. This shows that the two locations are located in an area with a sizeable amount of marine traffic. In figure 4.2, a more detailed analysis of the ship movement around Barranquilla is shown, in which the size of vessels is subdivided based on **Gross Tonnage (GT)**. This shows that, per year, approximately 100 medium sized vessels (GT 500-25K) and around 40 large sized vessels (GT 25-60K) are routing through or are in the vicinity of the 500 safety distance radius of the two floater locations. Also, figure 4.2(A) shows that it is on the routing of very large ships, but there is a smaller amount of traffic.

As there are many different types of ships, a more detailed analysis was made on the **type of ships** that are routing through (or in the vicinity of) the two locations. Figure 4.3 shows the types of vessels that are frequently passing through or near the 500 meter safety zones. The full analysis of the other types of vessels that pass through the area is shown in appendix D. Figure 4.3 has the same scale as table D.1 for figure 4.2. This means that the brightest color has 140 or more vessels per year etc.

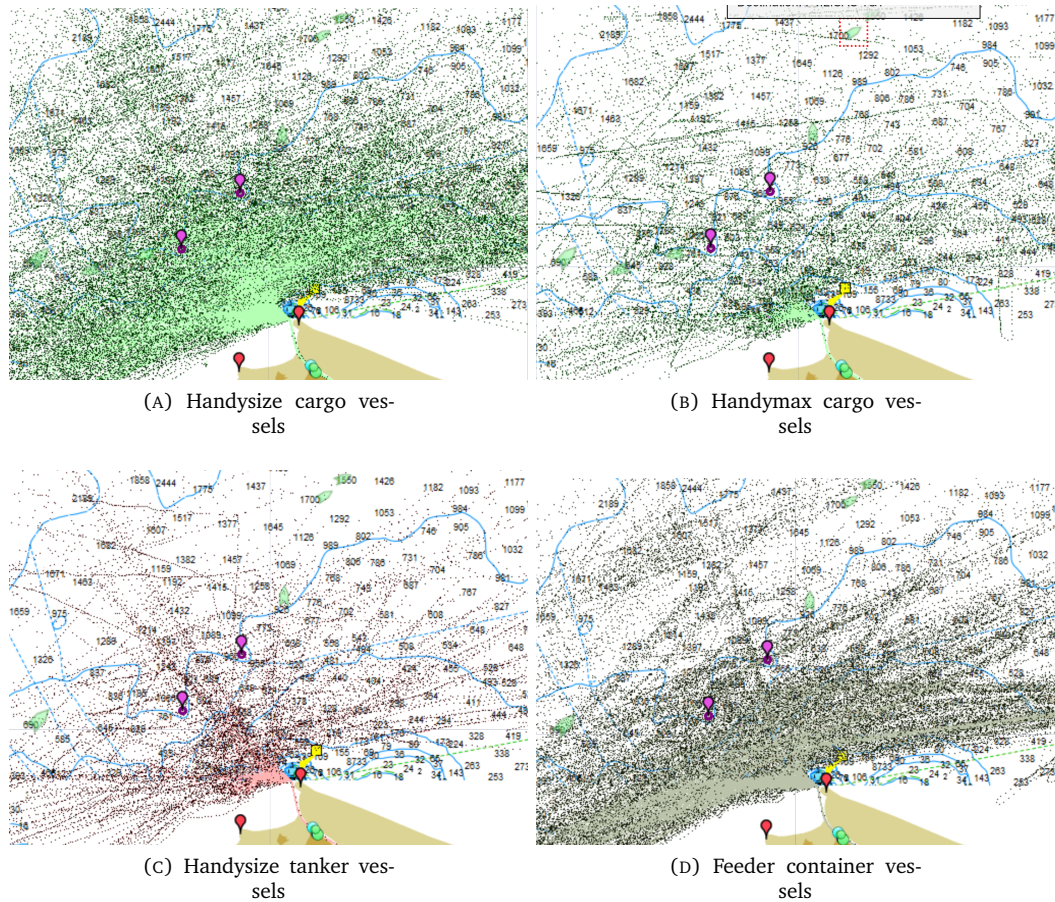


FIGURE 4.3: Average density of ships per vessel type per year near Barranquilla

It is clear from figure 4.3 that mainly Handysize and Handymax cargo vessels, Handysize tanker vessels and feeder container vessels pass through and near the 500 meter safety zone. The analysis of 2015 gives the same results and is shown in appendix D.

Forecast on marine traffic

In the master plan of the Port of Barranquilla from 2012, a marine traffic forecast was made for 2018, 2023 and 2030. (Rotterdam Maritime Group, 2012). These are shown in table 4.2.

TABLE 4.2: Forecast on number of vessels for the Port of Barranquilla

Number of vessels	2018	2023	2030
Deep-sea containers vessels	184	336	427
Container feeders	185	345	353
Carbon	58	90	104
Hydrocarbons	54	85	183
Total	481	856	1067

Converted into percentages, this gives a gross estimate of the growth in marine traffic for the upcoming years. These percentages are shown in table 4.3, and are based on table 4.2. The values for 2018 are taken as base case. From thereon, the growth in percentage is calculated.

TABLE 4.3: Percentage of growth for number of vessels

Number of vessels (in % increase)	2018	2023	2030
Deep-sea containers vessels	BASECASE	83%	132%
Container feeders	BASECASE	86%	91%
Carbon	BASECASE	55%	79%
Hydrocarbons	BASECASE	57%	239%
Average	BASECASE	70%	122%

These values give a gross estimate of the growth of marine traffic. This remains a gross estimate as there is a substantial amount of traffic in the area that does not enter the port of Barranquilla but only passes by. This traffic has not been included in the report. Table 4.3 shows a gross 70% growth of vessels for 2023 and a 122% growth for 2030.

4.3 Conclusion

The two locations with safety zones are located in a traffic dense area. The area is getting more traffic intense in the upcoming years, but is not getting too crowded. A 100 vessels per year means that approximately $100/365 \approx 0.27$ vessels per day (or one vessel every three days), pass through or near the safety zone. As stated in section 4.1, the state of Colombia is responsible for the distribution of information and protection of the safety zones. Therefore, as there is no responsibility for Bluerise, both locations are equally attractive. As location 2 has slightly less traffic, it would be preferable from a safety point of view.

5

Anchor mooring design

In the following chapter the anchor mooring design will be discussed. As mentioned earlier the bathymetry offshore of Barranquilla does not allow the OTEC system to be onshore, meaning the in- and outflow pipes cannot follow the seabed to reach the desirable depths. It will therefore be placed on a floating platform. In the first section the location will be discussed based on the previous chapters. The details of the floater will be discussed in section 5.2. The installation needs to be positioned stationary. The positioning of the floater will be maintained by an anchor mooring system. In section 5.3 the basis of design is given and in section 5.4 the different considerations with respect to the anchor mooring design are elaborated on. The calculations and modelling of the floater and its mooring system have been performed with the programs HydroSTAR and Ariane8. The procedures regarding the programs and the assumptions and considerations that have been made are stated in sections 5.5 and 5.6, respectively.

5.1 Location

Chapter 3 concludes that there is no difference in environmental conditions between the two locations. Chapter 4 concludes the same for marine traffic. Based on bathymetry data no conclusions can be made on which seabed topography is preferable regarding the configuration of the static part of the power cable. Therefore there is no preference with respect to both locations. A definitive choice of location is not necessary as the input for the anchor mooring design, the environmental analysis, is equal for both locations.

5.2 Floater

In the feasibility study conducted by Bluerise BV (Acevado et al., 2017), the possibilities of how to deploy an OTEC plant offshore have been examined. This study states that the conversion of an existing ship, specifically a second hand bulk carrier, to host the OTEC plant is the best option. In this report the concept design made by Guerrero Galán (2017) for an offshore location near Curacao is used to derive all the floater specifications. In this concept design the conversion of the Protefs bulk carrier is proposed.

TABLE 5.1: Main dimensions Protefs bulk carrier

LWL [m]	221.2
B [m]	32.2
T [m]	12.5
D [m]	19.2
Cb	0.83

Guerrero Galán (2017) recommends increasing the draft of the floater. Without any ballast the draft of the fully installed floater would be only 2.5 meters, which in turn results in very short roll periods similar to the most frequent wave periods. The environmental analysis appendix shows that in regular daily conditions the mean wave period never exceeds 5 seconds, as can be seen in figure A.1. In the report by Groenewoud (2017) the mean period of the hurricane conditions is not given. However, the peak period of a 5-year return period wave is 10.6 seconds and the larger the wave the higher this peak period. Ideally, the floater has a roll period in between these values. The draft therefore needs to be increased. For the design it is assumed to be 8 meters.

5.3 Basis of design

5.3.1 Requirements for maximum tension in the mooring lines

According to API (2005), the maximum tension in mooring lines may not be more than 59 percent of the minimum break load of the line. The line tension may not exceed this value during operation with an intact mooring system. However, it must also hold in case one of the lines fails, known as a single line damage situation.

$$\text{Maximum Line Tension} = 0.59 * \text{Minimum Break Load} \quad (5.1)$$

5.3.2 Requirements for maximum FPSO offset

The maximum horizontal offset for a taut mooring system is defined as 8 percent of the total water depth. This 8 percent is a commonly used value in the offshore industry for FPSO's with risers in deep water. Even though the OTEC platform does not have any risers connected to the seafloor the platform does have a power cable that extends to the seabed. For this situation a maximum horizontal offset of 8 percent is therefore applicable. It is beneficial to design the system close to this 8 percent because the system becomes stiffer when the maximum offset decreases. A stiffer system needs stronger lines, which increases the price of the lines. The maximum horizontal offset must hold for an intact mooring system as well as a system with a single line damage.

$$\text{Maximum Horizontal Offset} = 0.08 * \text{Water Depth} \quad (5.2)$$

5.4 Mooring system

In the following subsections the different options regarding the design of an anchor mooring system are discussed.

5.4.1 Mooring arrangement

Spread moored system

The wave and wind forces, which are the dominant environmental loads acting on the OTEC platform, have one dominant direction as we have seen in chapter 3. A spread moored system is the best option if the daily environmental loads are mainly from a single direction. The floater can be positioned in this dominant direction to minimize the fatigue build up in the mooring lines. The spread moored system is an economically favourable option in comparison with a turret moored system, which can rotate around a turret to position itself in an optimal direction like a wind vane. As can be seen in the article from Offshore magazine by M. Bozorgmehrian (2013) the spread moored option is common for the Caribbean sea offshore of Colombia and Venezuela.

Taut mooring design

The choice between a taut mooring design or catenary mooring design is a financial consideration. Taut mooring systems, which have pre-tensioned lines and use the elasticity of their lines

to create a restoring force if the floater moves, need shorter lines in comparison with catenary mooring systems which reduces the price significantly, especially regarding the depth of 1000 meters. The catenary mooring system, which creates restoring forces through the suspended weight of the mooring lines if the floater moves, need compensation for the weight of the chain lines. This weight is compensated by buoys. The buoys make the design more complex and even more expensive. Taut mooring systems use fibre lines, mostly polyester, which are relatively light, so there is no need to compensate these lines with buoys. The taut mooring design is therefore the the cheapest option.

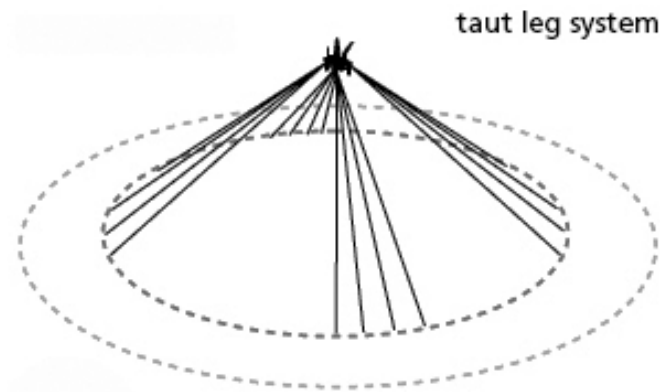


FIGURE 5.1: Taut Mooring System (ABCMoorings, 2014)

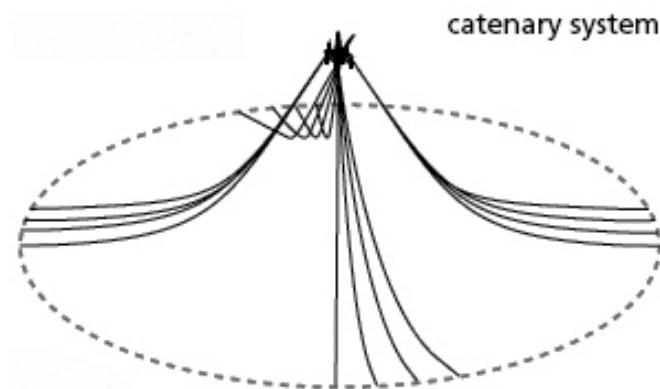


FIGURE 5.2: Catenary Mooring System (ABCMoorings, 2014)

5.4.2 Mooring lay-out

The mooring lay-out is designed in such a way that the ship is headed in the optimal direction regarding the environmental loads that are acting on the ship. It is symmetrically designed with a 4x3 lay-out. The advantage of a symmetrical lay-out is that several parts of the ship will be identical and can be copied (e.g. the foundations and the mooring equipment on deck). This will reduce overall costs. Another advantage is that spare parts will be identical and a smaller amount of items needs to be kept in stock.

The design has three lines per corner because the single line damage analysis shows that two lines are not sufficient. The angle between each line on a corner is 3 degrees which is a standard that is used to prevent the lines from colliding. If the environmental loads primarily come from one direction, which is the case, another option could be to place extra lines at the corners at which the maximum line tensions are highest. This could be beneficial for optimization reasons.

5.4.3 Anchors

The mooring lines of a taut leg system are pre-tensioned lines that, at the anchor point, make an angle with the seabed. This is in contrast to a catenary system where the lines lay on the seabed at the anchor point. This situation, where the line makes an angle with the seabed, creates a horizontal and vertical force on the anchors. The anchor line has an angle of 45° compared to the sea bottom. Not all types of anchors are suitable for these vertical loads. Suction piles, vertical load anchors like Vryhof's Stevmanta VLA, dynamic penetration anchors or torpedo anchors are several of the possibilities. The choice of which anchor should be used depends on the soil conditions at the location. Unfortunately these are not known at this moment and a soil investigation needs to be conducted to ensure that the best decision can be made. Preferably a regular vertical load anchor is used because this is economically the best option. According to the DNV (2017) offshore standard the maximum load that an anchor should be capable of holding is twice the minimum breaking load of the mooring line.

5.4.4 Position of the fairleads

A fairlead is an integral part of the mooring system. It is the piece of equipment in the mooring arrangement where the line enters the ship and it guides the mooring lines along the ships hull. To get maximum stability, the fairlead groups, consisting of three fairleads on each corner of the floater, need to be placed as far apart from each other as possible over the floater. The locations of the fairleads are chosen to be at the full width of the ship symmetrically placed on starboard and port side of the ship as close to the bow as possible for the front part and as far to the stern as possible for the aft part.

5.4.5 Line composition

An anchor mooring line consists of three parts: a chain of 50 meters from the ships' fairleads into the water, a fibre line in the middle part and a chain of 150 meters at the end which is attached to the anchor.

Fibre lines are mainly used due to its low cost, low stiffness (which induces less dynamic tension), good creep resistance and good strength to weight ratio. Because of this, they are often used for deep water applications. Because of the relatively low weight, there are no buoys needed to add to the design to reduce the weight of the lines.

The first part of the line (the part that is attached to the ship) is made of chain, because it is easier to pre-tension and lock the chain in comparison with a polyester line.

If there is less tension in one of the lines, it happens that a part of the line lies on the sea floor. Fibre lines wear very fast when they get in contact with the sea bottom. To prevent that the fibre line gets damaged the last parts of all the lines will also be chain. It is also essential that the connector does not touch the bottom because there is a chance that, in case of repetitive contact, the connector will fail.

The diameter of a polyester line with a break strength of 10.000 kN made by Phillystran, which is a typical supplier of offshore ropes, is 184mm (*Product Catalog Phillystran® Large Diameter Offshore Ropes - Polyester*). A similar line from Dyneema, also sold by Phillystran, has a diameter of 133mm (*Phillystran® Large Diameter Offshore Ropes - Spectra® / Dyneema® (High Modulus Polyethylene) Rope*). The diameter of the chain links is 95mm for R5 grade steel and goes up to 114mm for R3 grade steel (*The Future of Mooring*).

5.5 HydroSTAR

As discussed in chapter 2, HydroSTAR, together with Bureau Veritas' Ariane8, is used to design the anchor mooring system of the OTEC floater. In the following subsections the different steps in the process regarding HydroSTAR will be discussed. All the steps that have been taken to complete the HydroSTAR analysis can be found in appendix E, including all the input files.

5.5.1 Automatic Mesh Generator

HydroSTAR comes with an integrated mesh generator package called the Automatic Mesh Generator (AMG). With this package simple geometries and ship hull meshes can be made. In section 5.2 the dimensions of the Protefs bulk carrier have been determined. Since there was no detailed lines plan available another bulk carrier mesh has been scaled to the measurements of the Protefs. All dimensions and the shape of the hull are similar except for the block coefficient which slightly differs. With the assumed draft of 8 meters the block coefficient of the underwaterbody is $C_b = 0.81$ instead of the $C_b = 0.83$ of the Protefs. Note that the block coefficient of the Protefs is determined at the design draft. In figure 5.3 the mesh of the ship with a draft of 19.2 meters is depicted, to show the complete hull of the ship. For all the calculations a mesh with a draft of 8 meters is used.

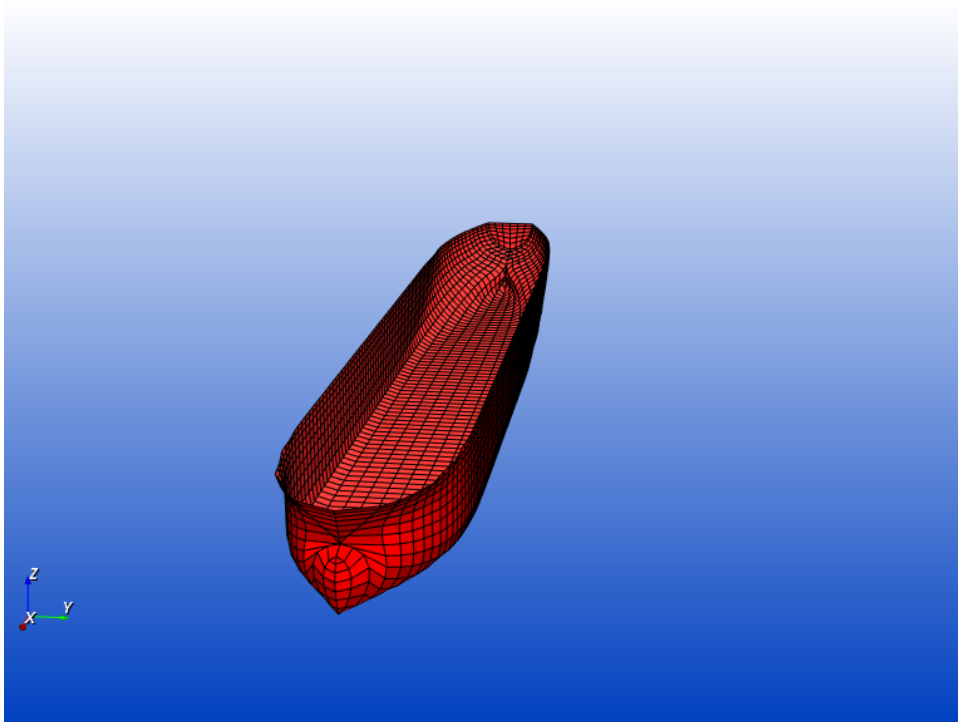


FIGURE 5.3: Mesh made with the HydroSTAR AMG

5.5.2 Calculations

In the following subsection the different choices that have been made regarding the calculations in HydroSTAR to generate the input for Ariane8 are discussed. Most of the steps need their own text input file, for these steps the name of the file that is used is given. In appendix E these files can be found. The different choices and considerations regarding the input for the three most important input files are re listed below.

HSrdf: radiation and diffraction computations (*OTECF.rdf*)

For the radiation and diffraction calculations the different headings and wave frequencies are determined. Also the speed of the vessel and the water depth are defined. With a water depth of a 1000m this can be regarded infinite for the calculation. The speed of the floater is 0 m/s. As the hull is symmetric with respect to the longitudinal axis of the ship, it is sufficient to use different incoming wave headings from 0° to 180° . The step size is taken as 15° to give a high enough resolution for the RAO and QTF plots. The wave frequencies from 0.05 rad/s till 1.80 rad/s are analyzed. The natural periods of the horizontal motions (surge, sway and yaw) of the floater typically lie between 60 and 120 seconds. The analyzed frequencies correspond to periods of 125.7 and 3.5 seconds which covers the area in which the horizontal motion natural

periods will occur.

HSmcn: motions computation (*OTECF.mcn*)

The radii of gyration need to be defined in the input file for the HSmcn command. For the roll, pitch and yaw radii of gyration, empirical formulas from IMO (2009) for k_{xx} and J.M.J. Journée (2001) for k_{yy} and k_{zz} are used. The coupled radii of gyration are neglected because their influence is minimal and they are not easily calculated.

$$k_{xx} \approx c * B \quad (5.3)$$

$$c = 0.373 + 0.023 \frac{B}{T} - 0.043 \frac{L}{100} \quad (5.4)$$

$$k_{yy} \approx 0.22 * L \text{ to } 0.28 * L \quad (5.5)$$

$$k_{zz} \approx 0.22 * L \text{ to } 0.28 * L \quad (5.6)$$

The mass of the body is derived from the displacement that belongs to a draft of 8 meters. The centre of gravity of the body in horizontal and vertical direction is assumed to be 119 meter from the aft perpendicular and 9.1 meter from the keel.

After the HSmcn computation has been done the roll period can be calculated to check if the assumed draft satisfies the desire of a roll period between 5 and 10 seconds. $c = 0.315$ calculated as in formula 5.4 and GM can be found in appendix E in figure E.6. Formula 5.7 is recommended by IMO (2009) to estimate the roll period and gives $T \approx 8.7s$.

$$T = \frac{2cB}{\sqrt{GM}} \quad (5.7)$$

HSdft: second-order drift computation in uni-directional waves (*OTECF.dft*)

For the second order drift computation there are several options provided by HydroSTAR. The computation can be made with uni- or multidirectional waves and a far field, near field of middle field formulation needs to be chosen. In this case the unidirectional waves option is sufficient. Only when a large part of the sea states are multidirectional this option needs to be chosen, which is not the case. Regarding the different formulations the far field method is used in this report. The far field method is precise enough for our analysis and due to its better convergence and stability it is a more robust calculation. It is not capable of providing us with the vertical drift loads but these are not necessary for the scope of this project.

5.6 Ariane8

In this section the operation of Ariane8 will be described. A general introduction of Ariane8 is given in subsection 5.6.1. In subsection 5.6.2, all the assumptions and considerations that have been made regarding the input for the program will be elaborated on. In subsection 5.6.3, the line tensions and offset for extreme conditions will be discussed. The underlying calculation of Ariane8 will not be treated in this report, but can be found in the theoretical manual of the program.

5.6.1 General

The Ariane8 program is a static time-domain mooring software which can handle multi-body systems. It is an interactive tool for anchor mooring project design. The program allows the user to create a mooring design based on a large number of input variables. A 3DOF simulation can test this design in imported environments and determine the forces in the line per time step. Based on these forces, the required minimum strength of the lines, the line layout and the offset of the floater is obtained. Appendix B shows the Ariane input values that are used in the final design of the mooring system.

5.6.2 Assumptions

Regarding the anchor mooring design the following two assumptions have been made.

Flat seabed

During the design phase, the exact bathymetry data for the location was not known. With the bathymetry data the precise length of the mooring lines can be determined. Because the exact bathymetry was not known, a flat seabed is assumed. Since the slope of the seabed is small compared to the total depth, this assumption will have no major consequences.

Cold water intake pipe

The design of the connection of the cold water intake pipe to the floater is not yet known, so it is not possible to determine the dynamic forces on the pipe and loads that it experiences. The presence of the pipes will be simplified for this project. For this project we assume that the pipes will provide for 5 percent extra current forces. So a factor of 1.05 is included in the calculation of the current loads on the floater.

5.6.3 Extreme and survival analyses results

In this subsection, the reliability of the system is tested against the extreme environmental conditions. By means of a number of standard tests, it is determined whether the chosen type of lines are suitable for the design. It is an iterative process that strives for the cheapest possible design which meets the basis of design of section 5.3.

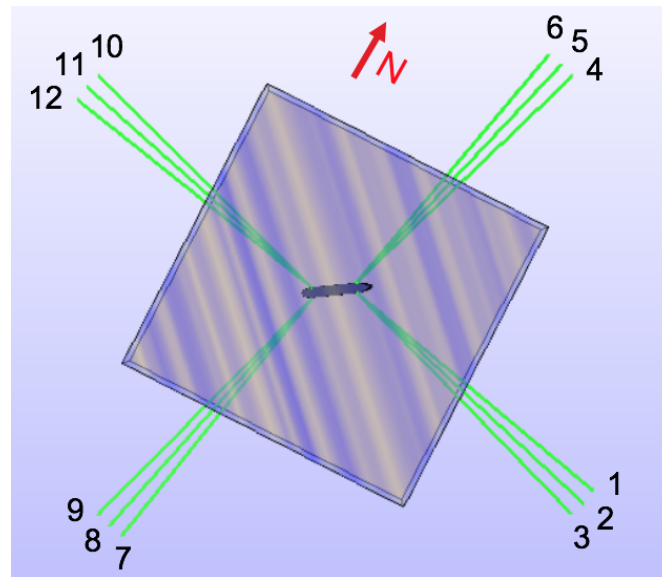


FIGURE 5.4: Mooring Lay-out

Tensions and offset for extreme environmental conditions

The simulation shows that line 6 has the biggest maximum tension. If the maximum tension in line 6 is below the stress limit, then all lines are below this limit. The simulation results of line 6 are shown in this subsection. The simulation results of the other lines are shown in appendix G.

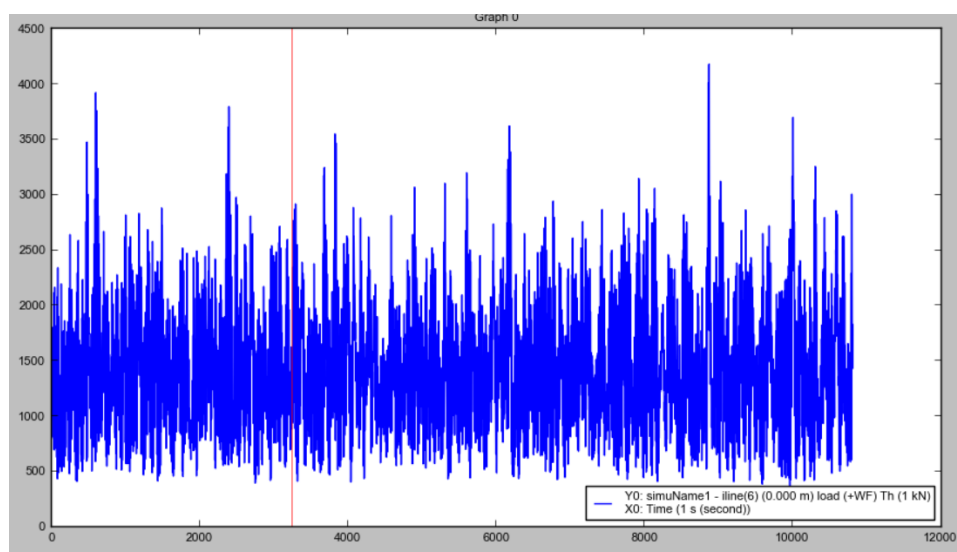


FIGURE 5.5: Tension in line 6

Graph 5.5 shows that the maximum tension is lower than the tension limit of 5900 kN. Therefore, the line meets the capacity requirements for maximum tension in the line.

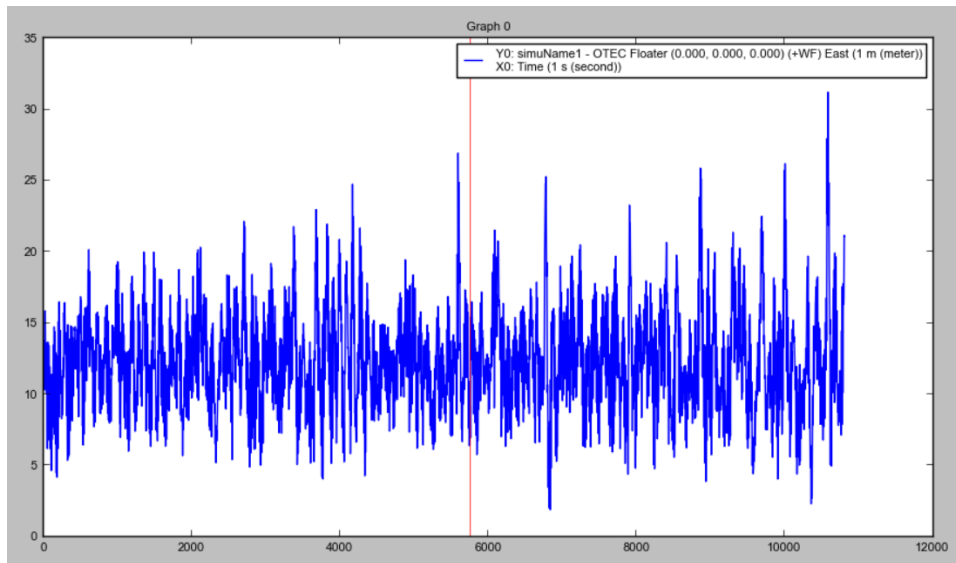


FIGURE 5.6: Horizontal offset in east direction

Graph 5.6 shows the offset in east direction under extreme environmental conditions.

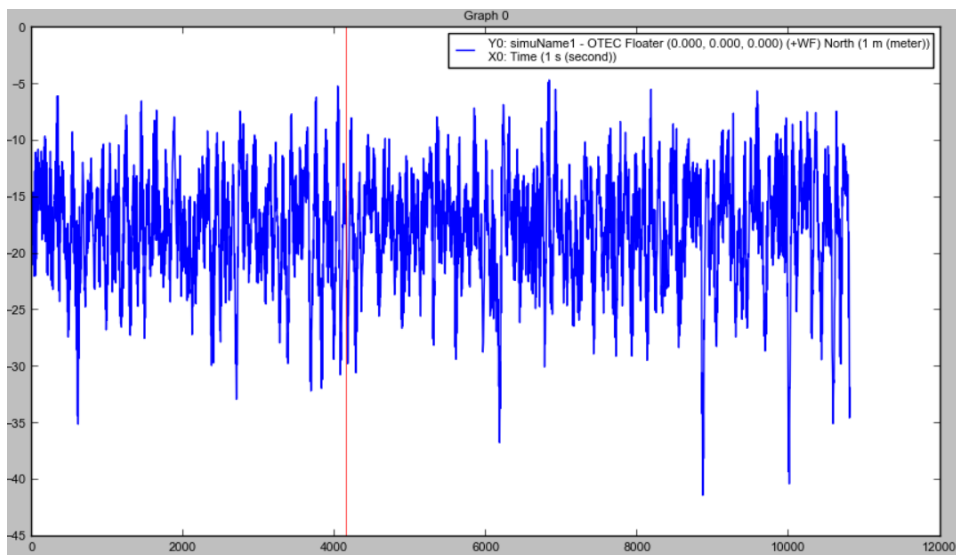


FIGURE 5.7: Horizontal offset in north direction

Graph 5.7 shows the offset in Z-direction under extreme environmental conditions.

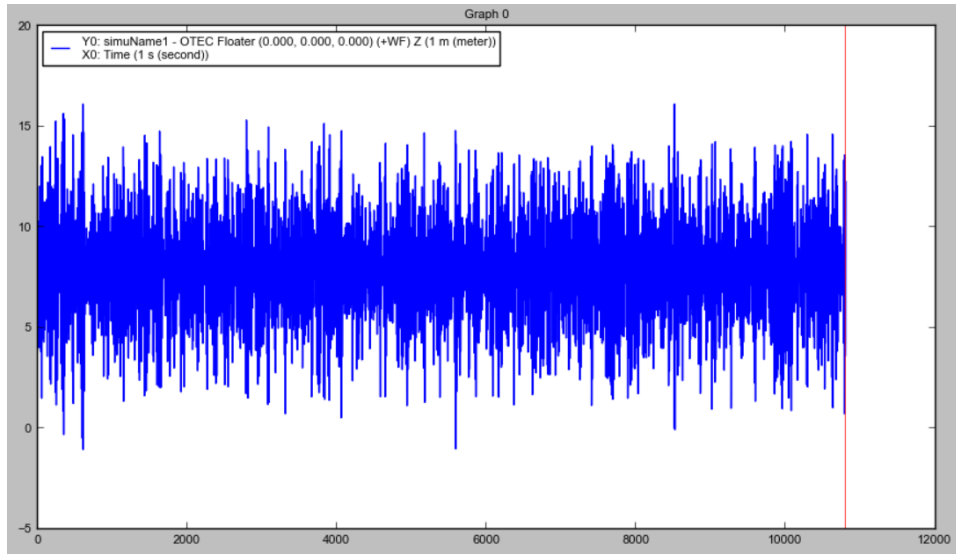


FIGURE 5.8: Horizontal offset in Z-direction

Graph 5.8 shows the offset in east direction under extreme environmental conditions.

5.6.4 Maximum offset analysis

To ensure the reliability of the system the first test, a maximum offset analysis, is performed. The maximum offset analysis tests the system's reliability when the system reaches its maximum offset. To test the design under the biggest loads, the floater is replaced in the direction of the highest extreme environmental loads. The graphs of appendix I show that the maximum tension in the lines does not exceed the minimum break load of 5900 kN. The design is therefore reliable at a maximum offset of 80 meters in the most stressful direction.

5.6.5 Single line damage analysis

To ensure the reliability of the system, the second test, a single line damage analysis, is performed. The line with the highest tension, line 6, is additionally loaded by disconnecting line 5 next to it. If line 6 can handle the resulting tension, then the system is reliable for a single damage in one of the lines.

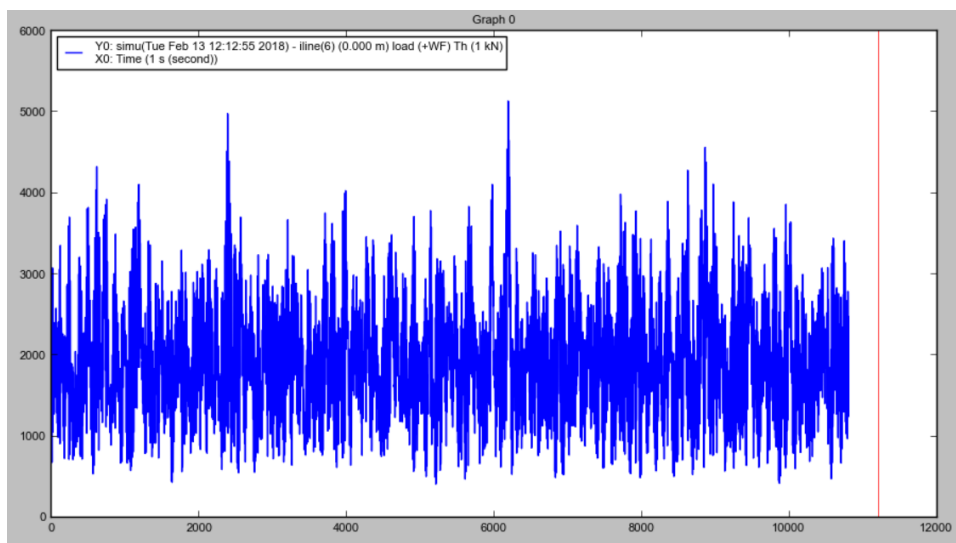


FIGURE 5.9: Tension in line 6 with single line damage of line 5

Graph 5.9 shows that the maximum tension of line 6 is lower than the tension limit of 5900 kN. Therefore, the line meets the capacity requirements for maximum tension in the line.

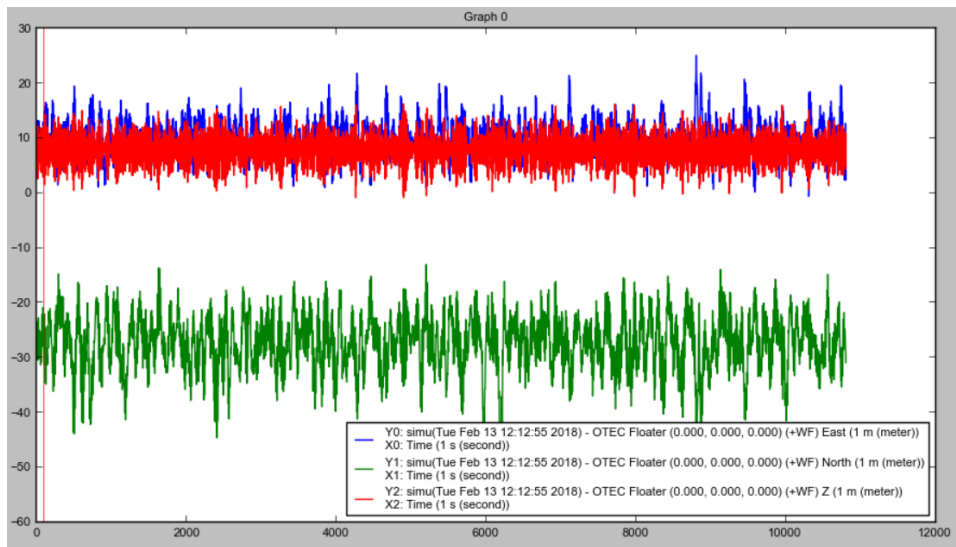


FIGURE 5.10: Average density of ships per year near Barranquilla

Figure 5.10 shows the horizontal offset of the floater during the single line damage analysis. The maximum horizontal offset in east direction is 25 meter and in north direction it is -45 meter, so according to the Pythagorean theorem, we have a total offset of 51.5 meter. This offset is lower than the offset limit of 80 meters.

5.6.6 Calibration system

With the hydrodynamics obtained from Hydrostar and the Ariane input values from appendix F, the system can be copied in a follow-up research. To make sure that the design is reconstructed the same as the design analyzed in this research, the created design will be calibrated. By comparing the reaction forces in the lines for a certain displacement of the ship, with the reaction forces of the ship in the original design, it can be determined whether the system is the same. The environmental conditions are not included in this analysis. In appendix H, the reaction forces of the lines of the original system are represented for two different displacements.

5.7 Conclusion

After the simulations we can conclude that the proposed anchor mooring system is indeed a good fit for the location. Also the 4x3 system with mooring lines that have a minimum breaking load of 10.000 kN complies with the DNV code and after the Ariane8 analysis we can conclude that it also holds for the basis of design. The angle between the lines in the horizontal plane is 3° and between the line and the seabed 45° . The line consists of three different parts. The first part, which is attached to the floater, is a 50m chain. The part in the middle will be a fibre line of 1290 m. The final part, to which the anchor is connected, is again a chain. This part has a length of 150 m to make sure the fibre part does not touch the seafloor. The diameter of the chain link will be in between 95 mm and 114 mm and the fibre line in between 133 mm and 184 mm depending on steel grades and fibre type.

6

Seawater intake- and return pipes

In this chapter, advice is given on the length of the intake and return pipes. Bluerise uses three pipes for their OTEC plant: a warm water intake pipe, a cold water intake pipe and a mixed water return pipe (Acevado et al., 2017).

6.1 Warm water intake pipe

For the seawater intake and outflow pipes it is assumed that the temperatures of the intake water is equal to the temperatures determined in section 3.5. Most optimal would be having intake water that has a temperature as high as possible, as but at least at a depth where the seawater is 27°C. For now, 27°C is taken as a design criterion. The Table B.1 and figure B.1 in Appendix B show that the seawater temperature of 27°C can be found at a depth of 30 meters, with a small deviation to a minimum of 26°C and a maximum of 28°C. It is clear from 3.11 and figure 3.12 that the water is getting warmer over time. Therefore, 30 meters would be an optimal depth as it is getting less likely over time that a 26°C low happens. It is advised to design the warm water intake pipe with 30 meters length.

6.2 Cold water intake pipe

The same principle used to calculate the warm water intake pipe is used for determining the length of the cold water intake pipe. The optimum cold water intake temperature is 5°C (Kirkenier, 2014). Table B.1 and figure B.1 in Appendix B show that at a depth of approximately 1000 meters the temperature of the seawater is 5°C with a deviation of 0.3°C. Figure 3.11 and figure 3.12 show that temperatures at greater depth stay almost constant. Therefore, it is advised to design the cold water intake pipe at 1023 meters length.

6.3 Mixed water return pipe

The warm and cold water that is pumped up for the OTEC installation is mixed and discharged back into the ocean through an outflow pipe. The depth at which this mixed seawater is discharged depends on two things:

- Density of the outflow mixture and the seawater in which it is discharged
- The thickness of the 'euphotic zone'

6.3.1 Density

The discharge should have a neutral buoyancy in the seawater in which it is discharged in order to minimize environmental impact (Vega, 2013). To reach neutral buoyancy, the density of the

discharge water should be equal to the density of the surrounding seawater, which is varies over depth. The density of seawater is a function of the salinity, temperature and pressure: $\rho(S, T, P)$. The density of seawater can be calculated using the Equation of State.

Temperature

The temperature of the discharge water is determined by taking the discharge temperatures of the warm surface water and the cold deep sea after it has been used for heating or cooling. The ratio warm to cold water is 2:1. This means that for every liter cold deep sea water is pumped up, two liters of warm surface water is pumped up. The discharge temperature of the warm seawater after it has been through the evaporator is 23.76°C (Kirkenier, 2014). The discharge temperature of the cold deep seawater after it has been through the condenser is 12.74°C (Kirkenier, 2014). With the ratio 2:1, this gives a discharge temperature of:

$$T_{out} = \frac{1}{3} * T_{deepsea} + \frac{2}{3} * T_{surface} = \frac{1}{3} * 12.74 + \frac{2}{3} * 23.76 = 20.087^{\circ}C \quad (6.1)$$

Salinity

The same principle can be applied to the salinity of the discharge water. In contrast to temperature, the salinity doesn't change when it passes through the installation. Therefore, the intake values of the salinity of warm surface water and cold deep sea water are used to calculate the salinity of the discharge water. The values for the salinity at 30 meters depth and 1000 meters depth are taken from data from Centro de Investigaciones Oceanográficas e Hidrográficas (CIOH) (Andrade Amaya, Rangel Parra, and Herrera Vásquez, 2015), which are also shown in appendix J. This gives a salinity of:

$$S_{out} = \frac{1}{3} * S_{deepsea} + \frac{2}{3} * S_{surface} = \frac{1}{3} * 34.87620 + \frac{2}{3} * 36.2007 = 35.7592PSU \quad (6.2)$$

Pressure

The pressure component of the Equation of State can be determined with the depth at which the discharge water is released. One decibar equals 1 meter of depth. However, the depth of the discharge is unknown if the density of the discharge is not known, as the discharge needs to be natural buoyant. It is therefore an iterative process which begins with an initial guess for the pressure. Together with the values for the salinity and the temperature, the density can be calculated with the Equation of State. With depth-based density data from CIOH (Andrade Amaya, Rangel Parra, and Herrera Vásquez, 2015), also shown in appendix J, the depth can be determined at which the discharge is natural buoyant. As the discharge depth gives a new value for the pressure, a new iterative cycle begins.

Equation of State for sea water

With the values of the salinity and temperature known, and with iteration for pressure, the density of the discharge water can be determined using the Equation of State for seawater. As this is a large non-linear formula (Fofonoff and Millard Jr, 1983), MatLab is used to compute the output values (Scripps Institution of Oceanography, 2017). The use of MatLab is further explained in appendix J. With a few iterations, the density of the discharge water, as a function of $T = 20.087^{\circ}C$, $S = 35.759$ PSU and $P = 130$ decibar, becomes $\rho = 1025.886 \text{ kg/m}^3$. This gives a discharge depth of 130 meters. The difference between the intake and the outtake is large enough in order for the discharged water not to be re-used again (Vega, 2013).

6.3.2 Euphotic zone

The thickness of the euphotic zone is determined by the depth at which the percentage of sun-light intensity is 1% of the surface layer. Is it therefore also referred to as $z_{1\%}$. It is important because it is a measure for the depth below which no algae can grow. The discharged water mixture is very nutrient rich and would very likely stimulate the growth of (possible harmful)

algae if it was released in the euphotic layer (Acevado et al., 2017). The euphotic layer is the most important factor for the determination of the discharge depth.

The intensity of sunlight can be determined by doing in-situ observations or with satellite remote sensing techniques. With in-situ observations light intensity can be measured directly. In certain conditions, satellite observations can determine the $z_{1\%}$ with the Chlorophyll concentration at the water surface. Whether or not this is possible is determined by whether one can assume 'Case-1 water' (Lee et al., 2007). Case-1 waters are those whose inherent optical properties (Preisendorfer, 1976) can be adequately described by phytoplankton (represented by chlorophyll concentration, or [Chl]) (Lee and Hu, 2006). In appendix J, figure J.4 we can see that the area of interest can be assumed Case-1 water.

The chlorophyll concentrations at the surface are determined at both possible floater locations (Loc 1: -75.0003, 11.2028; Loc 2: -74.9208, 11.2772) from Mercator data for the year 2017. The associated euphotic layer depth is calculated with the formula of Lee et al. (2007):

$$z_{1\%} = 34 * (C * [Chl])^{-0.39} \quad (6.3)$$

"It is necessary to emphasize that "the $z_{1\%}$ relationship developed in Morel [1988] and Morel and Maritorena [2001] requires either the mean chlorophyll concentration – or the water-column-integrated concentration – within the euphotic zone as input. Because of the existence of subsurface maxima of chlorophyll concentration, the mean value is normally greater than the surface value. Consequently, if surface chlorophyll (e.g., the product from current ocean-color remote-sensing algorithms) is used for the calculation of $z_{1\%}$, it is very likely that significant overestimation of $z_{1\%}$ values will result, as shown by Figure 5. Here $z_{1\%}$ is calculated simply using the relationship developed in Morel and Maritorena [2001]. Since we do not always know the details of the vertical distribution of chlorophyll concentration for each station (especially from remote sensing), it is assumed arbitrarily that the mean concentration of chlorophyll within the euphotic zone is 1.3 times that derived by the OC4v4 algorithm. With this consideration, the average error for $z_{1\%}$ is 34.3%. The average error is much larger (= 49.9%) when no such adjustment is considered, but can be reduced to 22.3% if the mean concentration is assumed as 1.8 times the OC4v4 derived surface value" (Lee et al., 2007).

Also, according to Vega (2013), using the $z_{1\%}$ is "unduly conservative because most biological activity requires radiation levels of at least 10% of the sea surface value." For a case study of the Hawaiian islands he uses the $z_{10\%}$.

These considerations lead to the following profiles:

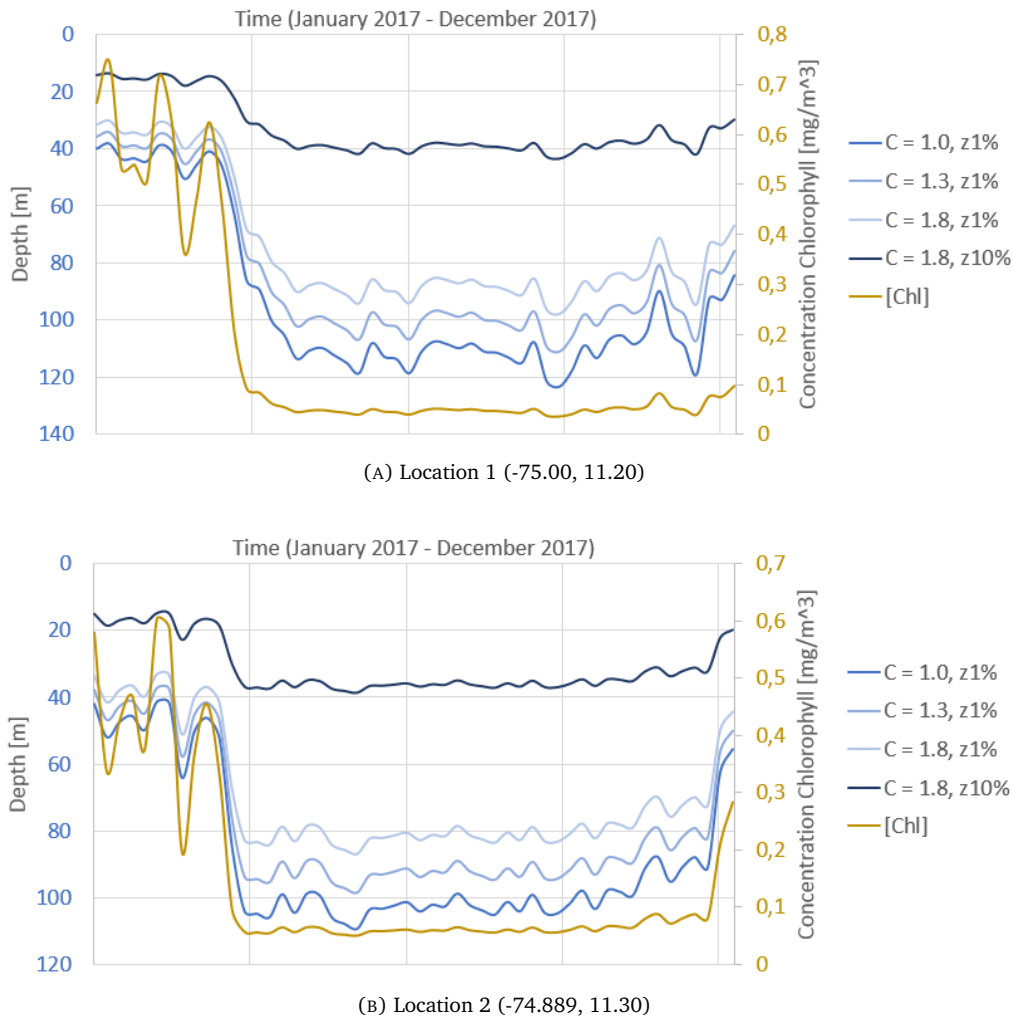


FIGURE 6.1: Euphotic layer depths and Chlorophyll concentration at the surface for both possible floater locations. Note that using the $z_{10\%}$ gives very low estimates of the euphotic layer depths. The $z_{1\%}$ plot for $C = 1.8$ stays above 90 m but keep in mind that the average error is still 22.3%.

It is assumed that the true euphotic depth is in between the theories of Lee et al. (2007) and Vega (2013) meaning the euphotic depth is approximately (50-70 meters), which is closer to the surface than the calculated return flow pipe depth. Because the depth at which the discharge is naturally buoyant is higher than the depth of the euphotic layer it is advised to design the mixed water return pipe based on the depth where the the discharge is naturally buoyant, which is **130 meters**.

6.4 Conclusion

Assuming a cold seawater intake temperature of 5°C and a warm seawater intake temperature of 27°C, the intake pipe lengths become 1023 and 36 meters, respectively. Based on the equation of state, the mixed water return flow pipe length becomes 130 m. At this depth, the effects of a difference in density between the surrounding seawater and the mixed returned water are minimized. Also, the depth is outside of the euphotic zone which minimizes algae growth.

If the intake water is higher than 27 degrees, the discharge temperature will have a higher temperature. Calculations with the Equation of State reveal that the warmer the discharge temperature, the less density the discharge water has. Whenever the discharge temperature is higher than output temperatures calculated in section 6.3.1, less depth is needed in order for

the discharge water to be naturally buoyant. As the intake temperature fluctuates throughout the year, it is therefor advised to design the length of the discharge return pipe at 120 meters.

If however, the preference lies to make the pipe as short as possible, it's possible to make the pipe shorter around 100 meters depth. As long as the discharge is below the euphotic layer, no severe environmental consequences are expected. At 100 meters depth the density of the discharge water is heavier than the density of the surrounding water, and thus will sink to the depth where it is naturally bouyant.

7

Contractors/Suppliers Analysis

In the following chapter the contractors/suppliers analysis for the modification of the floater and the anchor mooring system is discussed. For the modification of the floater and the realization of the anchor mooring system offshore of Barranquilla, many companies and organizations will be involved. This research considers companies and organizations from Colombia and abroad. Given the complexity of certain parts, the stakeholders are mainly specialized offshore companies which are located outside Colombia.

7.1 Modification of the floater

The conversion of a second-hand cargo ship to an OTEC-floater will have to be carried out in a shipyard with the necessary capacity, including a drydock that has the right dimensions. Colombia does not have a shipyard that meets this requirement, so the conversion of the ship needs to be carried out outside of Colombia. The company SBM Offshore has a lot of experience and a big track record regarding the conversion of second-hand ships to FPSO's, which is very much comparable with the conversion of an old bulk carrier to an OTEC-system. SBM offshore has confirmed that they could be a partner for the conversion. They usually do such projects in shipyards in Asia. Their shipyard in Brasil is not suitable for this operation.

The modification of the floater will include the installation of mooring equipment on deck, such as chainstoppers, fairleads and gearboxes. The companies Remazel, Righini and PH Hydraulic and Engineering are experienced suppliers of these components for SBM Offshore projects.

7.2 Installation of the anchor mooring system

The installation of the anchor mooring system is similar to the anchor mooring system installation of an FPSO. In Colombia there are no contractors that have experience with these types of jobs. Outside of Colombia, however, several offshore contractors have experience with the anchor mooring system installation of an FPSO. The contractor Boskalis has confirmed that the scope of the installation of an anchor mooring system for this project is quite comparable with one required for a FPSO, with which they have a lot of experience. The price of an anchor mooring system installation can vary significantly depending on the availability of installation vessels at the time of installation, the composition of the mooring lines and the side works that are needed, such as transport, storage, ROV surveys and testing. Other contractors capable of installing the anchor mooring system are Van Oord and SBM Offshore.

7.3 Lines

The design of the lines consists of two chain parts and a fibre part. These different types of lines are commonly provided by different specialized suppliers. The contractor Boskalis often works with the chain suppliers Vicinay and Ramnas and for the fibre lines they often work with suppliers like Bexco, Lankhorst and CSL. For the connectors between the different line components the Dutch company Vryhof and the French company Le Beon are experienced suppliers.

7.4 Anchors

There are many different suppliers of offshore anchors for application in a taut leg mooring system, which can handle the maximum design loads of our design. An example is the experienced Dutch supplier Vryhof, which has an extensive collection of different anchor types.

8

Conclusion and discussion

8.1 Conclusion

From the environmental analysis we now know that both locations are suitable for an offshore OTEC plant. There is no significant negative effect from upwelling and the temperature profiles show that the temperature differences are sufficient year round. The proposed anchor mooring design consists of a spread-moored 4x3 taut mooring system. The lines are composed of three parts: a 50 meter chain connected to the ship, a 1290 meter fibre line in the middle section and another 150 meter chain at the end that is connected to the anchor. The floater is positioned in a 58,05° angle with respect to the north (in a northeast direction). This ensures comfortable operation during daily conditions and will reduce fatigue build up. The hurricane conditions were found to be governing. The design complies with the basis of design stated in section 5.3 and with the DNV-OS-E301 code and the API Recommended Practice 2SK.

8.2 Discussion

Most of the data that was used for the environmental study has been obtained with satellite remote sensing. This has the advantage that a large area can be analyzed but it does mean that the data has a relatively low resolution. On-site measurements provide more accurate data. On-site measurement services are offered by commercial companies or can be done by investing in measurement devices. These are more expensive solutions than using the freely and publicly available Copernicus data however.

8.3 Recommendations

In this section, recommendations are done for different components of the design.

8.3.1 Environmental study

The resolution of the bathymetry used in this report is quite low. It is recommended that higher resolution bathymetry is acquired. This will lead to a more optimized location of the floater. Using a wave buoy for the wave data increases the reliability of the wave analysis, under the condition that it accurately measures tropical storm, tropical depression and hurricane conditions. CIOH owns a wave buoy in the Caribbean Sea that measures this data but it is far from the location of interest. It is recommended to measure wave data on or near the floater. Measuring temperature profiles is also recommended. Placing temperature, salinity and pressure gauges along the cold water pipe would provide valuable data with which future offshore OTEC designs can be further optimized. It is recommended that the same is done for current data.

8.3.2 Seawater intake- and return flow pipes

The length of the discharge return pipe could be further optimized if information is available of the discharge temperature whenever the water intake temperature is higher than 27°C. The OTEC system will have a higher yield when intake temperatures are higher, but as a consequence the discharge temperatures are higher as well. Therefore, less depth is required for the return pipe. A secondary consequence is that the warm water intake pipe requires less depth, as it is now designed to have an average intake temperature of 27 °C. Higher intake temperatures require less depth.

8.3.3 Anchor mooring design

Regarding the mooring system there are several recommendations to make. First of all it is unknown at this moment how the coldwater intake pipe would be attached to the hull. For this reason the option of a disconnectable anchor mooring system is not looked into because difficulties regarding transportation of the entire OTEC plant including pipes or the disconnecting of the pipes is also unknown. Secondly the system can be further optimized. As discussed the system presented in this report is suitable for the location and its purpose but is a little conservative in some aspects (e.g. the maximum offset is never reached). The optimization is an iterative process and there are several parameters which can be optimized. A fibre line with a smaller minimum breaking load which still complies with the basis of design can be searched for. However, it is also possible to increase the number of lines on the side where the environmental loading is largest or change the pay-out length of the lines. Note that the lay-out of the mooring system is thus also a matter of preference. Thirdly, at this moment it is unknown what the soil conditions at the location are. It is therefore not possible to give advice on what type of anchor is best suited for this situation. A soil investigation is therefore necessary. Furthermore, when designing the plant layout and the general arrangement of the ship, space will have to be reserved for the deck equipment which is needed for the anchor mooring system (e.g. chain jacks and winches). Lastly, a fatigue analysis has not been conducted during the research. This topic should be looked into further. However, because the entire system is designed to withstand hurricane conditions it is presumed not likely that fatigue damage will play a major role regarding the structural integrity of the system.

8.3.4 Power cable

The choice for a dynamic power cable or a combination of dynamic and static power cable depends on the irregularity of the bed. This means that the resolution of bathymetry data must be such that sand waves and other small scale bed irregularities can be distinguished. Unfortunately, the bathymetry data received from CIOH had a low resolution and missed spatial information. Because of this, no advice could be given on the configuration of the power cable. It is recommended to use more accurate bathymetry data (which is not yet available) for this purpose. The soil conditions must also be known.

A: Wind and wave data

Scatter table

[Download the scatter table](#)

Percentage of occurrence of wave height (m) in rows versus mean wave period (s) in columns

	lower	03	04	05	06	07	08	09	10	11	12	13	14	
lower	upper	04	05	06	07	08	09	10	11	12	13	14	15	total
0.0	0.5	0	0	0	0	0	0	0	0	0	0	0	0	0.0
0.5	1.0	0	0.6	0.6	3.2	3.2	1.9	0	0.6	0	0	0	0	10.1
1.0	1.5	0	0	7.0	6.3	3.2	0.6	0	0	0.6	0	0	0	17.7
1.5	2.0	0	0	8.2	11.4	1.3	0.6	0	0	0	0	0	0	21.5
2.0	2.5	0	0	4.4	14.6	3.2	0	0	0	0	0	0	0	22.2
2.5	3.0	0	0	0	9.5	6.3	0.6	0	0	0.6	0	0	0	17.1
3.0	3.5	0	0	0	0.6	5.7	0.6	0	0	0.6	0	0.6	0	8.2
3.5	4.0	0	0	0	0	0.6	0	0	0	0	0	0	0	0.6
4.0	4.5	0	0	0	0	1.3	0.6	0	0	0	0	0	0	1.9
4.5	5.0	0	0	0	0	0	0	0.6	0	0	0	0	0	0.6
5.0	5.5	0	0	0	0	0	0	0	0	0	0	0	0	0.0
total		0.0	0.6	20.3	45.6	24.7	5.1	0.6	0.6	1.9	0.0	0.6	0.0	100.0

Copyright ARGOSS, March 2018

Your choices :

Centre of area is at 11° 32'N, 75° 17'W

Size of area is 200x200 km

Season is all year

First and last year analysed 1993-2003

Variables are wave height (m) and mean wave period (s)

Data source is sar

Results are based on 158 samples from 158 passes

FIGURE A.1: Distribution of mean wave period of the daily wave conditions

	Velocity	0-3 m/s	3-6 m/s	6-9 m/s	9-12 m/s	12-15 m/s	15-18 m/s
Degrees							
0	9	39	209	32	5	1	0
10	19	36	281	110	15	1	0
20	29	54	407	304	68	1	1
30	39	44	649	947	451	9	0
40	49	51	862	2525	2990	373	1
50	59	46	1017	4481	9258	3873	155
60	69	52	949	4010	9192	6608	758
70	79	48	853	2590	4253	1682	80
80	89	29	703	1585	678	30	0
90	99	54	585	702	54	0	0
100	109	53	451	306	4	0	0
110	119	38	412	124	0	0	0
120	129	41	377	75	0	0	0
130	139	48	288	67	0	0	0
140	149	38	268	73	2	0	0
150	159	37	280	71	4	0	0
160	169	30	256	74	4	0	0
170	179	30	238	79	5	1	0
180	189	31	224	77	9	2	0
190	199	39	256	93	12	2	0
200	209	36	242	88	15	4	0
210	219	41	227	85	9	1	0
220	229	46	240	83	7	2	0
230	239	32	187	78	13	3	0
240	249	43	195	54	5	2	0
250	259	33	185	35	4	0	0
260	269	38	165	17	1	1	0
270	279	44	145	10	1	0	0
280	289	40	118	5	1	0	0
290	299	35	101	2	0	0	0
300	309	28	98	4	0	0	0
310	319	31	96	1	2	0	0
320	329	48	102	8	1	0	0
330	339	30	108	5	1	0	0
340	349	41	131	8	2	0	0
350	359	51	169	26	4	0	0

TABLE A.1: Number of wind events per velocity and direction from 1992 until 2016 for an area of 200 km x 200 km centered at 11.50, -75.50 and dataset with a timestep of 3 hours (BMT Argoss, 2017)

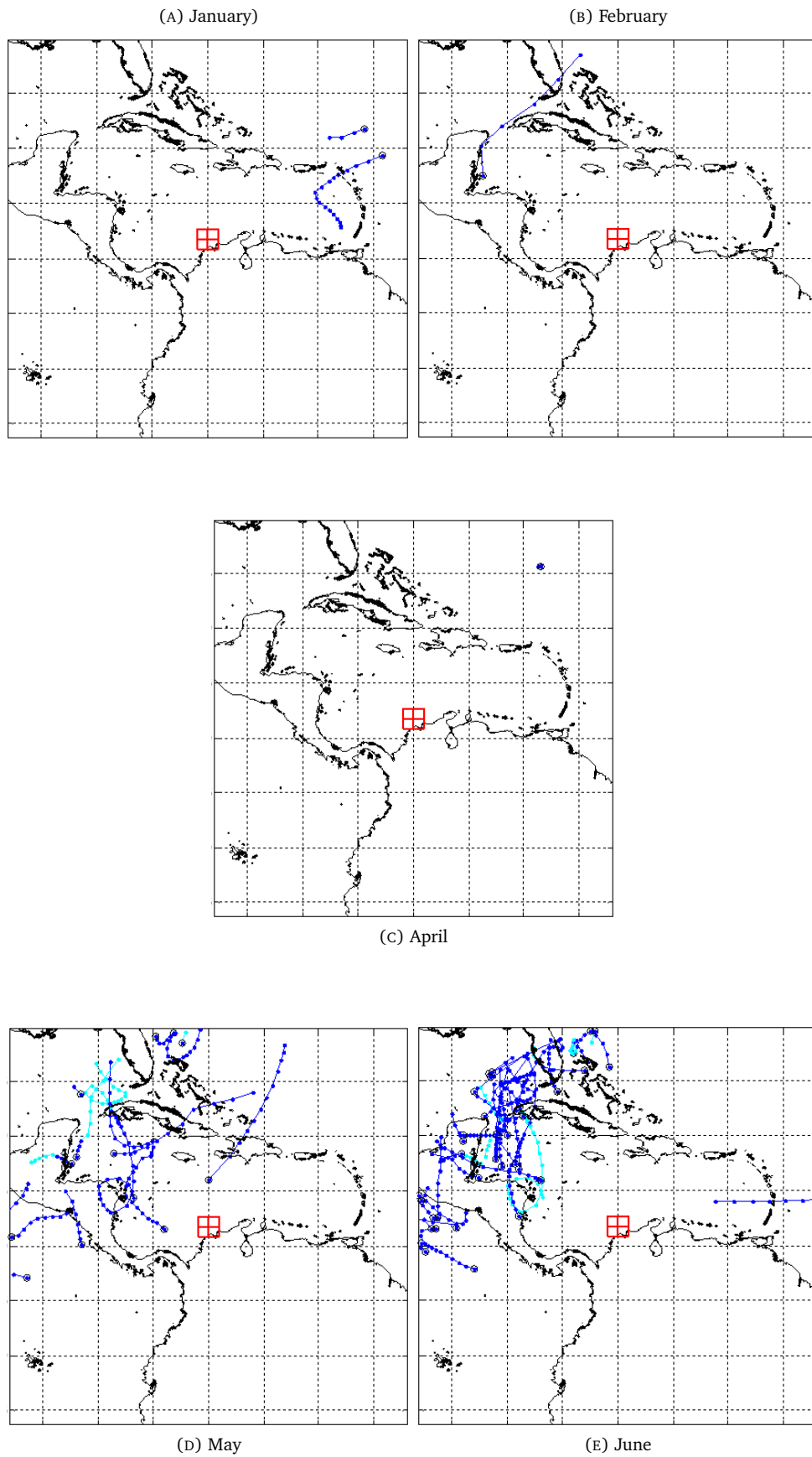
	Velocity	0-3 m/s	3-6 m/s	6-9 m/s	9-12 m/s	12-15 m/s	15-18 m/s
Degrees							
0	9	0,05 %	0,29 %	0,04 %	0,01 %	0,00 %	0,00 %
10	19	0,05 %	0,38 %	0,15 %	0,02 %	0,00 %	0,00 %
20	29	0,07 %	0,56 %	0,42 %	0,09 %	0,00 %	0,00 %
30	39	0,06 %	0,89 %	1,30 %	0,62 %	0,01 %	0,00 %
40	49	0,07 %	1,18 %	3,46 %	4,09 %	0,51 %	0,00 %
50	59	0,06 %	1,39 %	6,14 %	12,68 %	5,30 %	0,21 %
60	69	0,07 %	1,30 %	5,49 %	12,59 %	9,05 %	1,04 %
70	79	0,07 %	1,17 %	3,55 %	5,82 %	2,30 %	0,11 %
80	89	0,04 %	0,96 %	2,17 %	0,93 %	0,04 %	0,00 %
90	99	0,07 %	0,80 %	0,96 %	0,07 %	0,00 %	0,00 %
100	109	0,07 %	0,62 %	0,42 %	0,01 %	0,00 %	0,00 %
110	119	0,05 %	0,56 %	0,17 %	0,00 %	0,00 %	0,00 %
120	129	0,06 %	0,52 %	0,10 %	0,00 %	0,00 %	0,00 %
130	139	0,07 %	0,39 %	0,09 %	0,00 %	0,00 %	0,00 %
140	149	0,05 %	0,37 %	0,10 %	0,00 %	0,00 %	0,00 %
150	159	0,05 %	0,38 %	0,10 %	0,01 %	0,00 %	0,00 %
160	169	0,04 %	0,35 %	0,10 %	0,01 %	0,00 %	0,00 %
170	179	0,04 %	0,33 %	0,11 %	0,01 %	0,00 %	0,00 %
180	189	0,04 %	0,31 %	0,11 %	0,01 %	0,00 %	0,00 %
190	199	0,05 %	0,35 %	0,13 %	0,02 %	0,00 %	0,00 %
200	209	0,05 %	0,33 %	0,12 %	0,02 %	0,01 %	0,00 %
210	219	0,06 %	0,31 %	0,12 %	0,01 %	0,00 %	0,00 %
220	229	0,06 %	0,33 %	0,11 %	0,01 %	0,00 %	0,00 %
230	239	0,04 %	0,26 %	0,11 %	0,02 %	0,00 %	0,00 %
240	249	0,06 %	0,27 %	0,07 %	0,01 %	0,00 %	0,00 %
250	259	0,05 %	0,25 %	0,05 %	0,01 %	0,00 %	0,00 %
260	269	0,05 %	0,23 %	0,02 %	0,00 %	0,00 %	0,00 %
270	279	0,06 %	0,20 %	0,01 %	0,00 %	0,00 %	0,00 %
280	289	0,05 %	0,16 %	0,01 %	0,00 %	0,00 %	0,00 %
290	299	0,05 %	0,14 %	0,00 %	0,00 %	0,00 %	0,00 %
300	309	0,04 %	0,13 %	0,01 %	0,00 %	0,00 %	0,00 %
310	319	0,04 %	0,13 %	0,00 %	0,00 %	0,00 %	0,00 %
320	329	0,07 %	0,14 %	0,01 %	0,00 %	0,00 %	0,00 %
330	339	0,04 %	0,15 %	0,01 %	0,00 %	0,00 %	0,00 %
340	349	0,06 %	0,18 %	0,01 %	0,00 %	0,00 %	0,00 %
350	359	0,07 %	0,23 %	0,04 %	0,01 %	0,00 %	0,00 %

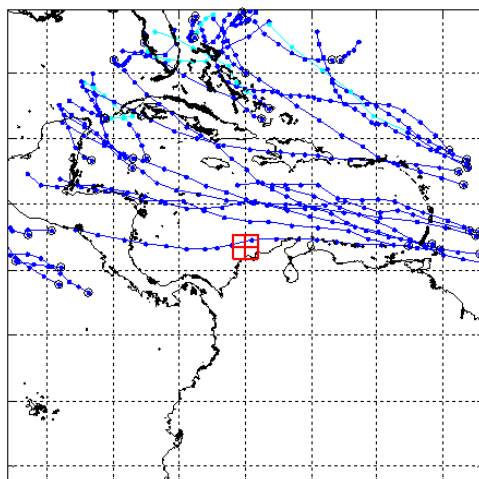
TABLE A.2: Percentage of occurrence of combinations of wind velocity and direction from 1992 until 2016 for an area of 200 km x 200 km centered at 11.50, -75.50 and dataset with a timestep of 3 hours (BMT Argoss, 2017)

SS-Cat	Min	Max	Jan	Feb	Mar	Apr	May	Jun	Jul	Aug	Sep	Oct	Nov	Dec	All
HR-5	69,4		0	0	0	0	0	0	0	0	0	0	0	0	0
HR-4	58,1	69,4	0	0	0	0	0	0	0	0	0	0	0	0	0
HR-3	49,2	58,1	0	0	0	0	0	0	0	0	0	0	0	0	0
HR-2	42,5	49,2	0	0	0	0	0	0	0	0	1	1	0	0	2
HR-1	32,5	42,5	0	0	0	0	0	0	1	0	1	2	1	0	5
TS	17,2	32,5	1	0	0	0	3	3	6	19	33	27	9	1	102
TD	0,1	17,2	1	1	0	1	11	29	29	92	121	72	20	4	381
-	0,0	0,1	0	0	0	0	0	0	0	0	0	0	0	0	0
			2	1	0	1	14	32	36	111	156	102	30	5	490

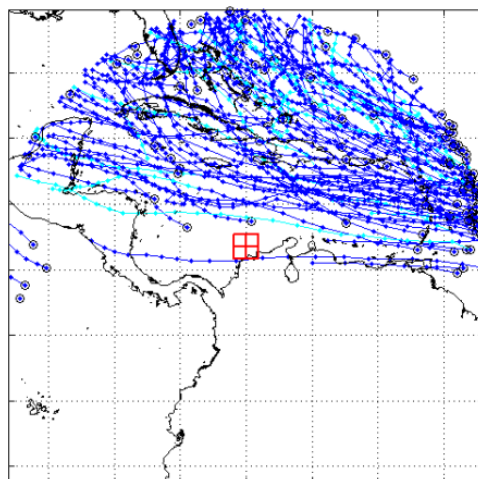
TABLE A.3: All storm events off the coast of Barranquilla (1946-2015)(Groenewoud, 2017)

FIGURE A.2: Tropical storm tracks per month (excluding March, for which no storms were recorded)

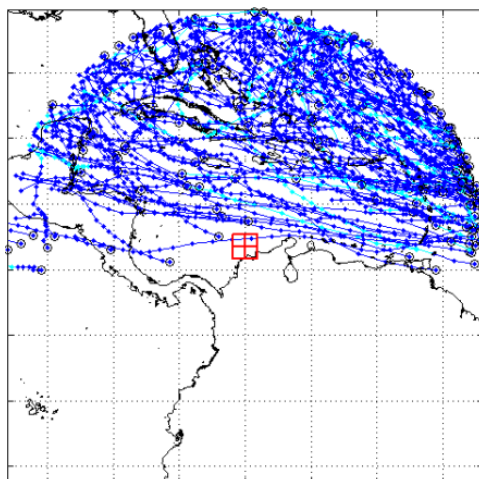




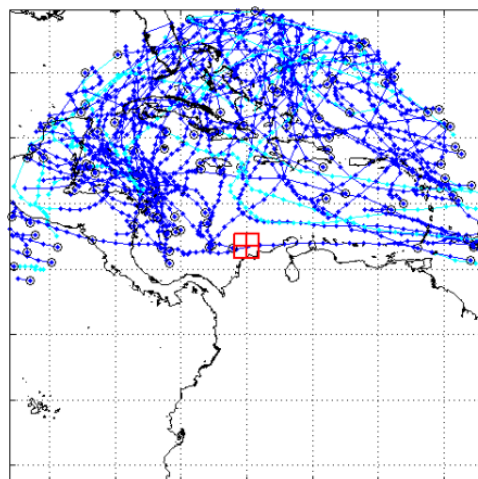
(F) July



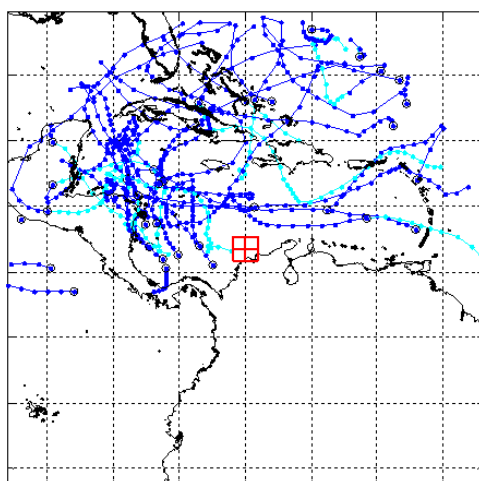
(G) August



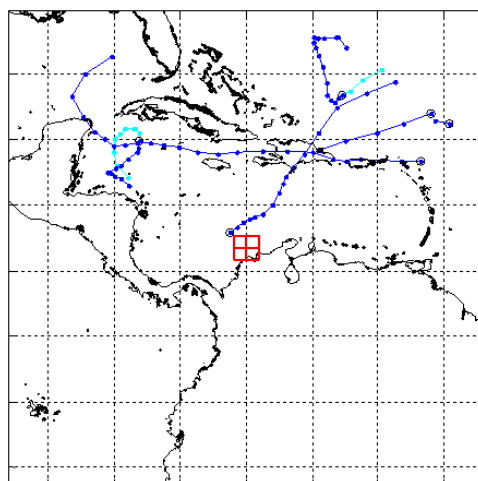
(H) September



(I) October



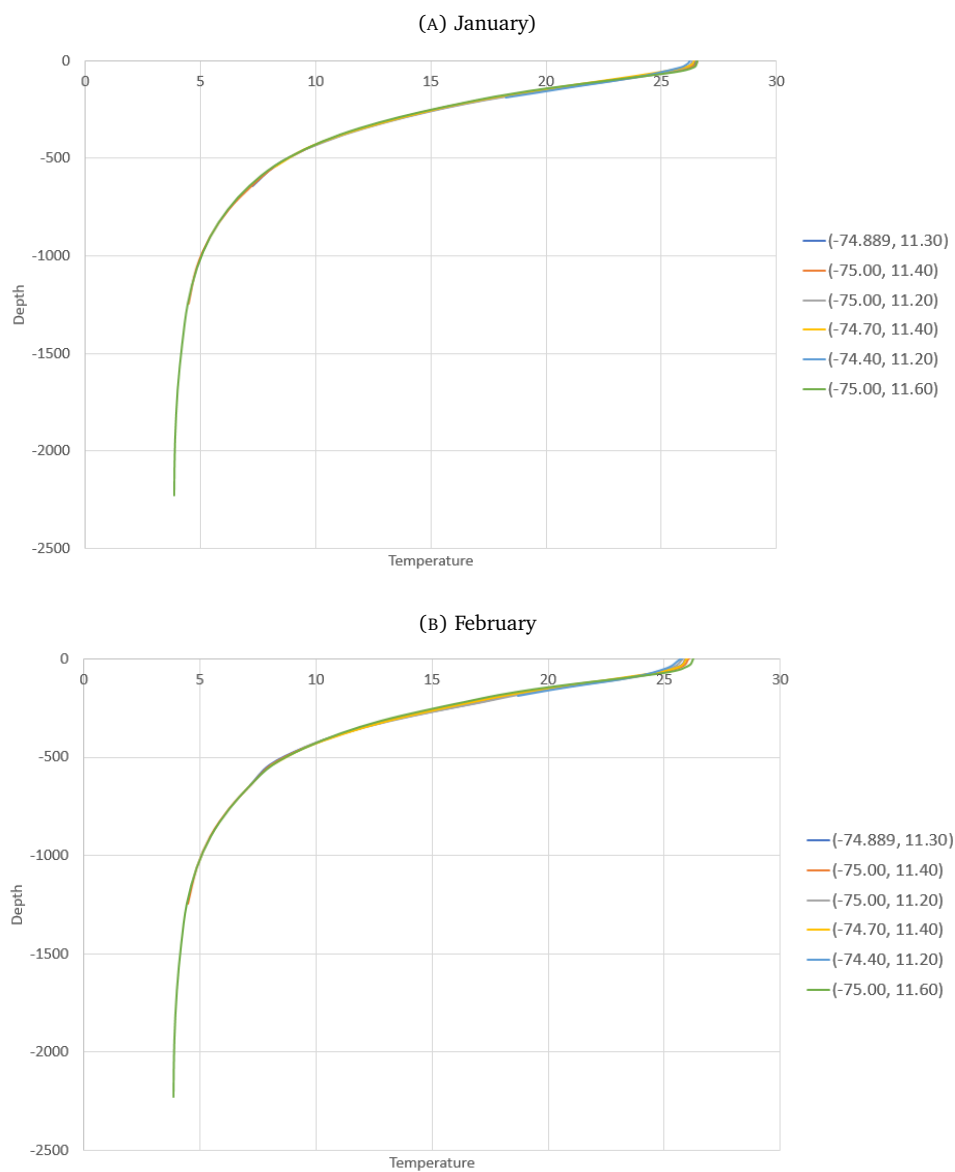
(J) November

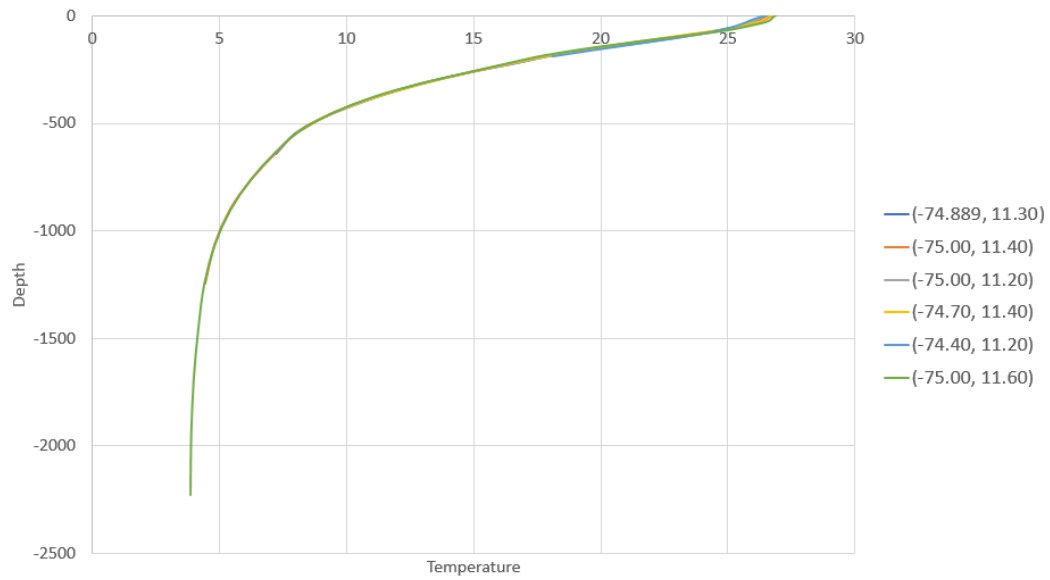


(K) December

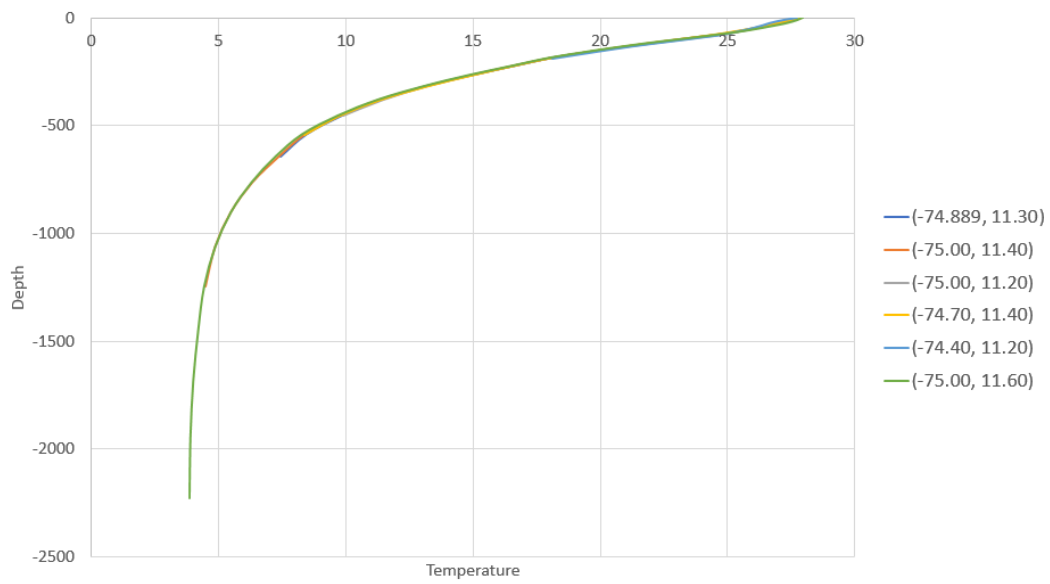
B: Temperature profiles

FIGURE B.1: Temperature profiles for 5 different locations with different depths off the coast of Barranquilla. Each profile is the average of the month from 2007 until 2016. (e.g. January is the average profile of all Januaries in the period 2007-2016)

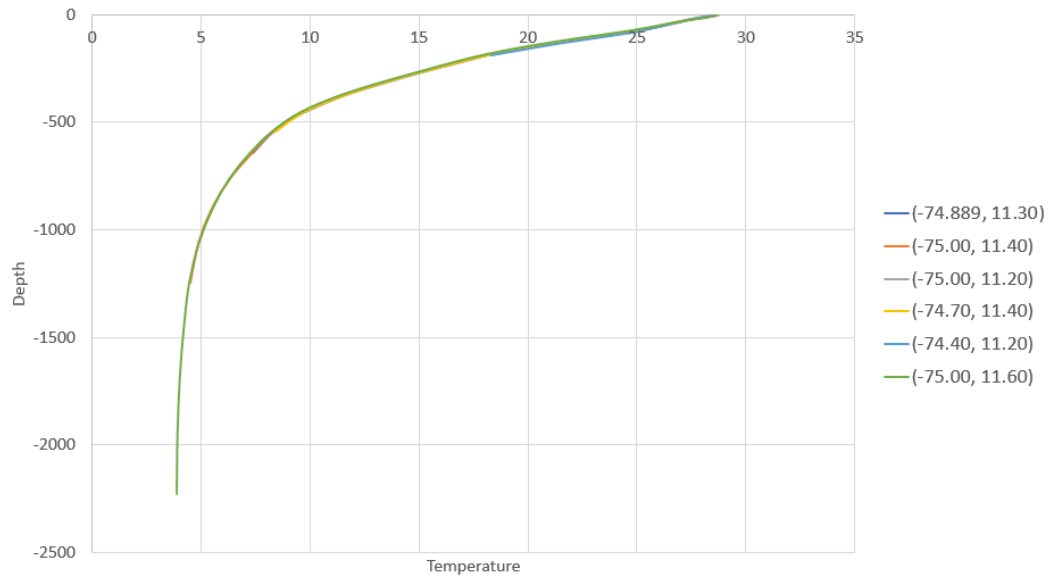




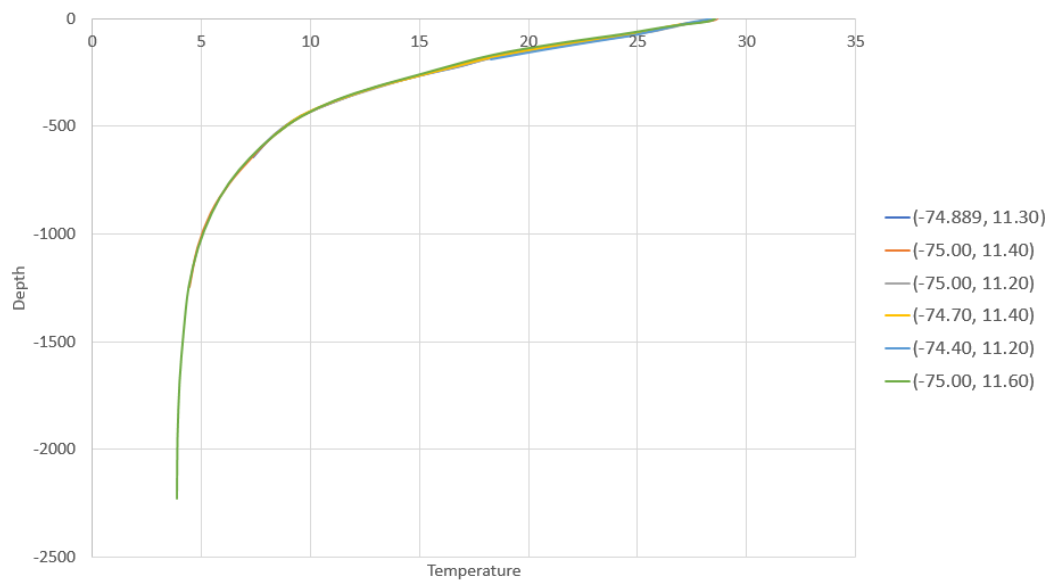
(c) March



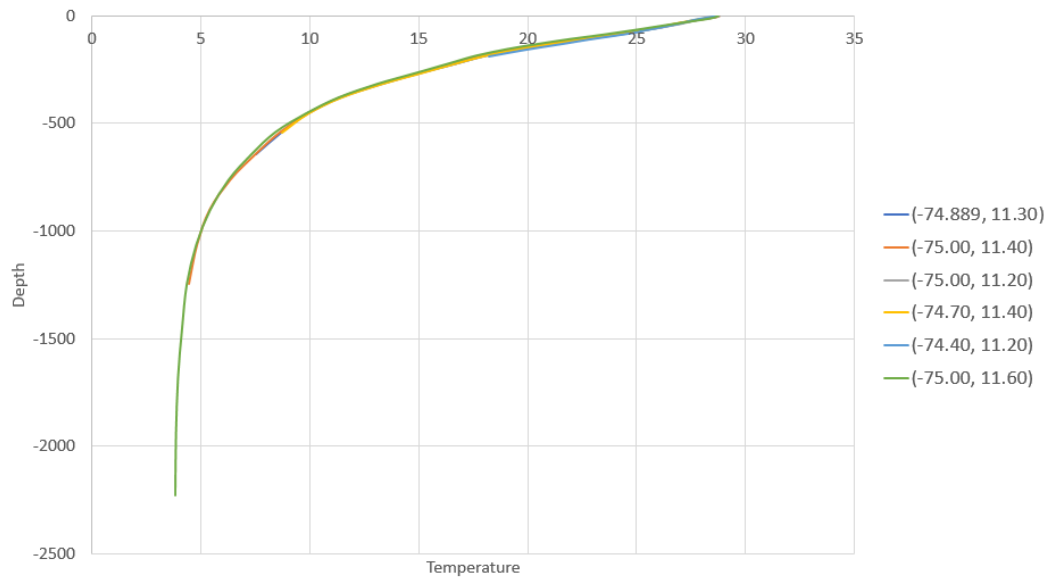
(d) April



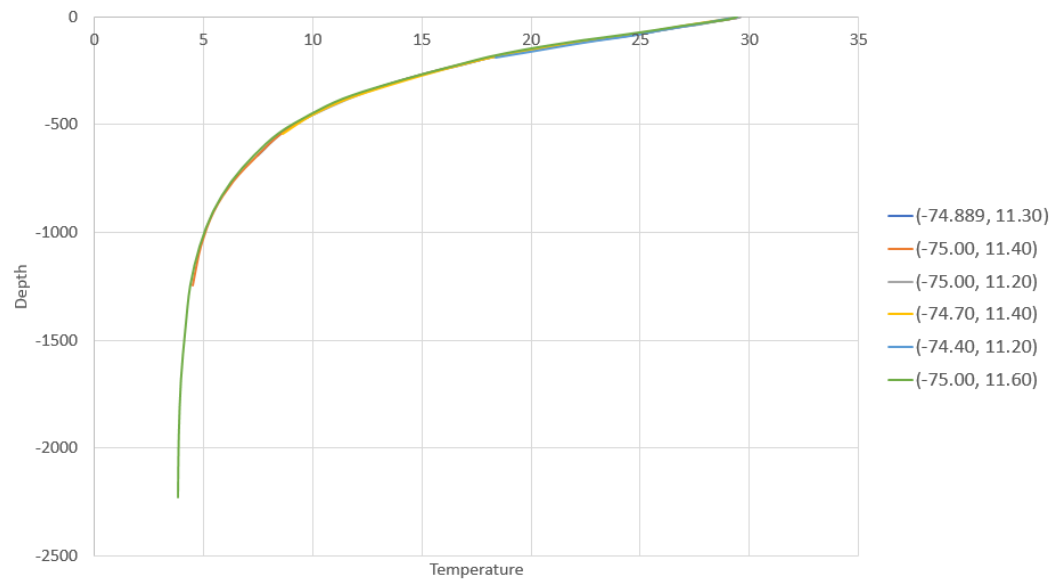
(E) May



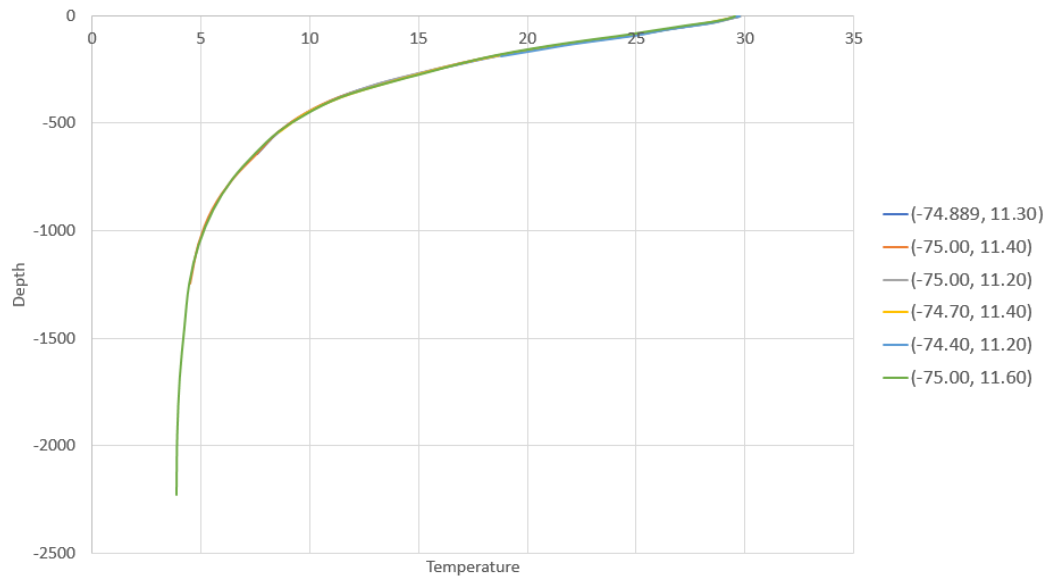
(F) June



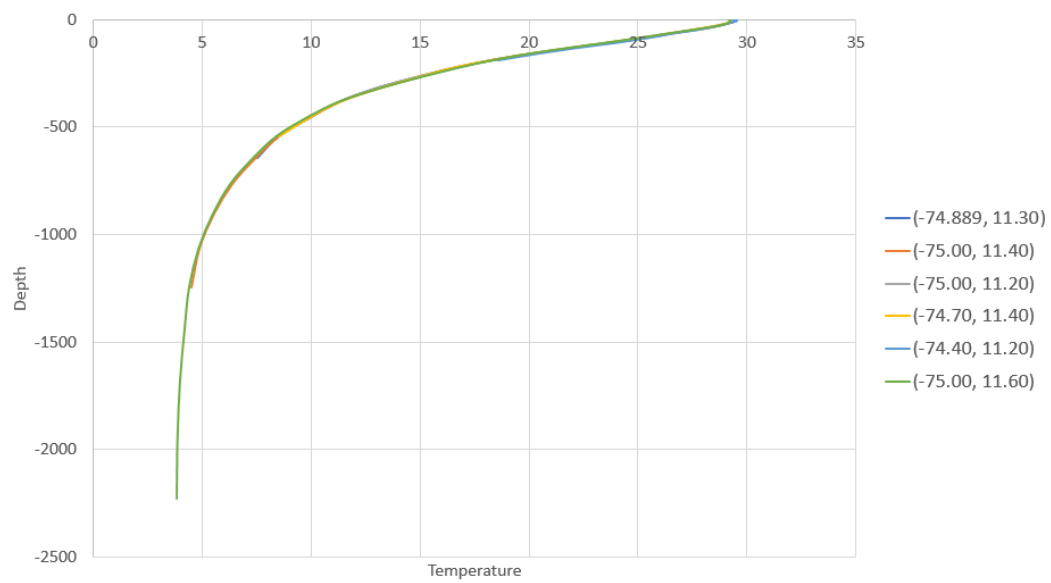
(G) July



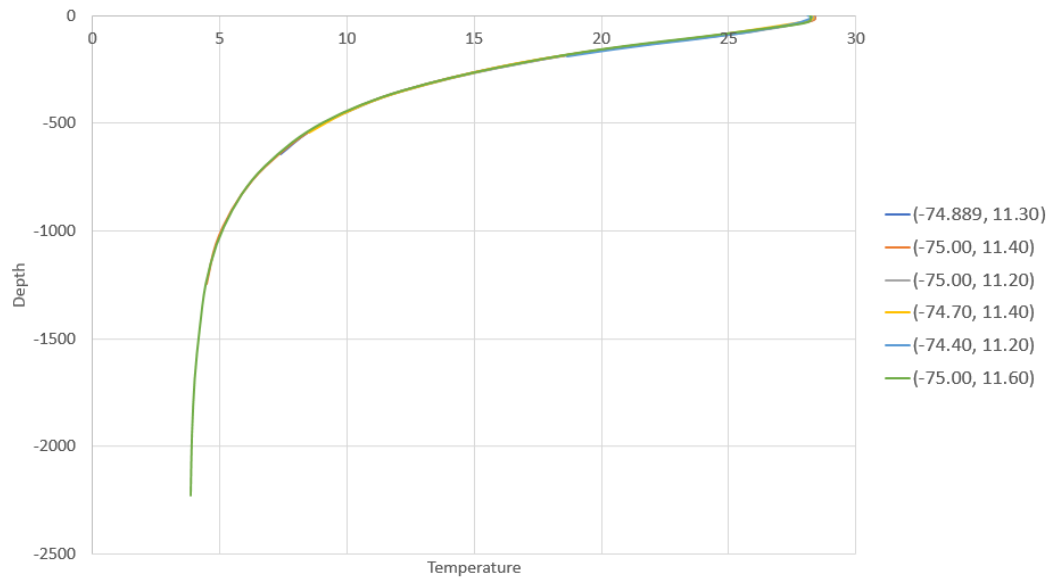
(H) August



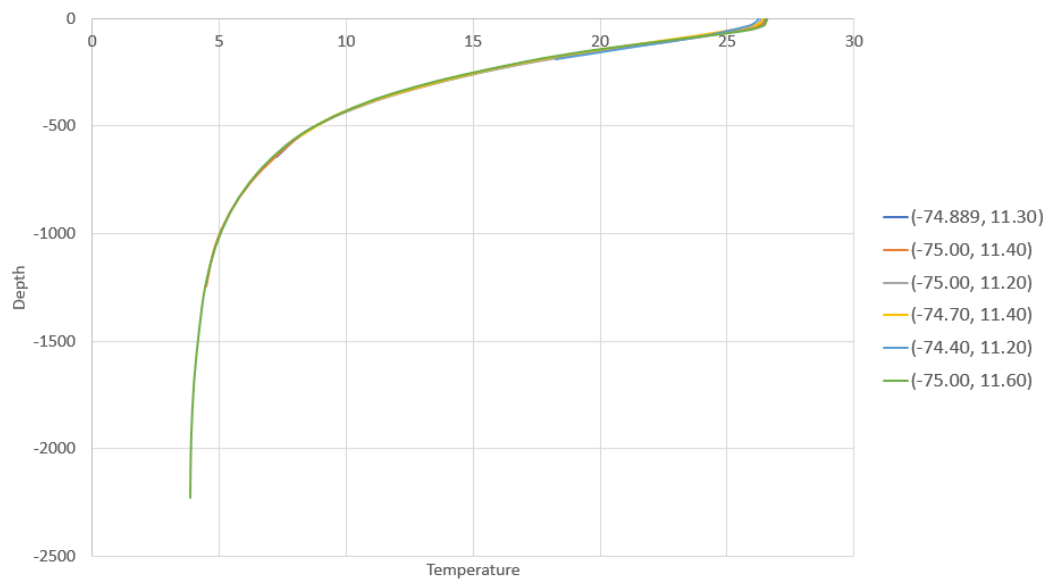
(i) September



(j) October



(K) November



(L) December

TABLE B.1: Sea temperatures and temperature differences over depth (2007-2016)

z [m]	$T_{minimum}$ [°C]	$T_{average}$ [°C]	$T_{maximum}$ [°C]	$dT_{average}$ [°C]	$dT_{min_{top}-max_{column}}$ [°C]
0,5	26,95	28,01	28,98	0,00	-2,03
1,5	26,94	28,00	28,97	0,01	-2,02
2,6	26,93	27,99	28,96	0,02	-2,02
3,8	26,92	27,98	28,97	0,03	-2,02
5,1	26,91	27,97	28,96	0,04	-2,01
6,4	26,89	27,96	28,94	0,05	-1,99
7,9	26,86	27,94	28,90	0,07	-1,96
9,6	26,83	27,91	28,87	0,10	-1,92
11,4	26,80	27,88	28,83	0,13	-1,88
13,5	26,76	27,84	28,78	0,18	-1,83
15,8	26,70	27,78	28,71	0,23	-1,76
18,5	26,62	27,70	28,62	0,31	-1,67
21,6	26,50	27,59	28,52	0,42	-1,57
25,2	26,36	27,46	28,41	0,55	-1,46
29,4	26,20	27,29	28,25	0,72	-1,30
34,4	26,01	27,08	28,03	0,93	-1,08
40,3	25,78	26,80	27,72	1,21	-0,77
47,4	25,49	26,46	27,35	1,55	-0,40
55,8	25,09	26,04	26,95	1,97	0,00
65,8	24,55	25,49	26,42	2,52	0,53
77,9	23,77	24,74	25,77	3,27	1,18
92,3	22,68	23,74	24,84	4,27	2,11
109,7	21,42	22,51	23,61	5,50	3,33
130,7	20,06	21,09	22,21	6,92	4,74
155,9	18,62	19,56	20,69	8,45	6,26
186,1	17,00	18,00	19,13	10,01	7,82
222,5	15,25	16,52	17,70	11,49	9,25
266,0	13,53	14,88	16,10	13,13	10,85
318,1	11,70	13,05	14,37	14,96	12,58
380,2	10,16	11,22	12,46	16,79	14,48
453,9	8,88	9,68	10,70	18,33	16,25
541,1	7,73	8,31	8,96	19,70	17,99
643,6	6,79	7,25	7,73	20,76	19,21
763,3	5,96	6,27	6,58	21,74	20,37
902,3	5,23	5,47	5,70	22,54	21,25
1062,4	4,65	4,85	5,04	23,16	21,91
1245,3	4,27	4,42	4,60	23,59	22,35
1452,3	4,07	4,18	4,30	23,83	22,65
1684,3	3,91	3,99	4,10	24,02	22,85
1941,9	3,83	3,89	3,94	24,12	23,01
2225,1	3,81	3,85	3,88	24,16	23,07

C: Current maps

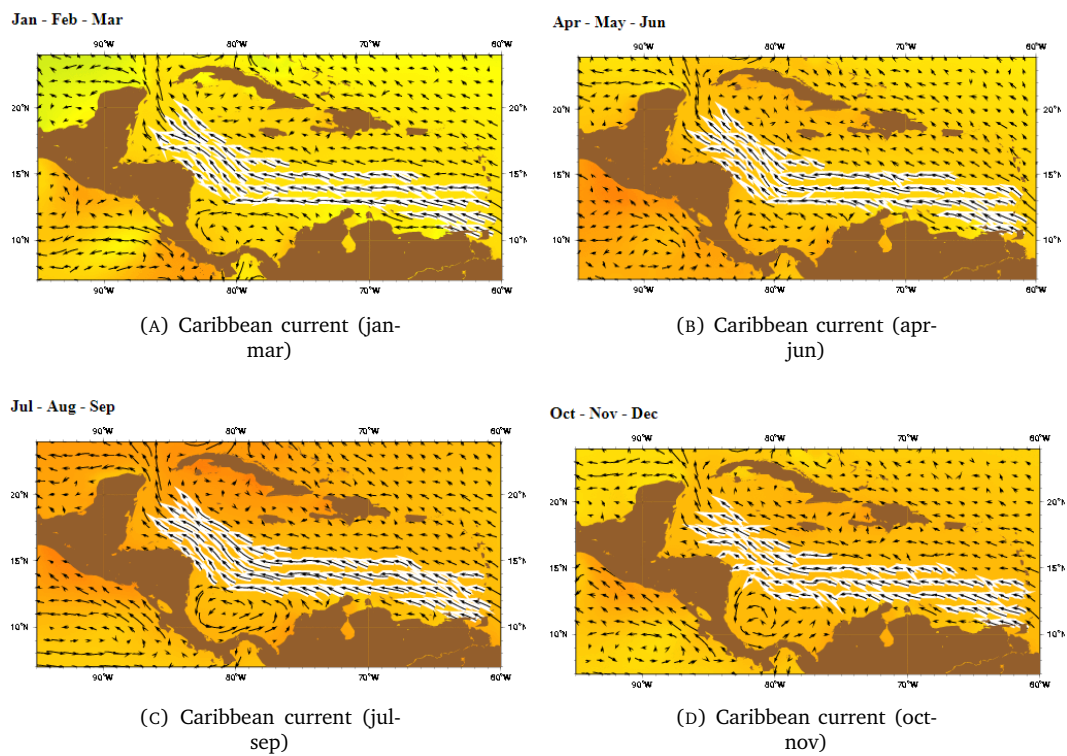


FIGURE C.1: Seasonal maps of the Caribbean surface current

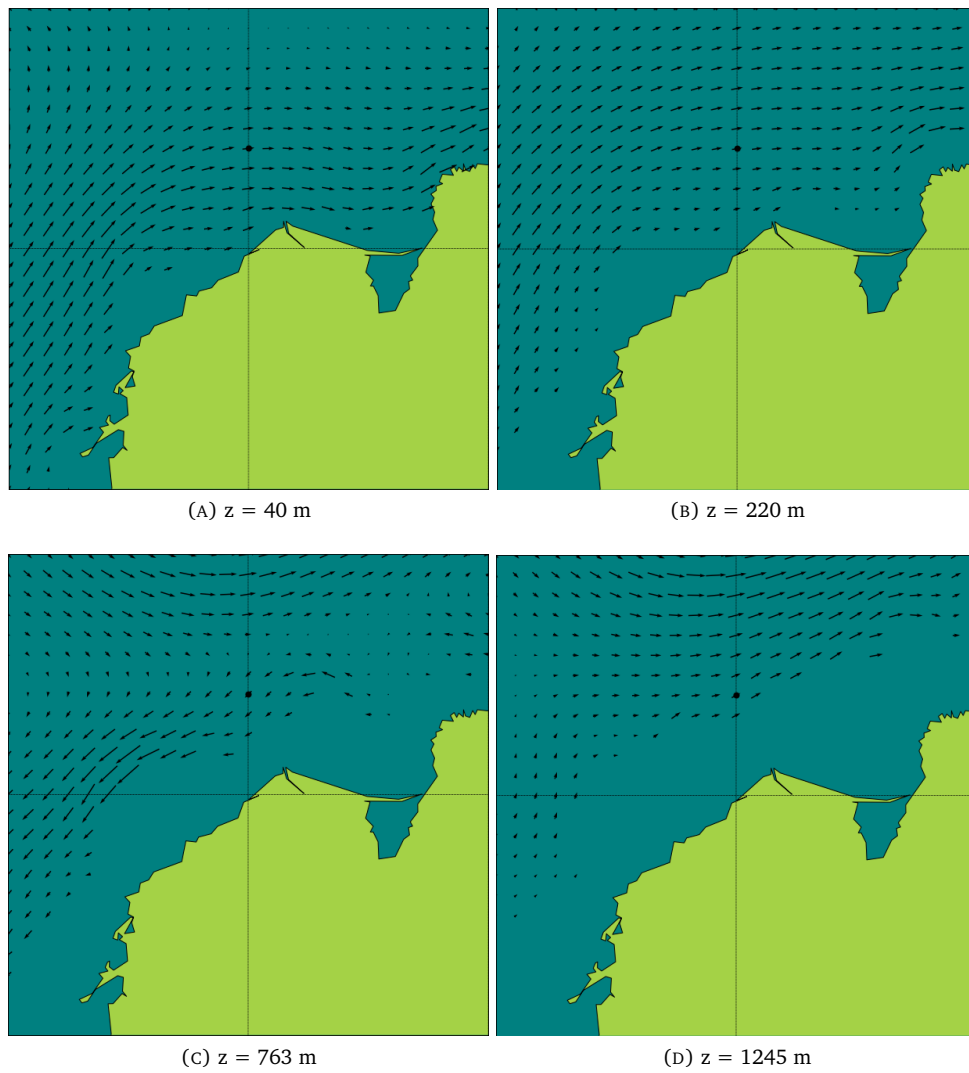


FIGURE C.2: Subsurface currents near Barranquilla (averaged over the period 2013-2017)

D: Marine traffic

The maps have a colour coding which is based on number of vessels per year. "The colour coding is based on a rather compound algorithm. An approximate estimation on the numeric values of the corresponding colours follows - the numbers refer to distinct vessels on a daily basis and count positions per square Km." (MarineTraffic, 2017)

TABLE D.1: Color coding of marine traffic density maps





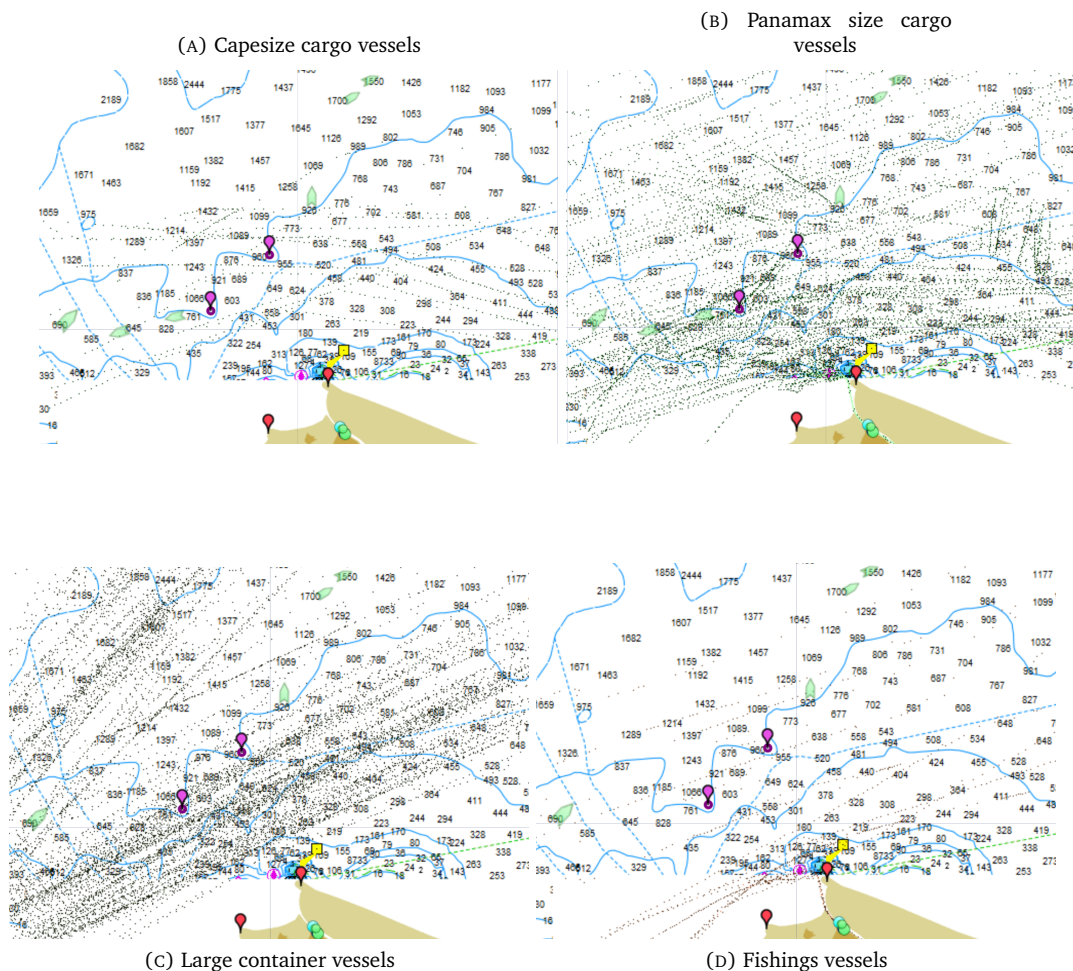
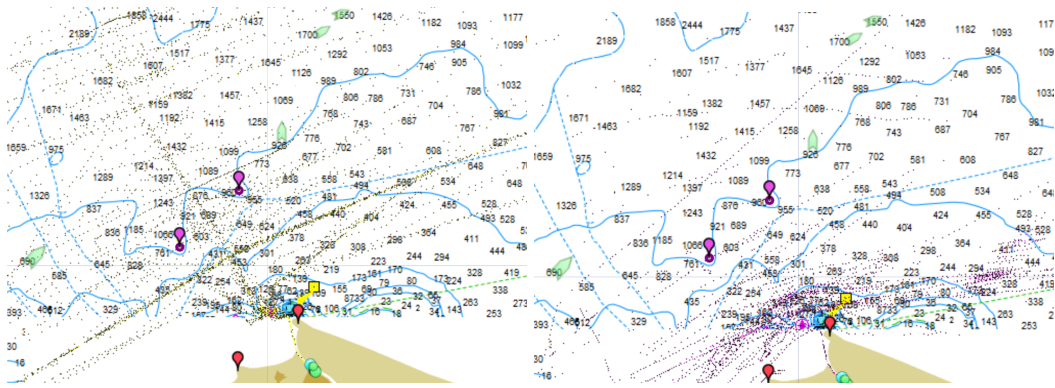
Legenda	Color	Number of vessels
	Blue	Less than 30
	Green	30 to 70
	Yellow	70 to 140
	Red	more than 140

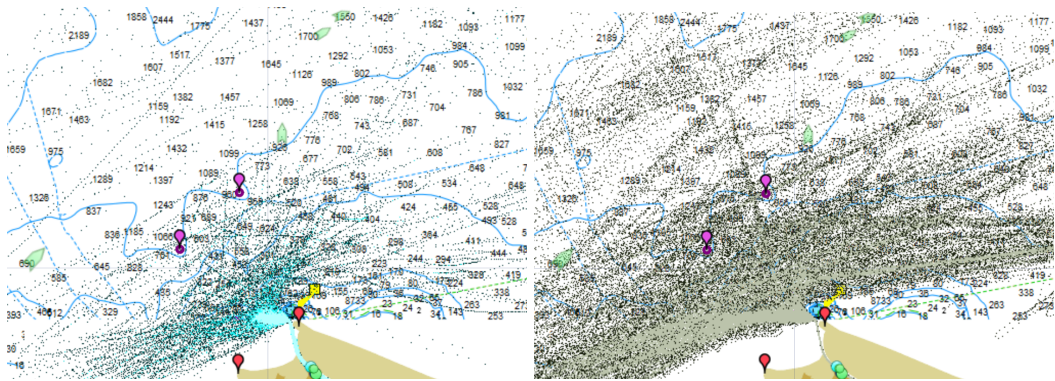
FIGURE D.1: Density of marine traffic (2016)





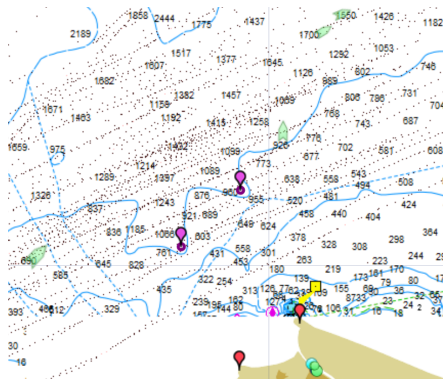
(E) Gas carriers

(F) Pleasure craft

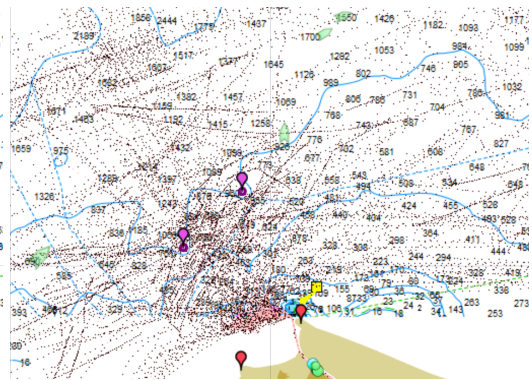


(G) Tugs and special craft

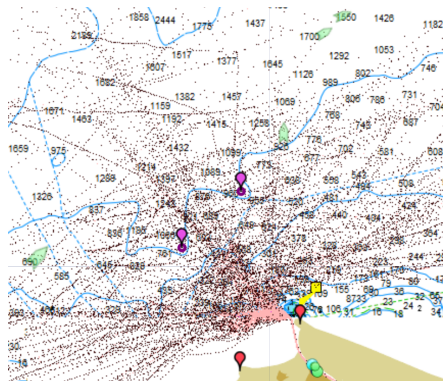
(H) Container feeder vessels



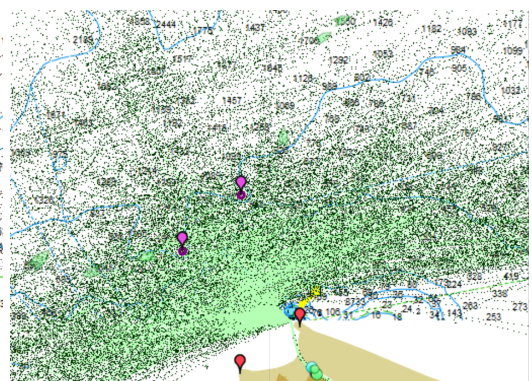
(I) Aframax tankers



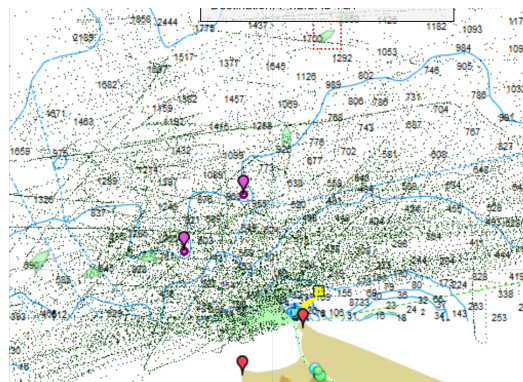
(J) Handymax and Panamax tanker vessels



(K) Handysize tanker vessels

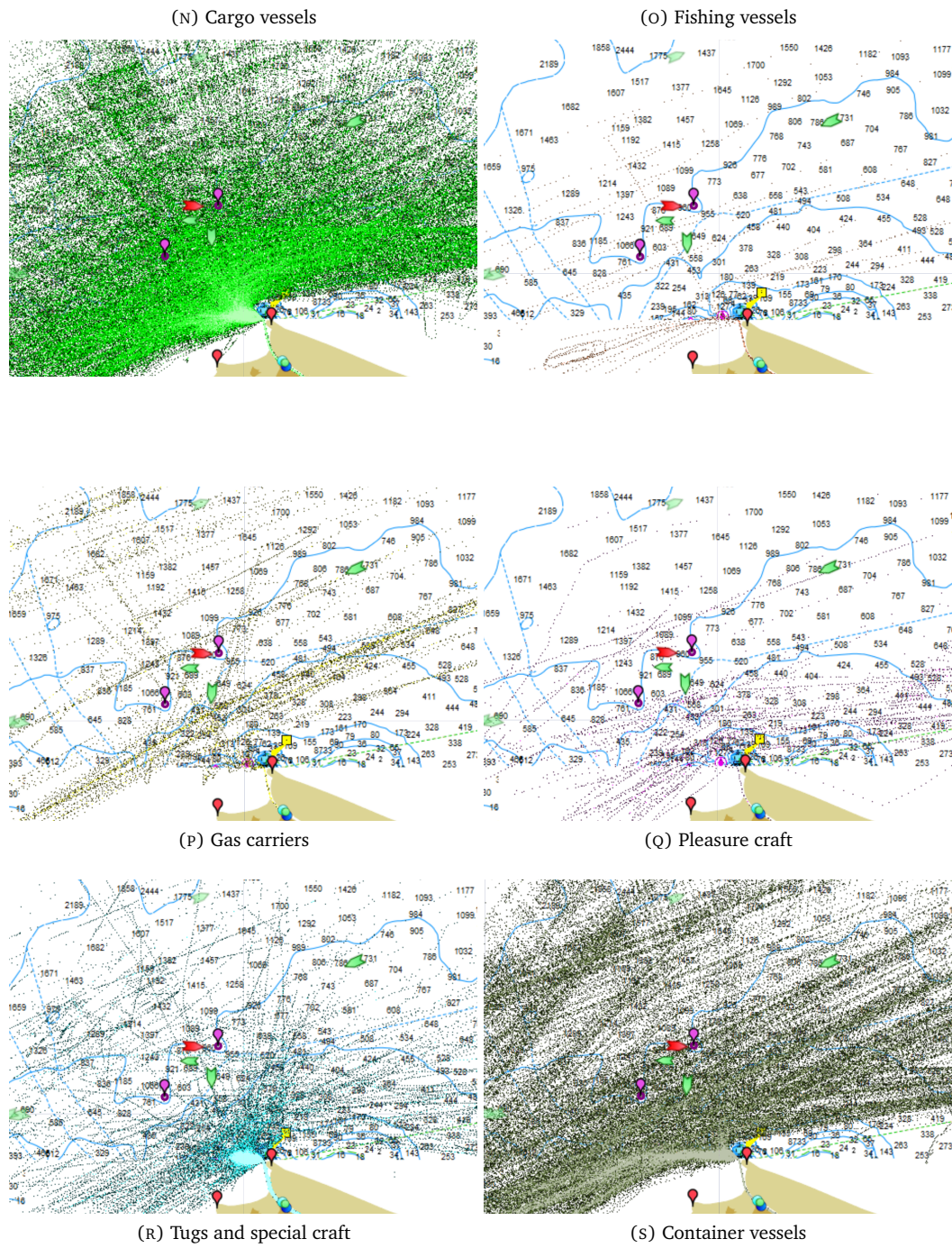


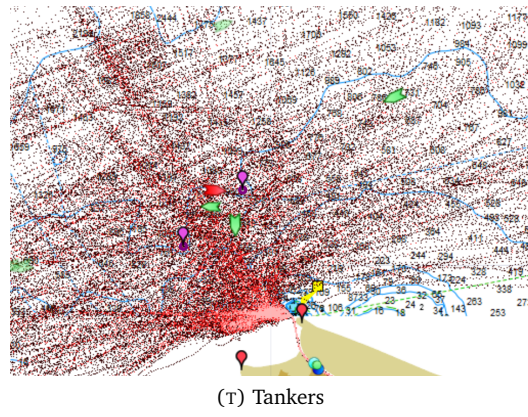
(L) Handysize cargo vessels



(M) Handymax cargo vessels

FIGURE D.-2: Density of marine traffic (2015). More detail on the size and type of vessels is not available for 2015





E: HydroSTAR

E.1 Input

The different calculation steps that have been taken in HydroSTAR and their corresponding input files are listed below.

HSmsg: Automatic mesh generator

OTECF.mri

OTECF.hul

The hull lines input file that was used to create the mesh used in the following step will be shared upon request.

HSlec: reading the mesh

OTECF.hst

The mesh file that has been generated with the automatic mesh generator package is read via the HSlec command. The mesh file can be shared upon request.

FIGURE E.1: HydroSTAR screenshot HSlec command

```

=====***** HydroStar For Experts V7.3 *****=====
-----x64----(c)BV/DR 1991-2016

HSlec - Reading geometrical data.

INPUT FILE : otecf.hst
PROJECT NAME : PRO
* 1th node called 1 is not used.
Nb of bodies to be analysed 1
Nb symmetry of hull geometry 1
Nb panels on hulls 1148
Nb segments along waterlines 82
Nb panels on the waterplanes 384
Nb panels over the free surface 0
Nb hull panels over the waterline 0

Reference length 1.000000
Gravity acceleration 9.810000
Reference point of incident wave ( 119.049630, 0.000000)
Body 1: reference point x= 119.049630 center of buoyancy x= 119.049630
y= 0.000000 y= 0.000000
z= -3.871866 z= -3.871866

Total clock time of operation was 0.28 s

```

HSchk: verification of the mesh

FIGURE E.2: HydroSTAR screenshot HSchk command

```

=====***** HydroStar For Experts V7.3 *****=====
-----x64----(c)BV/DR 1991-2016

HSchk - Checking input data.

It may take a few minutes ...
... Consistence checking finished.
... Superposition checking finished.
... Neighborhood checking finished.

In total: nb of zero-area panels = 0
          nb of panels over free surface = 0
          nb of panels at free surface = 0
          nb of superpositions = 0
          nb of inconsistencies = 0
          nb of neighbor-absences = 0
          nb of symmetry problem = 0

Congratulations! Felicitations! Parabens!
Write visualisation files... Done
Total clock time of operation was 1.12 s

```

HSinf -g: information about the mesh

FIGURE E.3: HydroSTAR screenshot HSinf -g command

```

=====***** HydroStar For Experts V7.3 *****=====
-----x64----(c)BV/DR 1991-2016

HSinf - Computation information.

Nb of bodies : 1

Body No : 1 Xmin= 4.56330 Xmax= 220.84000 => L= 216.277
          Ymin= -16.10000 Ymax= 16.10000 => B= 32.200
          Zmin= -8.00000 Zmax= 0.00000 => D= 8.000

          Nb of symmetries= 1
          Nb of panels = 2296

          Body's surface = 4366.64954
          Average panel surface= 3.80370
          Average panel size = 1.56074

          Body's buoyant volume= 0.45262E+05
          Body's buoyant center= 119.04963 0.00000 -3.87187

```

HStat: hydrostatic properties verification

FIGURE E.4: HydroSTAR screenshot HStat command

```

=====***** HydroStar For Experts V7.3 *****=====
-----x64-----(c)BV/DR 1991-2016

HStat - Hydrostatic-property computations.

Project: BLUERISE OTEC FLOATER
User   :
Nb of bodies to be analysed      1
Nb symmetry of hull geometry    1
Nb panels on hulls              1148
Nb segments along waterlines    82
Nb panels over waterplanes      384
Nb panels over the free surface  0

# Constants used in computations
# Reference length      : 1.000
# Water density (rho)  : 1025.000
# Gravity acceleration  : 9.810

# BODY No.1
# REFERENCE POINT : ( 119.050  0.000 -3.872)
# BUOYANT CENTER  : ( 119.050  0.000 -3.872)
# HULL VOLUME     : 0.45262E+05 m*m*m
# HULL SURFACE    : 0.87333E+04 m*m

# WATERPLANE AREA : 0.60477E+04 m*m
# Ctre : ( 116.136  0.000)
# Ixx  : 0.47167E+06 BMxx 10.42095
# Ixy  : 0.00000E+00 BMxy 0.00000
# Iyy  : 0.18469E+08 BMyy 408.03865

```

HSrdf: radiation and diffraction computationsInput file for the HSrdf command *OTECF.rdf*

FILENAME ww1

FREQUENCES TYPE 2

WMIN 0.05

WMAX 1.80

WSTP 0.05

ENDFREQUENCES

HEADINGS TYPE 2

HMIN 0.0

HMAX 180.0

HSTP 15.0

ENDHEADINGS

SPEEDS TYPE 0

1 0.0

ENDSPEEDS

WATERDEPTH INF

INFREQ

ENDFILE

FIGURE E.5: HydroSTAR screenshot HSRdf command

```

=====***** HydroStar For Experts V7.3 *****=====
-----x64----(c)BV/DR 1991-2016

HSrdf - Radiation and diffraction computations.

***** 64-bit version *****

Project: BLUERISE OTEC FLOATER
User :
Nb of bodies to be analysed      1
Nb panels on hulls              1148
Nb geometric symmetry           1
Nb segments along waterlines    82
Nb panels over waterplanes      384
Nb panels over the free surface  0

Reference length                 1.000000
Gravity acceleration             9.810000
Reference point of incident wave ( 119.049630,  0.000000)

Body 1: reference point x= 119.049630 center of buoyancy x= 119.049630
          y=  0.000000          y=  0.000000
          z= -3.871866          z= -3.871866

Option - Elimination of irr. freq. : Yes
Name of output files :          otecf.ww1

Method = Sources
Linear system solved by LU decomposition
Calculation in open sea
          Water depth is infinity
36 frequencies from 0.050 to 1.800
13 headings from 0.000 to 180.000
1 speeds from 0.000 to 0.000
-----

```

HSmcn: motions computationInput file for the command HSmcn *OTECF.mcn*

```

FILENAME ww1

MASS_BODY 1 46393738.0777663

COGPOINT_BODY 1 119.049630 0 1.1

GYRADIUS_BODY 1 10.13729792 56.25 56.25 0 0 0

LINVISCOUSDAMPING 1 6

INFFREQ

ENDFILE

```

FIGURE E.6: HydroSTAR screenshot HSmcn command

```

=====***** HydroStar For Experts V7.3 *****=====
-----x64----(c)BV/DR 1991-2016

HSmcn - Mechanical computations.

Project: BLUERISE OTEC FLOATER
User :
Reference length                 1.000000
Gravity acceleration             9.810000
Water mass density               1025.000000

Ref. point of incident wave ( 119.049630,  0.000000)
Body 1: Reference point is ( 119.049630,  0.000000,  1.100000)
          Centre of gravity ( 119.049630,  0.000000,  1.100000)
          Centre of buoyancy ( 119.049630,  0.000000,  -3.871866)
          GMxx , GMyy ( 5.408141, 403.033324)

```

HSdft: second-order drift computation in uni-directional wavesInput file for the HSdft command *OTECECF.dft*

```

NFORMULE NO
FFORMULE YES
MFORMULE NO

ENDFILE

```

FIGURE E.7: HydroSTAR screenshot HSdft command

```

=====***** HydroStar For Experts V7.3 *****=====
-----x64----(c)BV/DR 1991-2016

HSdft - Second-order drift load computations.

Haskind function based on the source distribution is used.
Near-field formulation is NOT used.
Far-field formulation by Maruo-Newman (1960-1967) is used.
Middle-field formulation is NOT used.

```

HSrao: construction of the transfer functionsInput file for the HSrao command *OTECECF.rao*

```

# Motion at the center of gravity
GSURGE BODY 1 FILE Surge.rao
GSWAY BODY 1 FILE Sway.rao
GHEAVE BODY 1 FILE Heave.rao
GROLL BODY 1 FILE Roll.rao
GPITCH BODY 1 FILE Pitch.rao
GYAW BODY 1 FILE Yaw.rao

# drift loads
DRIFTFX FILE DriftFxFF.rao MOM
DRIFTFY FILE DriftFyFF.rao MOM
DRIFTMZ FILE DriftMzFF.rao MOM

# Added mass and damping
CM FILE AddedMass.dat TERM 11 22 33 44 55 66
CA FILE Damping.dat TERM 11 22 33 44 55 66

# Excitation loads
FXF1ST FILE fxf1st.rao
FYF1ST FILE fyf1st.rao
FZF1ST FILE fzf1st.rao
MXF1ST FILE mxf1st.rao
MYF1ST FILE myf1st.rao
MZF1ST FILE mzf1st.rao

ARIANE7N FILE _newman.dat

ENDFILE

```

FIGURE E.8: HydroSTAR screenshot HSrao command

```
=====***** HydroStar For Experts V7.3 *****=====
-----x64----(c)BV/DR 1991-2016

HSrao - RAOs constructions.

GSURGE FILE Surge.rao BODY 1 COORD 119.0496 0.0000 1.1000
GSWAY FILE Sway.rao BODY 1 COORD 119.0496 0.0000 1.1000
GHEAVE FILE Heave.rao BODY 1 COORD 119.0496 0.0000 1.1000
GROLL FILE Roll.rao BODY 1 COORD 119.0496 0.0000 1.1000
GPITCH FILE Pitch.rao BODY 1 COORD 119.0496 0.0000 1.1000
GYAW FILE Yaw.rao BODY 1 COORD 119.0496 0.0000 1.1000
DRIFTFX FILE DriftFxFF.rao BODY 1
DRIFTFY FILE DriftFyFF.rao BODY 1
DRIFTMZ FILE DriftMzFF.rao BODY 1
CM FILE AddedMass.dat BODY 1
CA FILE Damping.dat BODY 1
FXF1ST FILE fxf1st.rao BODY 1
FYF1ST FILE fyf1st.rao BODY 1
FZF1ST FILE fzf1st.rao BODY 1
MXF1ST FILE mxf1st.rao BODY 1
MYF1ST FILE myf1st.rao BODY 1
MZF1ST FILE mzf1st.rao BODY 1
ARIANE7N
```

E.2 Output

Response Amplitude Operators

FIGURE E.9: RAO - Surge

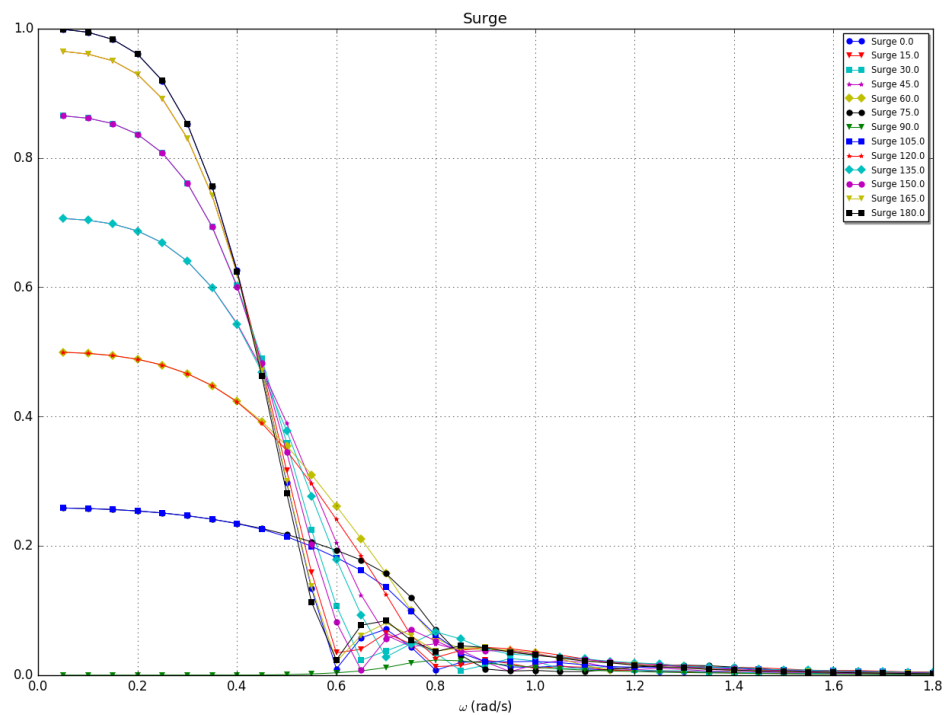


FIGURE E.10: RAO - Sway

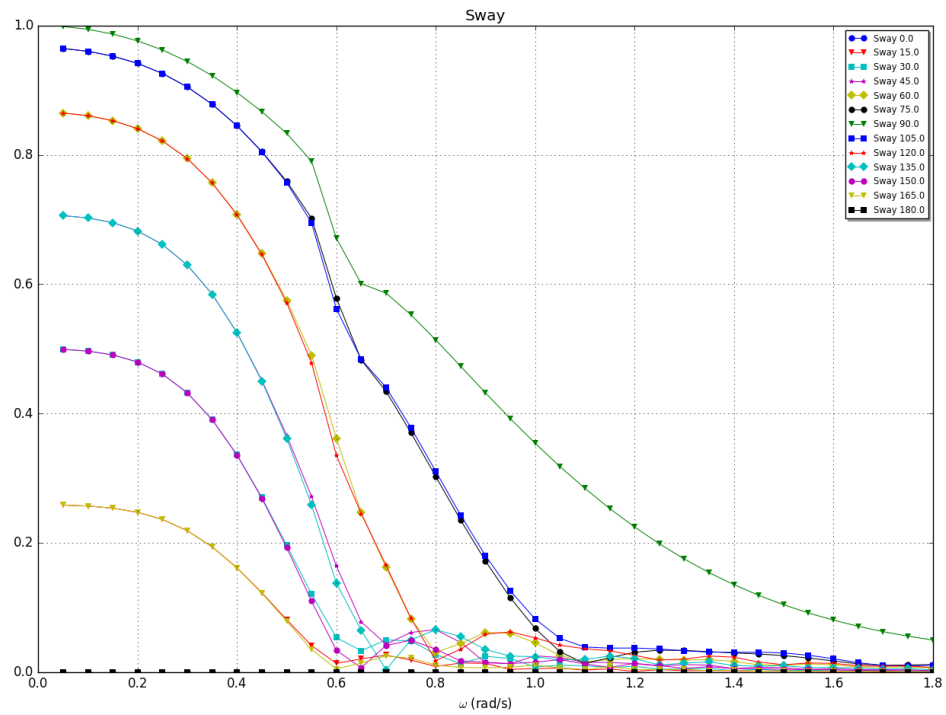


FIGURE E.11: RAO - Heave

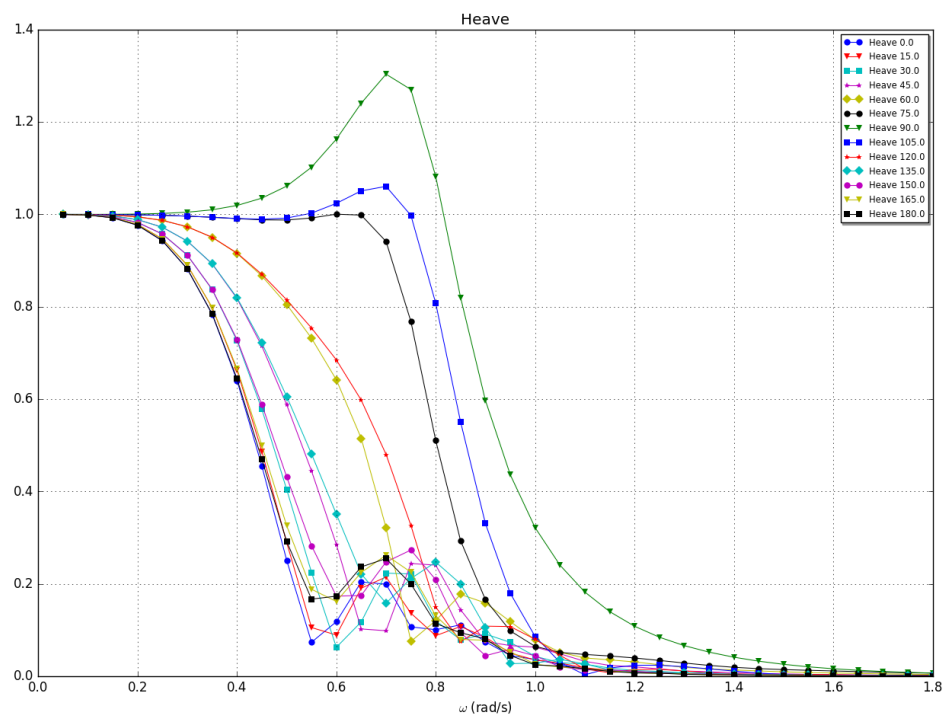


FIGURE E.12: RAO - Roll

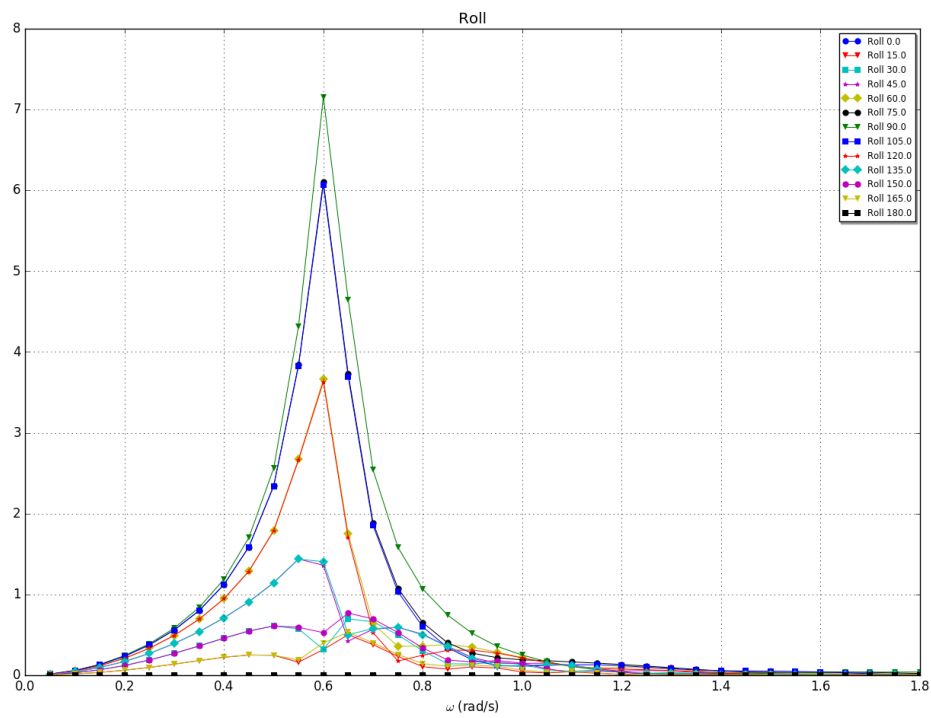


FIGURE E.13: RAO - Pitch

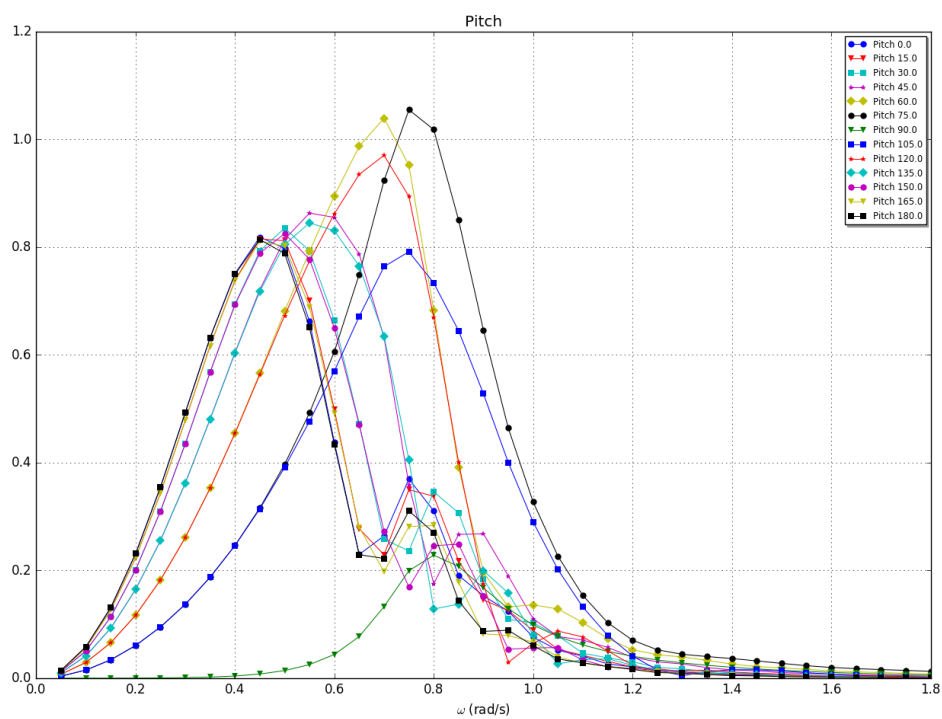
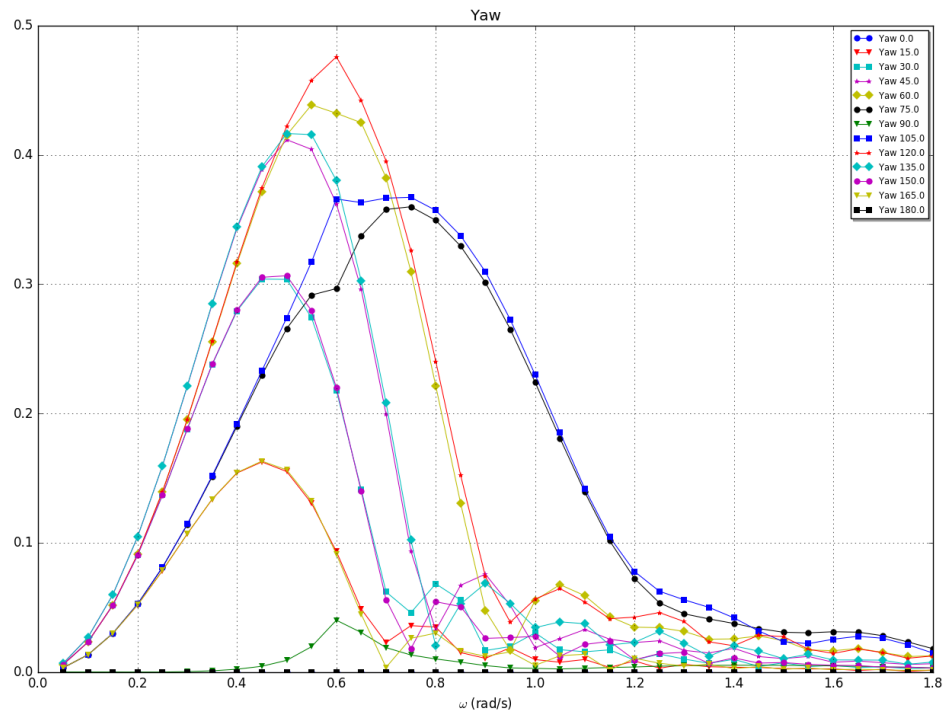


FIGURE E.14: RAO - yaw



Drift loads

FIGURE E.15: Drift load - Fx

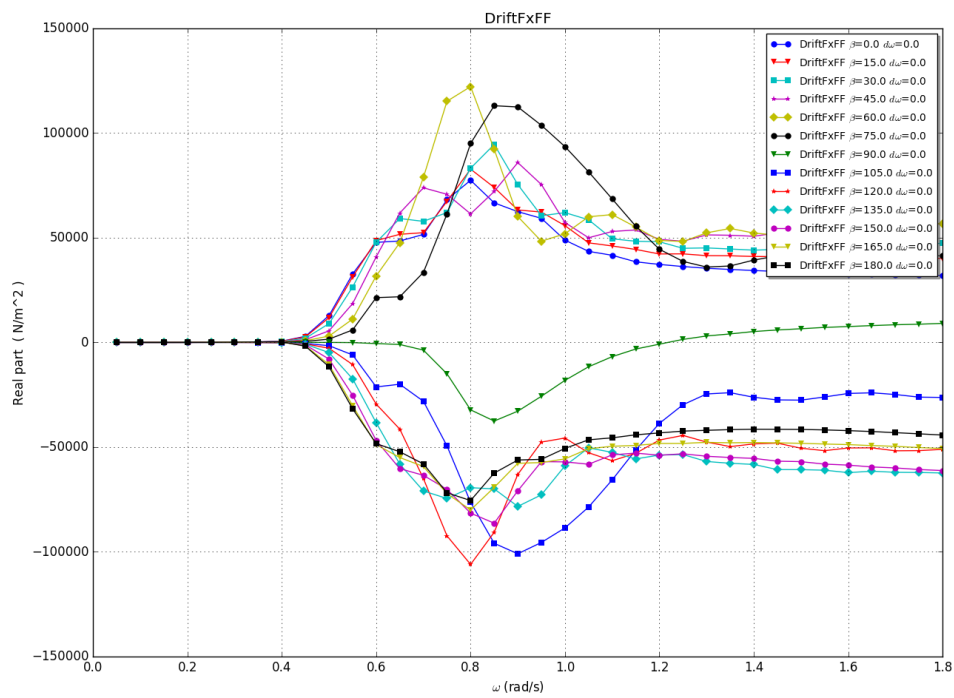


FIGURE E.16: Drift load - Fy

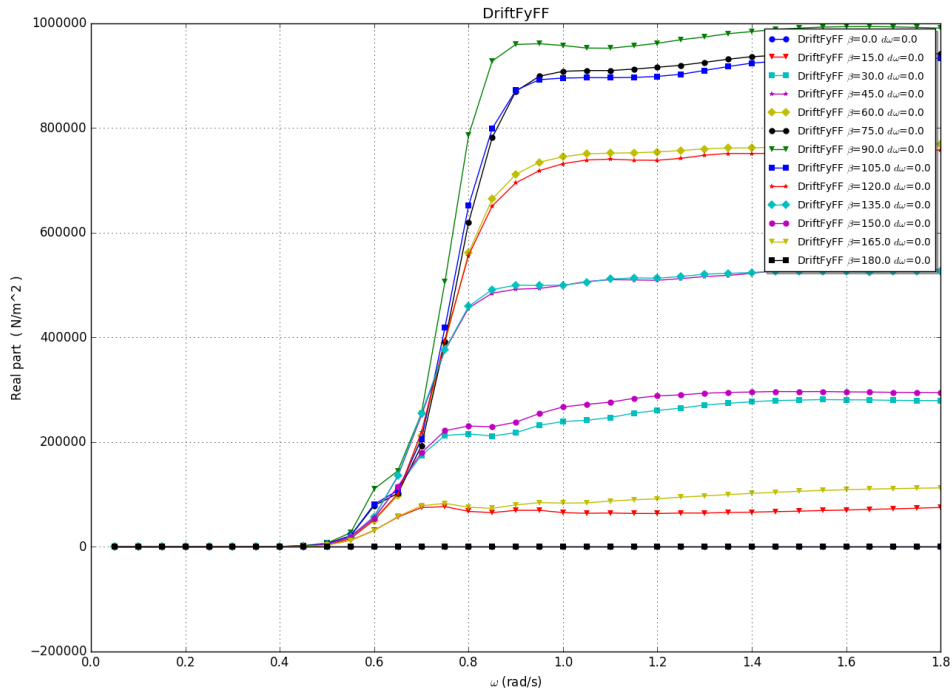
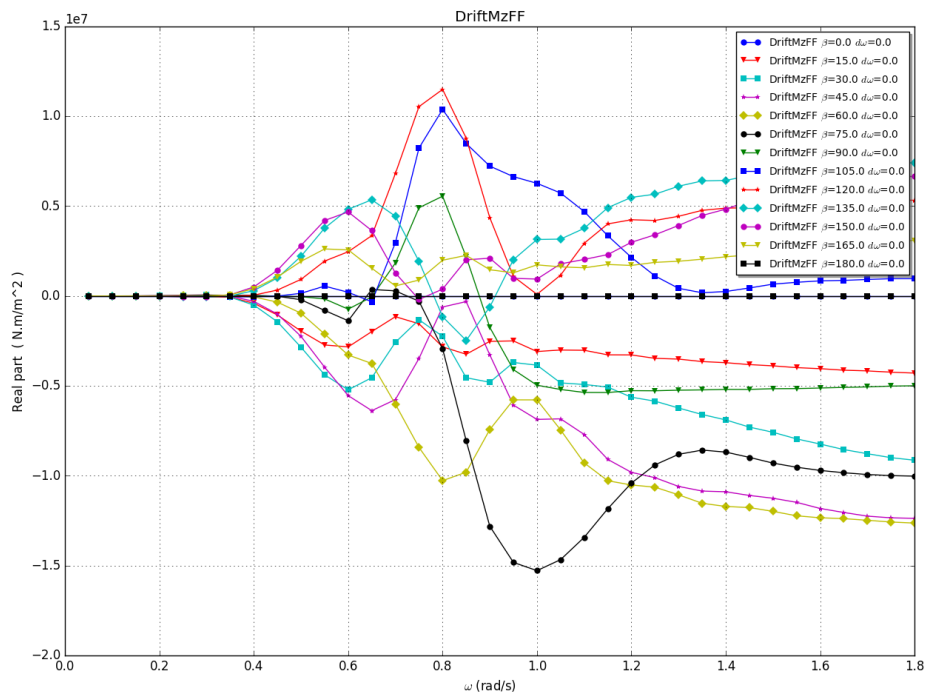


FIGURE E.17: Drift load - Mz



F: Input Ariane8

In this appendix, the input data for Ariane 8 is displayed expect of the hydrodynamic data that is described in appendix A.

TABLE F.1: Environment data

	Wave 0	Wave 1	Wave 2	Wave 3
Wave spectrum	Jonswap	Jonswap	Jonswap	Jonswap
Gamma	3,3	3,3	3,3	3,3
Sigma 1	0,07	0,07	0,07	0,07
Sigma 2	0,09	0,09	0,09	0,09
Significant wave height	8	8,1	8,7	8,6
Modal peak period	11,8	11,8	11,8	11,8
Min frequency	0,01	0,01	0,01	0,01
Max frequency	0,286	0,286	0,286	0,286
Heading	270	315	0	45
Wind spectrum	API	API	API	API
Factor fp/V1-hour	0,0025	0,0025	0,0025	0,0025
Mean Velocity (m/s)	29,1	29,1	29,1	29,1
Min Frequency	0,01	0,01	0,01	0,01
Max Frequency	0,3	0,3	0,3	0,3
Heading	270	270	270	270

TABLE F.2: Vessel coordinates

	East (m)	North (m)	Heading (Deg)
Vessel position	10,41	-20,4	58,05

TABLE F.3: Anchor coordinates

		East (m)	North (m)
Anchor global position	Anchor 1	1046,81	-186,85
	Anchor 2	1034,59	-237,76
	Anchor 3	1019,73	-287,96
	Anchor 4	361,59	1000
	Anchor 5	311,39	1014,87
	Anchor 6	260,48	1027,09
	Anchor 7	-260,48	-1027,09
	Anchor 8	-311,39	-1014,87
	Anchor 9	-361,59	-1000
	Anchor 10	-1019,73	287,96
	Anchor 11	-1034,6	237,76
	Anchor 12	-1046,82	186,86

G: Tensions and offset for extreme environmental conditions

In this appendix, the outcomes are given of the tensions and offset for the analysis under extreme environmental conditions. The resulting tension in every line and the offset in east, north and Z direction are displayed.

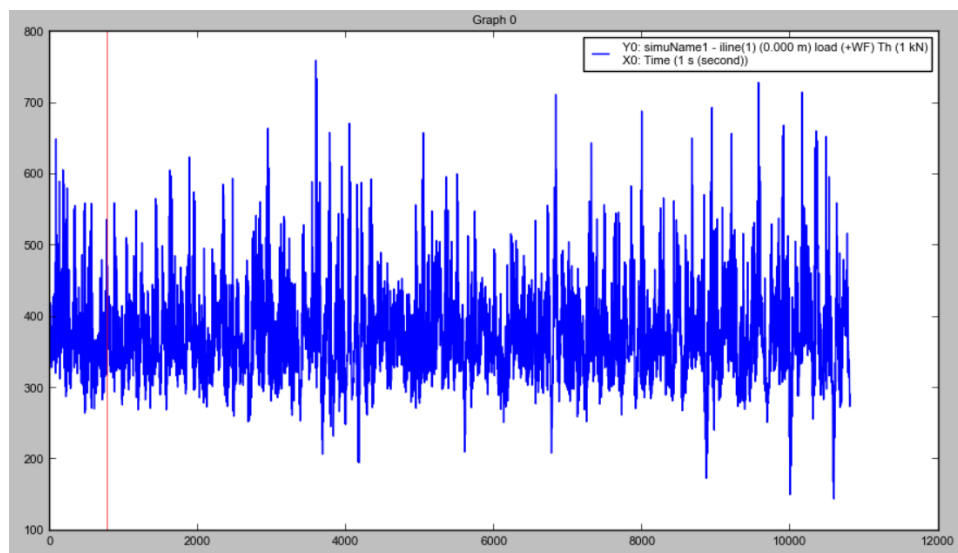


FIGURE G.1: Tension over time: line 1

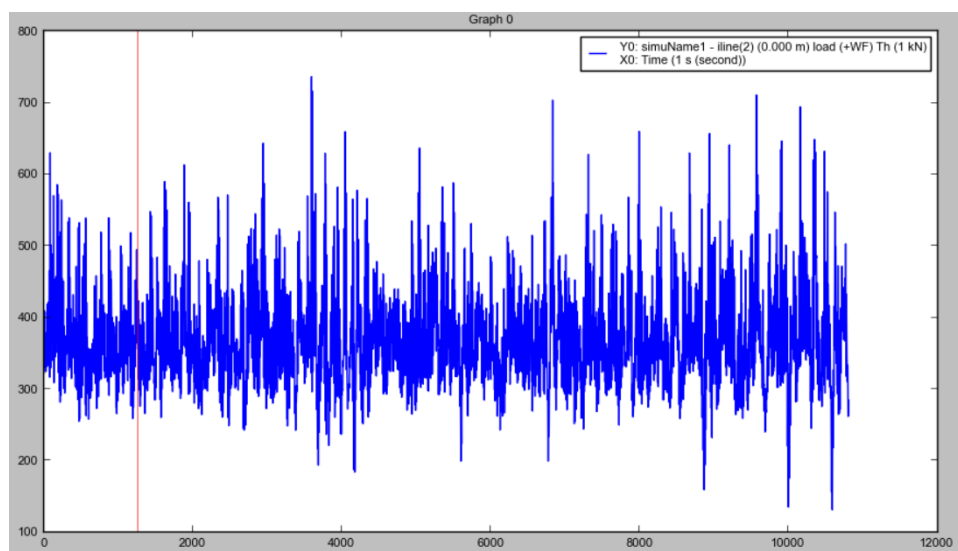


FIGURE G.2: Tension over time: line 2

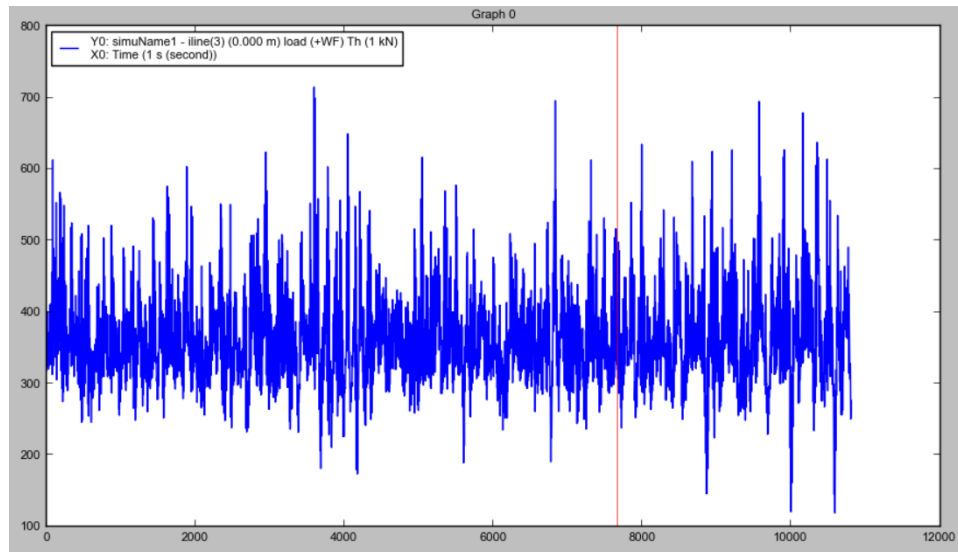


FIGURE G.3: Tension over time: line 3

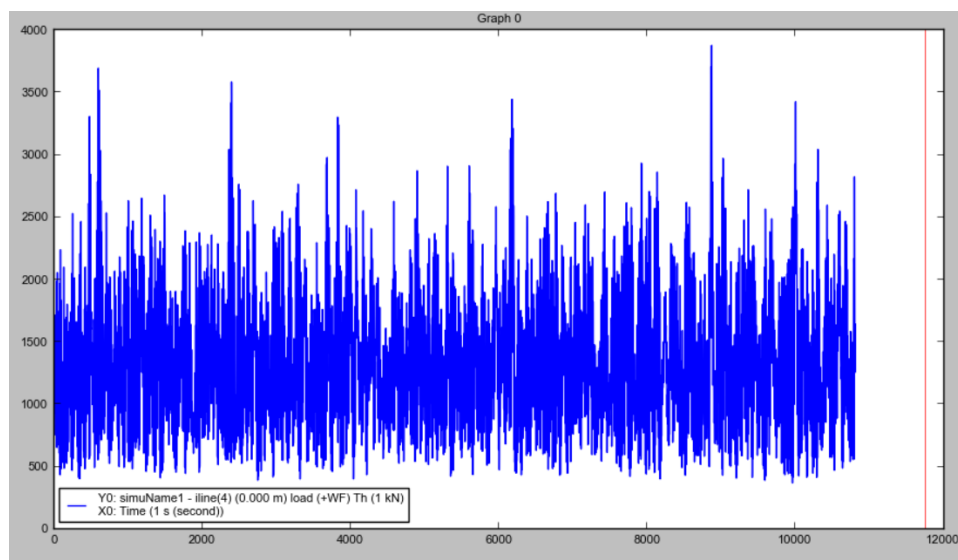


FIGURE G.4: Tension over time: line 4

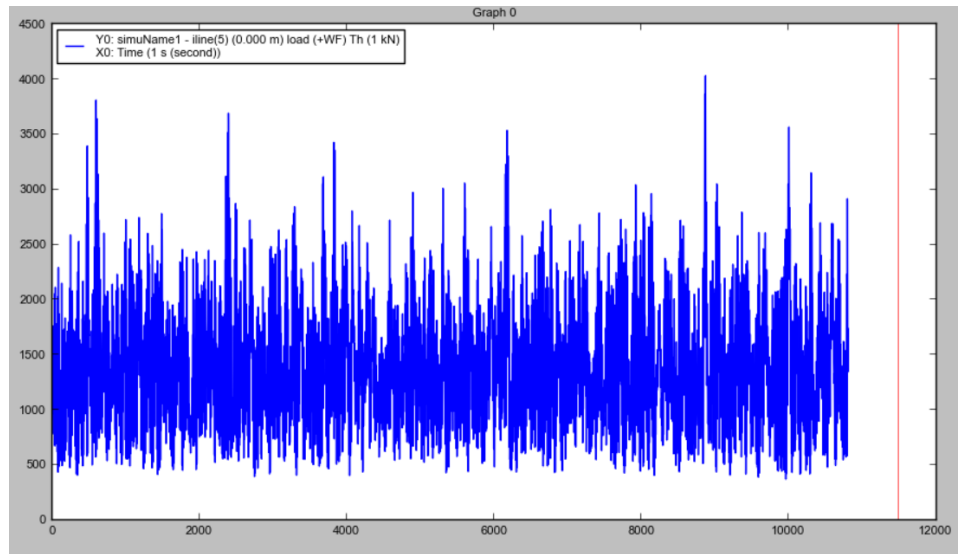


FIGURE G.5: Tension over time: line 5

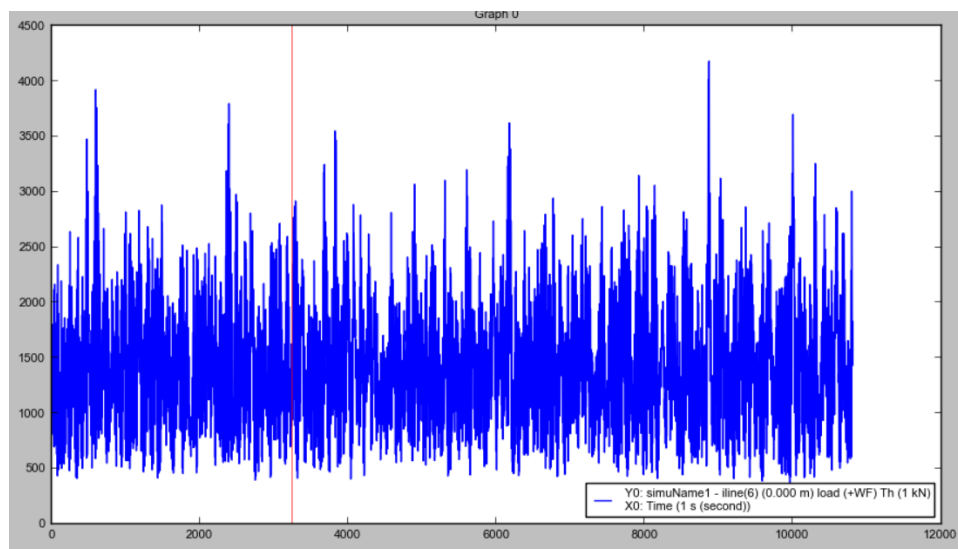


FIGURE G.6: Tension over time: line 6

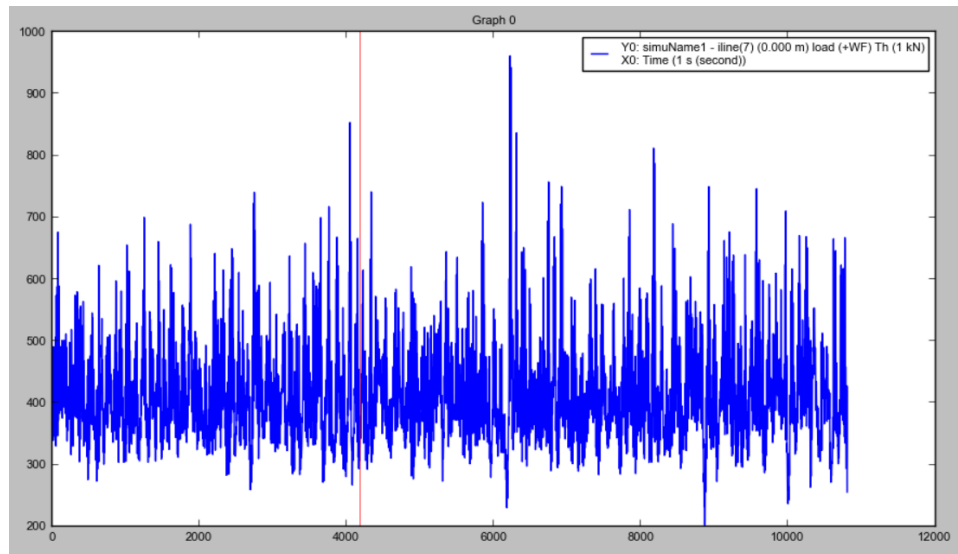


FIGURE G.7: Tension over time: line 7

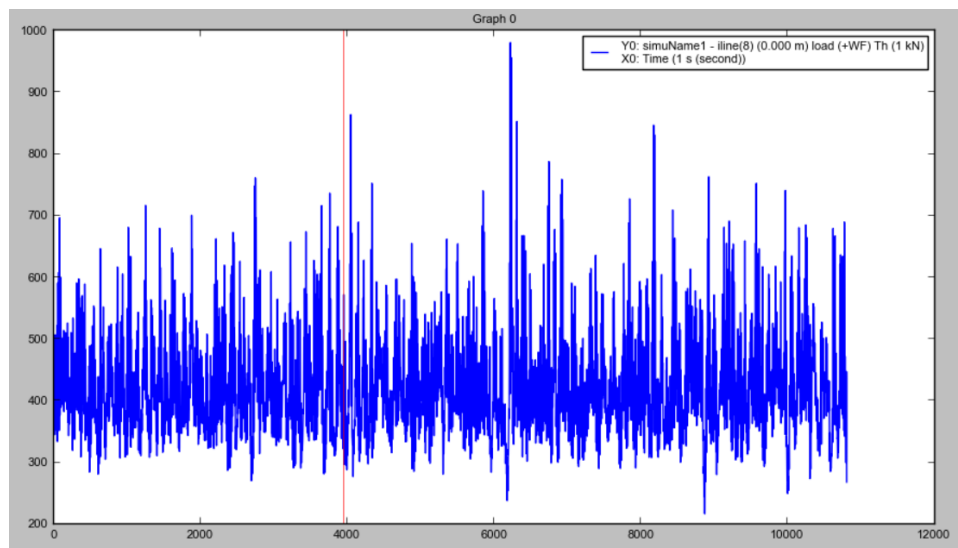


FIGURE G.8: Tension over time: line 8

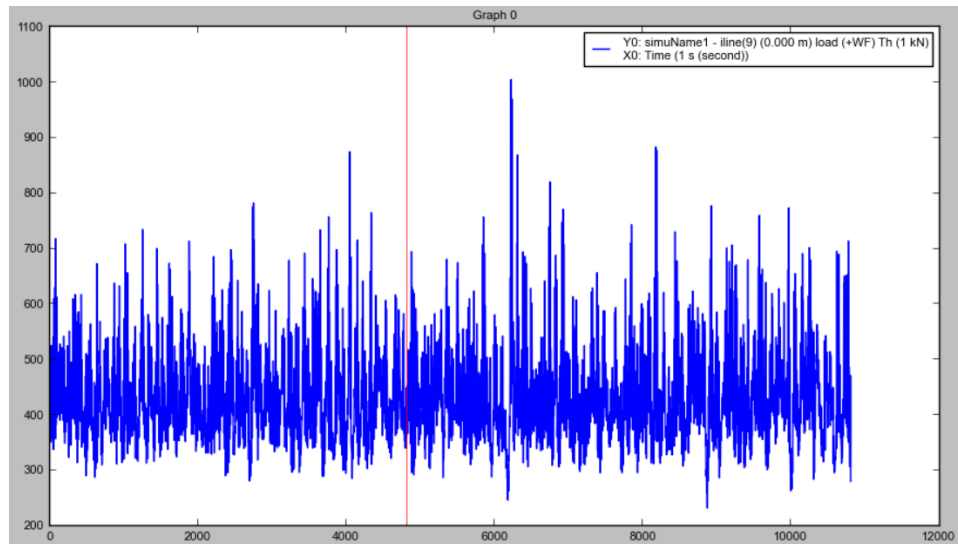


FIGURE G.9: Tension over time: line 9

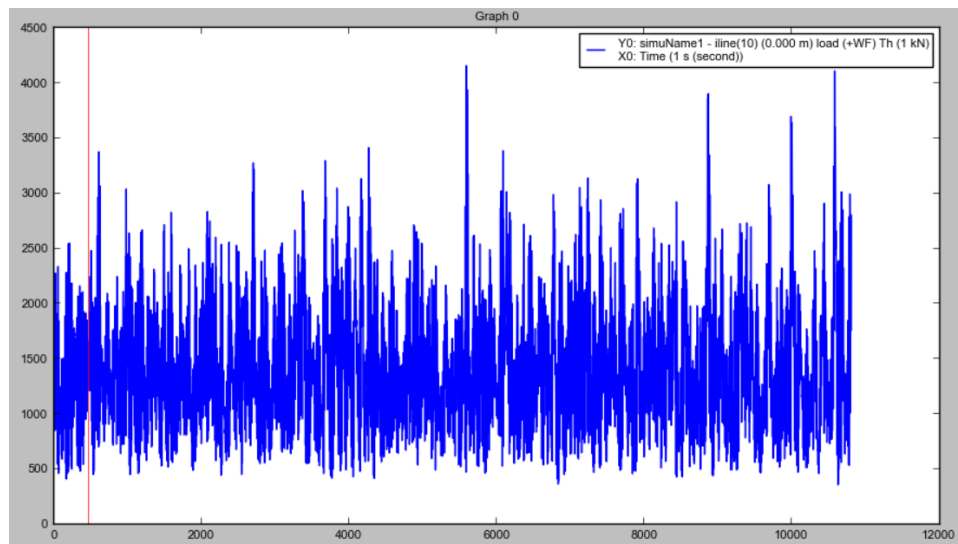


FIGURE G.10: Tension over time: line 10

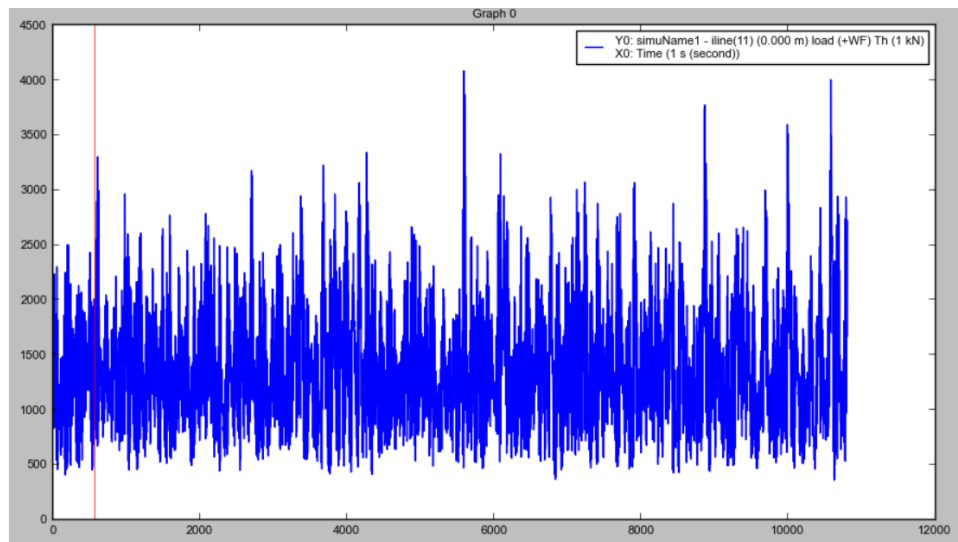


FIGURE G.11: Tension over time: line 11

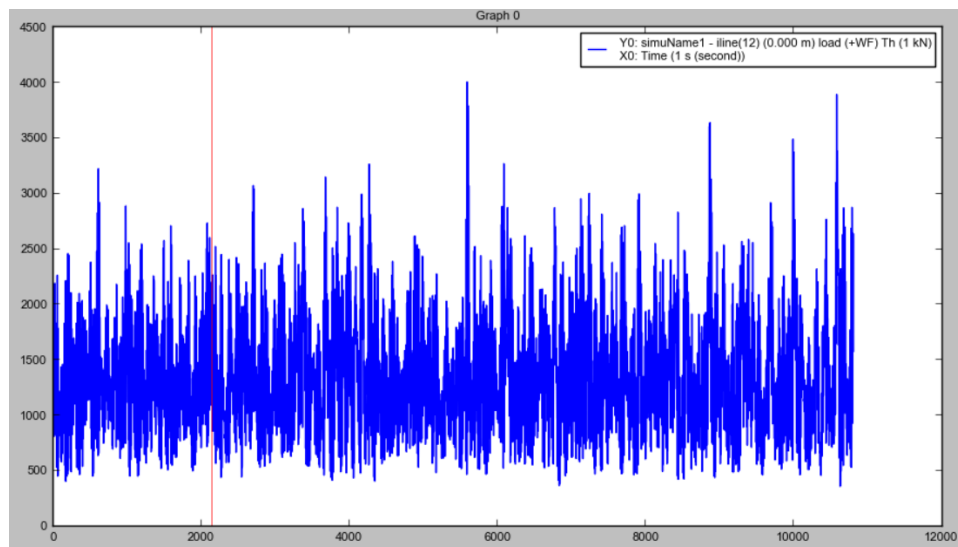


FIGURE G.12: Tension over time: line 12

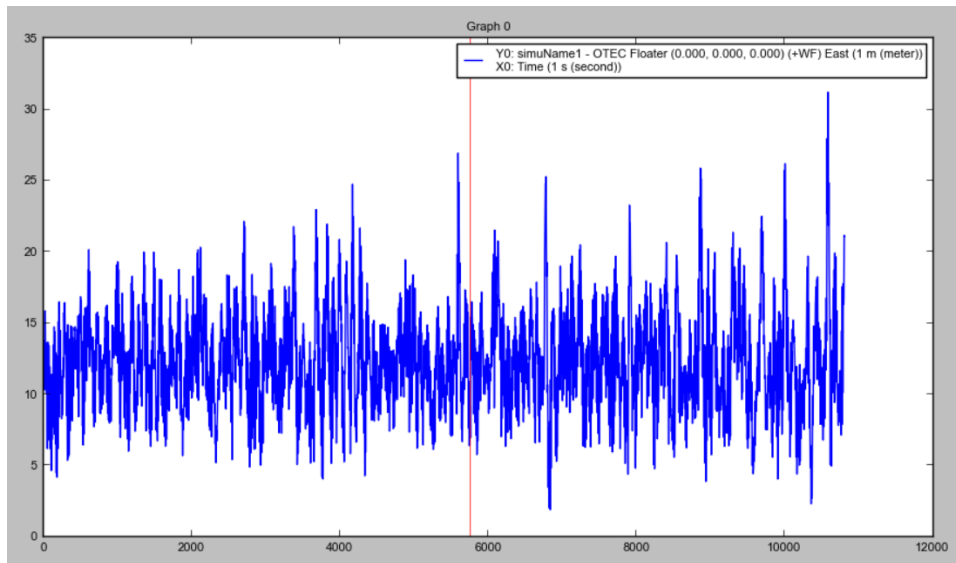


FIGURE G.13: Maximum horizontal offset in east direction

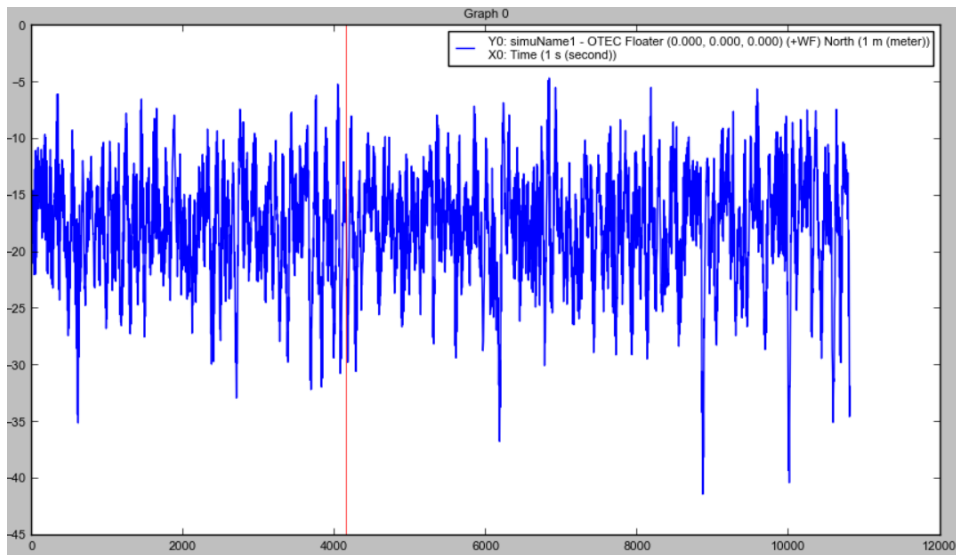


FIGURE G.14: Maximum horizontal offset in north direction

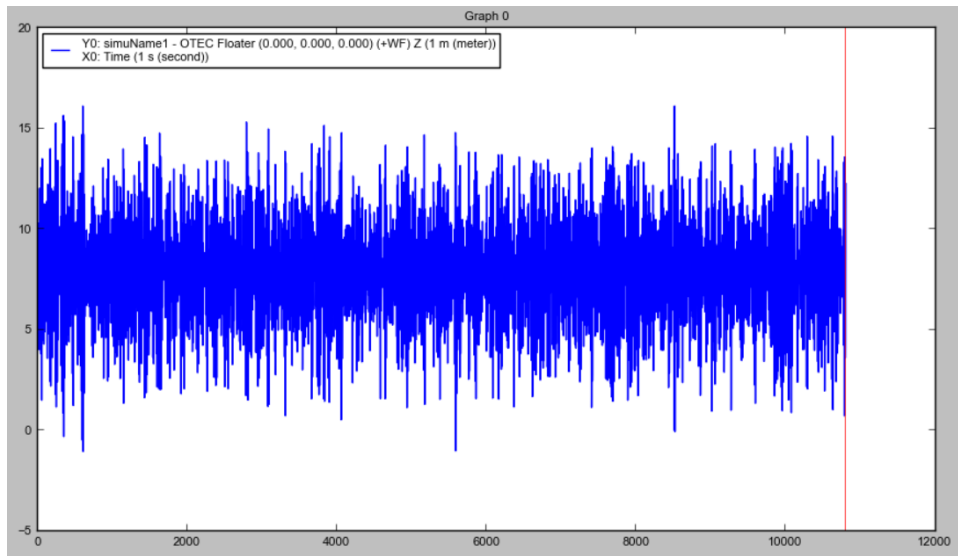


FIGURE G.15: Maximum horizontal offset in Z-direction

H: Calibration

In this appendix, the results of the calibration of the system are given. The line tensions are given for two different situations. The displacements for these two situations are displayed in table H.1.

TABLE H.1: Displacements

	Situation 1	Situation 2
East	100 m	-50 m
North	50 m	-50 m
heading	60 deg	60 deg

Results of situation 1

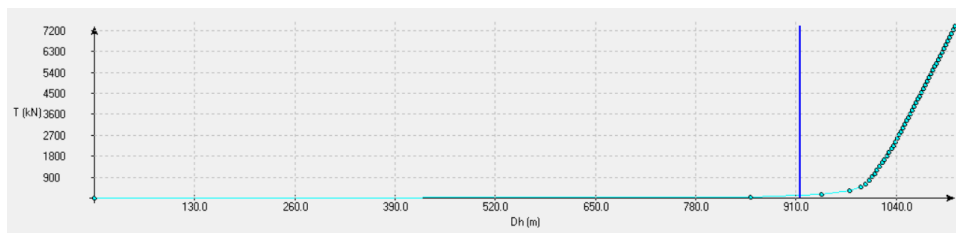


FIGURE H.1: Situation 1: tension in line 1

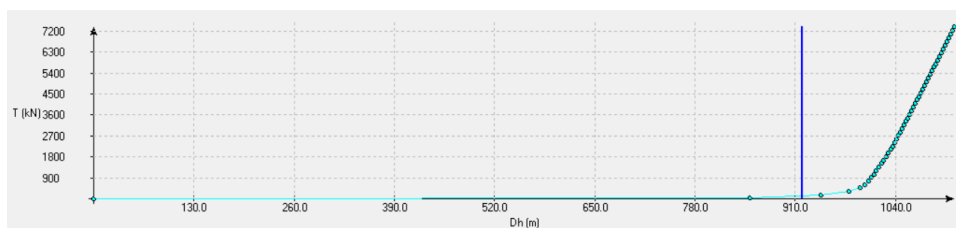


FIGURE H.2: Situation 1: tension in line 2

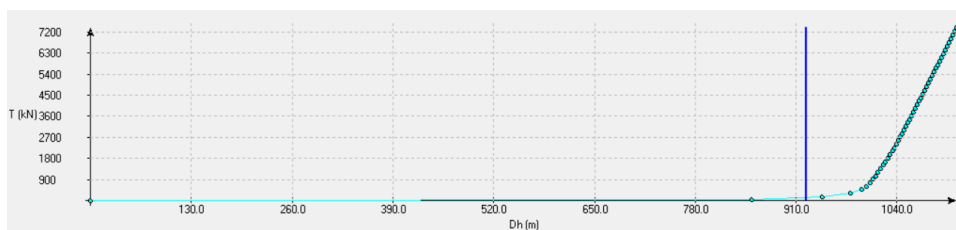


FIGURE H.3: Situation 1: tension in line 3

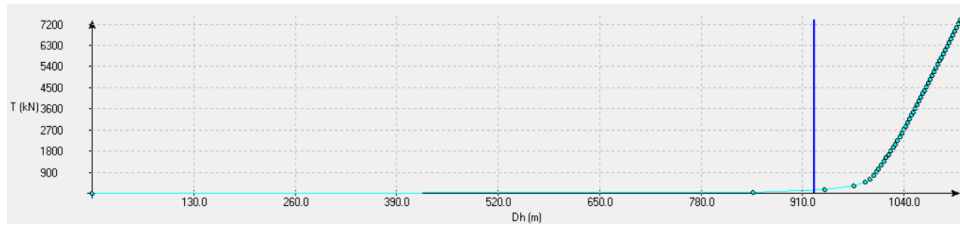


FIGURE H.4: Situation 1: tension in line 4

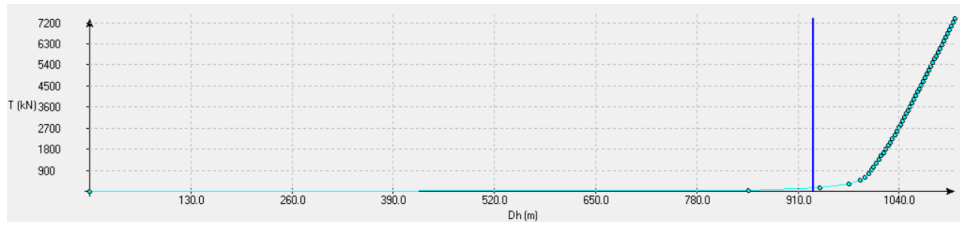


FIGURE H.5: Situation 1: tension in line 5

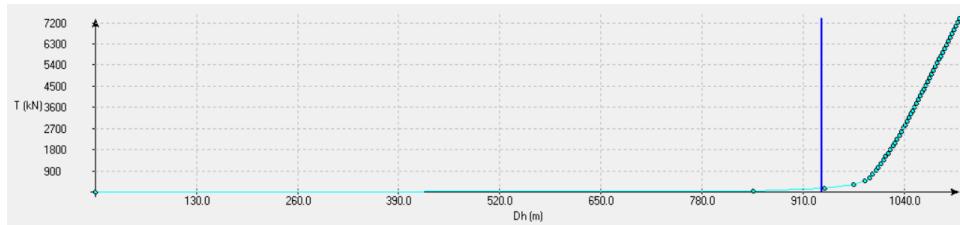


FIGURE H.6: Situation 1: tension in line 6

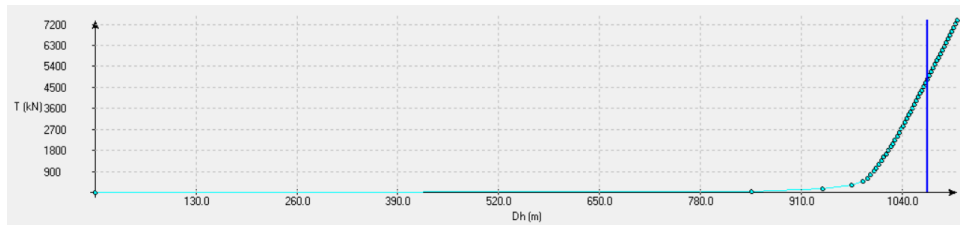


FIGURE H.7: Situation 1: tension in line 7

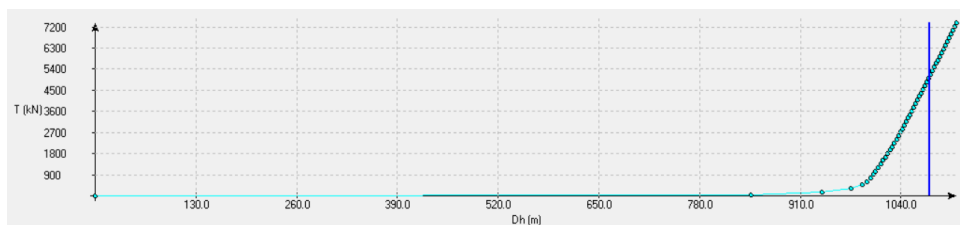


FIGURE H.8: Situation 1: tension in line 8

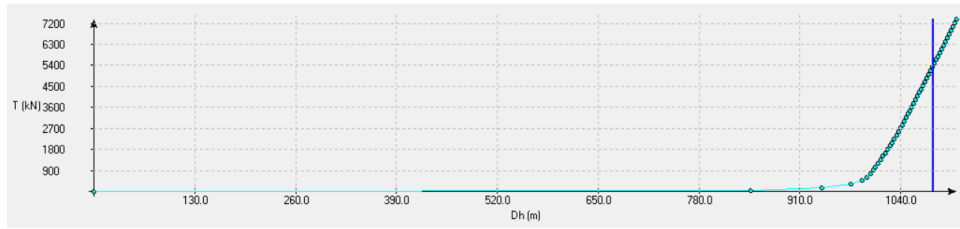


FIGURE H.9: Situation 1: tension in line 9

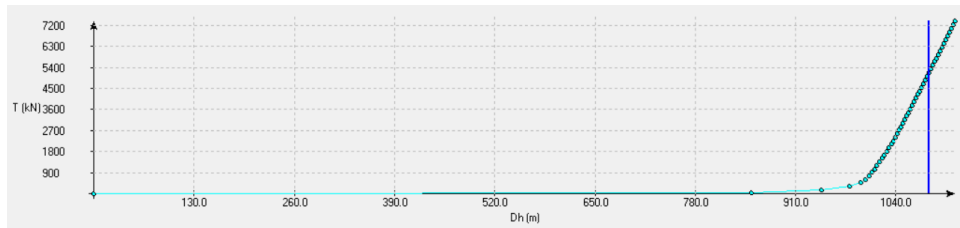


FIGURE H.10: Situation 1: tension in line 10

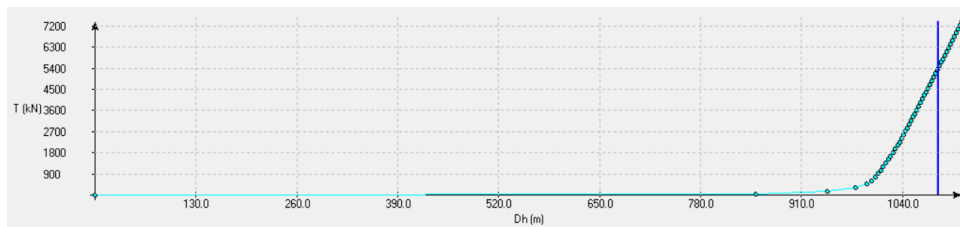


FIGURE H.11: Situation 1: tension in line 11

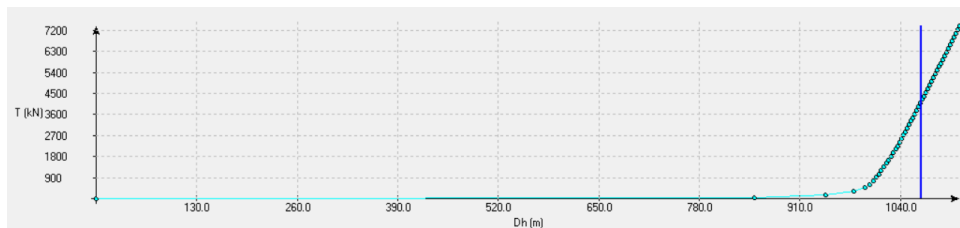


FIGURE H.12: Situation 1: tension in line 12

Results of situation 2

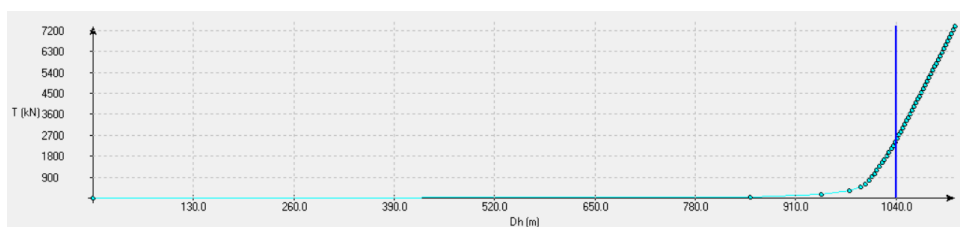


FIGURE H.13: Situation 2: tension in line 1

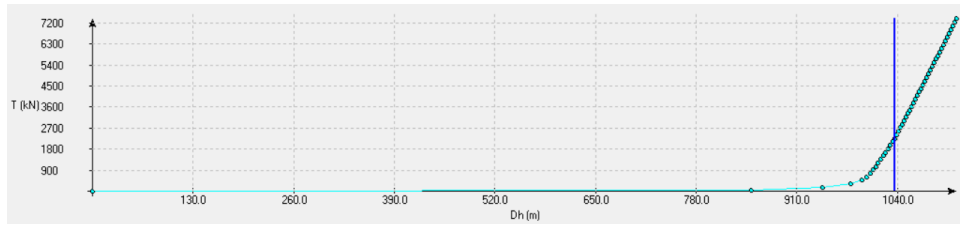


FIGURE H.14: Situation 2: tension in line 2

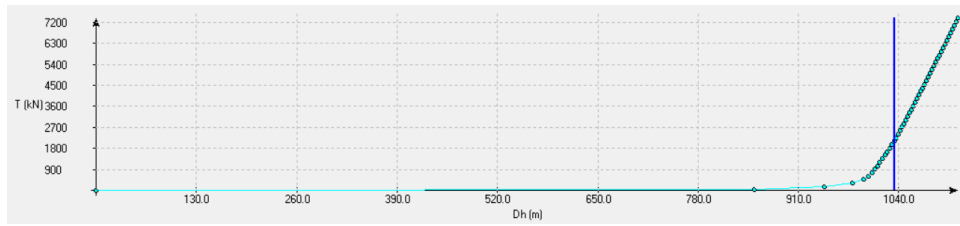


FIGURE H.15: Situation 2: tension in line 3

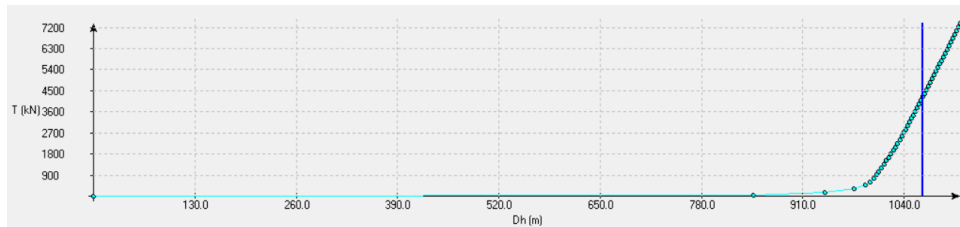


FIGURE H.16: Situation 2: tension in line 4

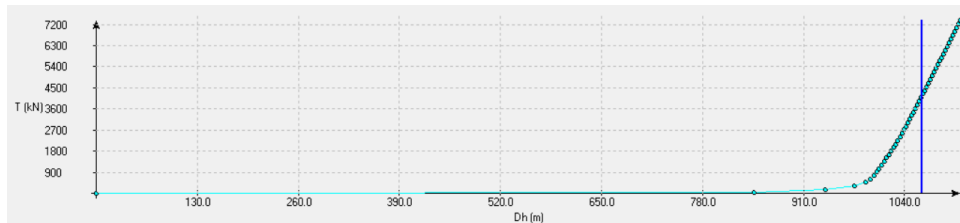


FIGURE H.17: Situation 2: tension in line 5

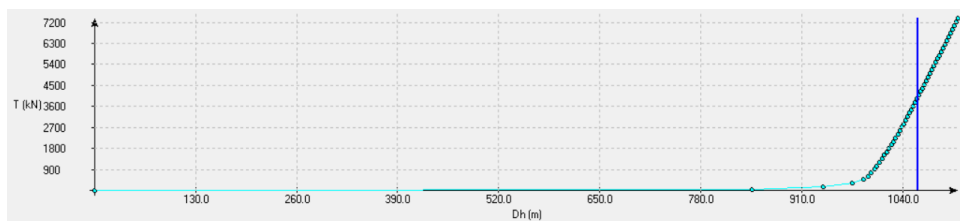


FIGURE H.18: Situation 2: tension in line 6

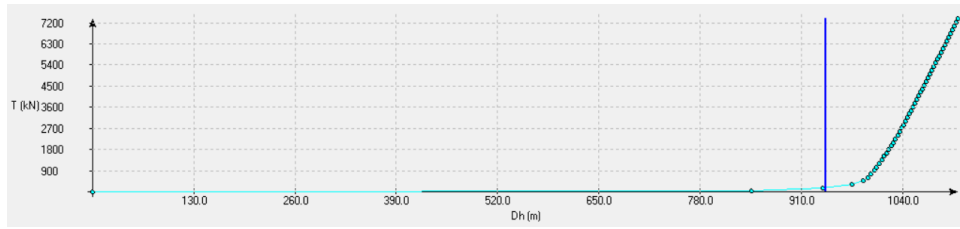


FIGURE H.19: Situation 2: tension in line 7

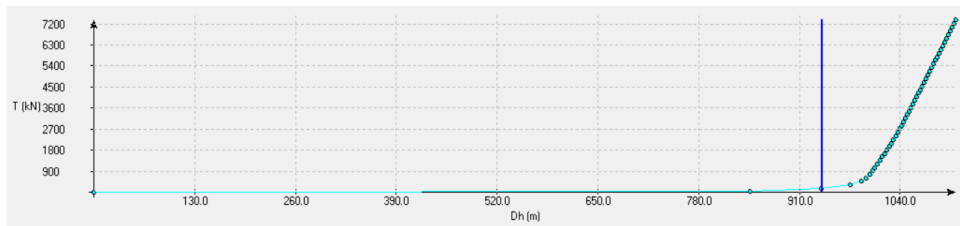


FIGURE H.20: Situation 2: tension in line 8

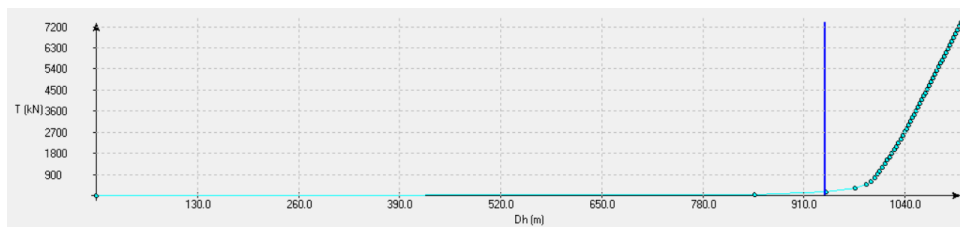


FIGURE H.21: Situation 2: tension in line 9

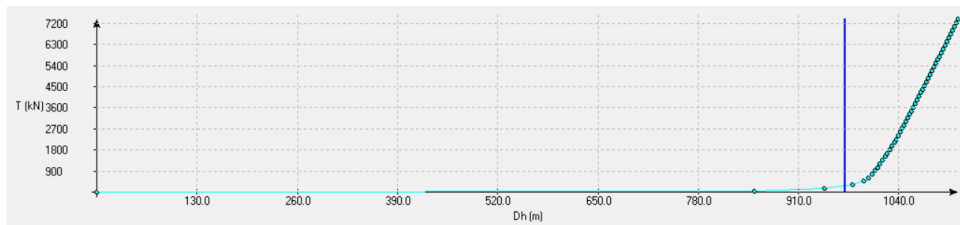


FIGURE H.22: Situation 2: tension in line 10

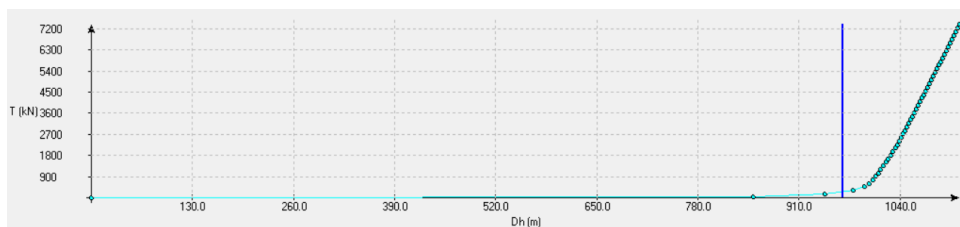


FIGURE H.23: Situation 2: tension in line 11

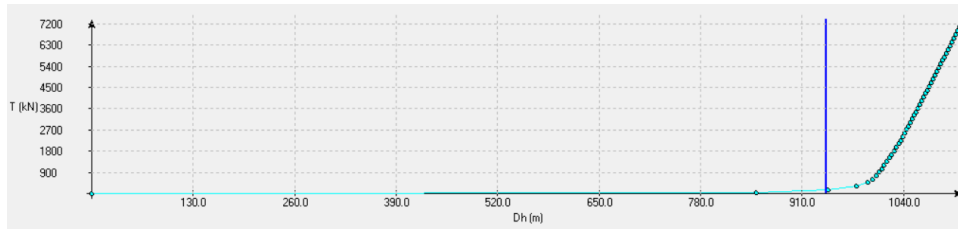


FIGURE H.24: Situation 2: tension in line 12

I: Maximum Offset Analysis

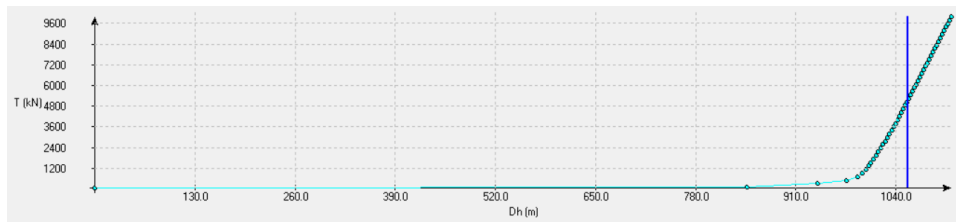


FIGURE I.1: Maximum offset analysis: line 4

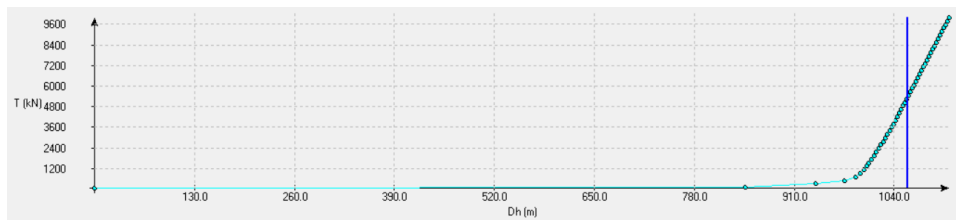


FIGURE I.2: Maximum offset analysis: line 5

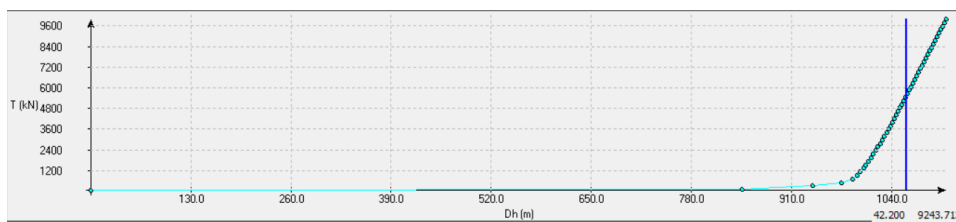


FIGURE I.3: Maximum offset analysis: line 6

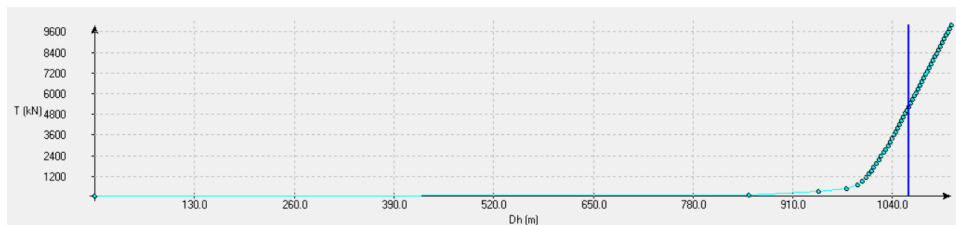


FIGURE I.4: Maximum offset analysis: line 10

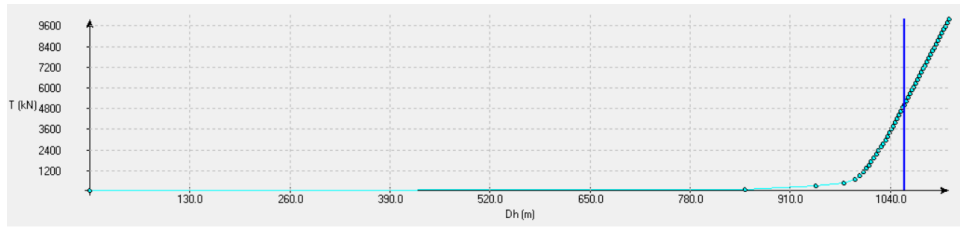


FIGURE I.5: Maximum offset analysis: line 11

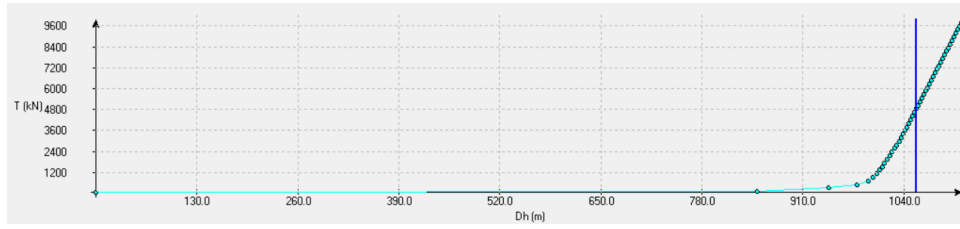


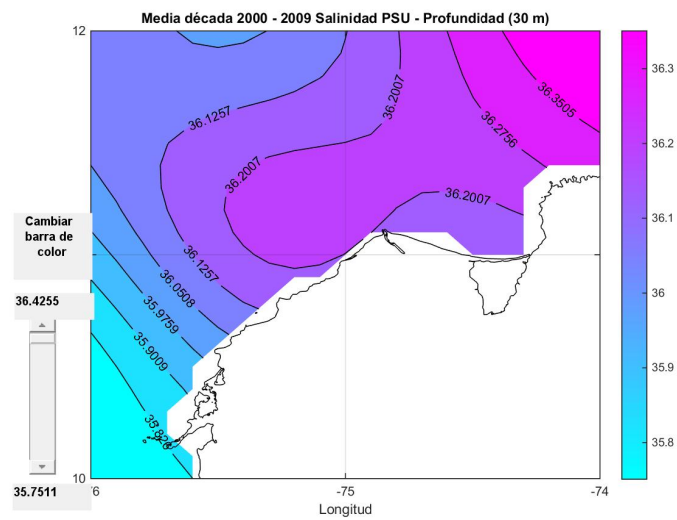
FIGURE I.6: Maximum offset analysis: line 12

J: Intake- and return pipes

In this section, the data obtained from Centro de Investigaciones Oceanográficas e Hidrográficas (CIOH) is shown. This includes depth based salinity and depth based density.

FIGURE J.1: Average salinity in PSU at different depths (2000-2009)

(A) 30 meters



(B) 1000 meters

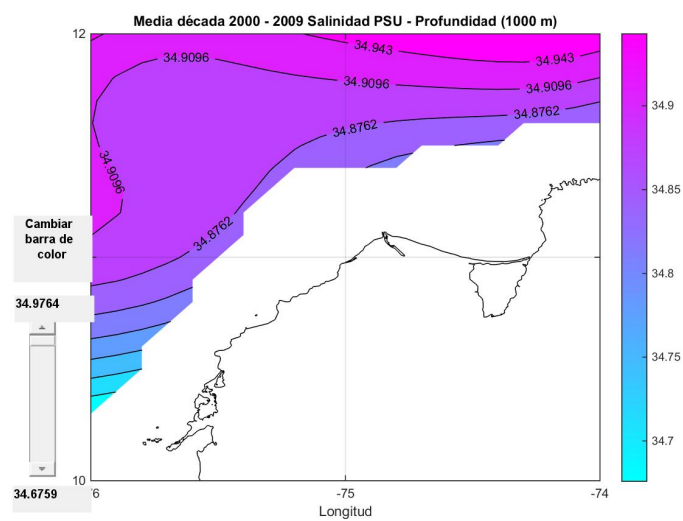
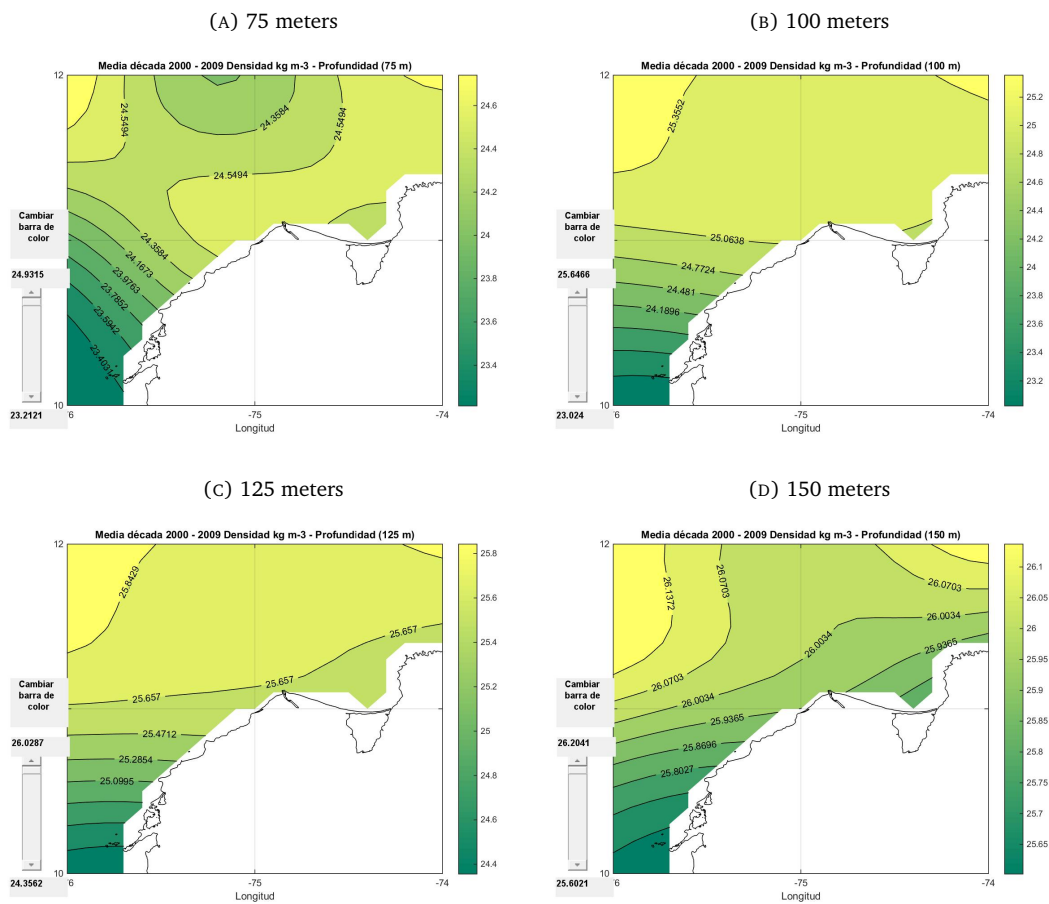


FIGURE J.2: Average density in $kg/m^3 - 1000$ at different depths (2000-2009)

The MatLab file that was used for the calculation of the equation of state was obtained from the Scripps Institute of Oceanography. It is based on the paper 'UNESCO technical papers in marine science: Algorithms for computation of fundamental properties of seawater' (Fofonoff and Millard Jr, 1983). A short description of the MatLab code is given in figure J.3 and is available ¹.

¹<http://mooring.ucsd.edu/software/matlab/doc/ocean/index.html>

FIGURE J.3: Short MatLab code description

```
SIGMA Density of Seawater
SIG = SIGMA( P , T , S , [Pref] )

computation of density of seawater
referenced to arbitrary pressures
based on 'alpha.m'

input :   P           : pressure [dbar]
         T           : in situ temperature [degC] IPTS-68
         S           : salinity [psu] IPSS-78
         Pref [p]    : optional reference pressure
                        use: SIGMA(Pref,THETA(P,T,S,Pref),S)

output :   SIG           : density of seawater at pressure P (adiabatic)
                        [kg/m^3]

check values :   sigma(0,40,40) = 21.6788 kg/m^3
                 sigma(0, 0,35) = 28.106331 kg/m^3

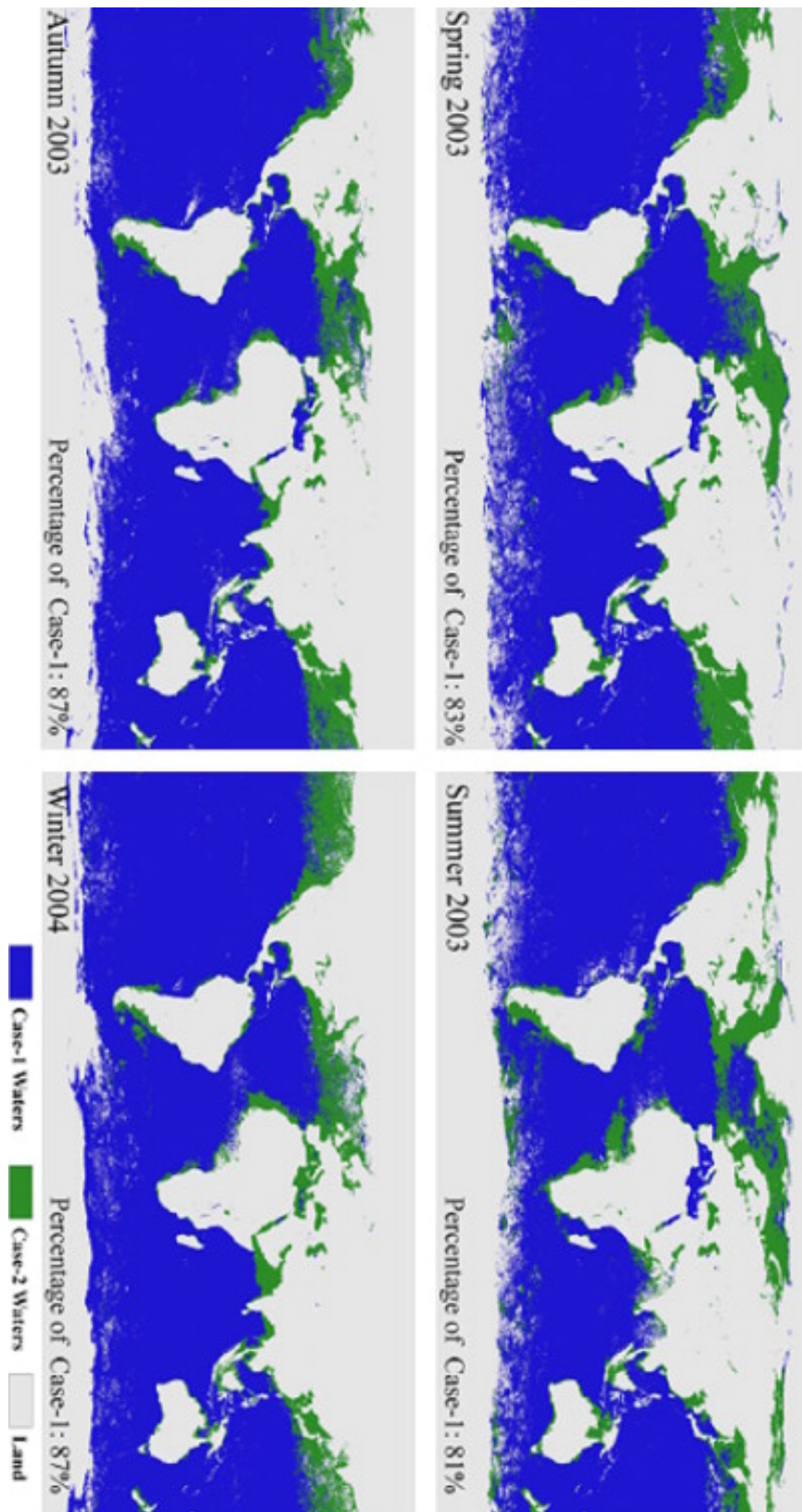
        P could be a [ M by 1 ] Vector if T,S 2-dimensional,
        or a [ 1 x 1 x N ] Vector if T,S 3-dimensional,
        (the last Matlab 5.# only)

NOTE: The Conversion from IPTS-68 to ITS90 is:
      T90 = 0.99976 * T68
      T68 = 1.00024 * T90

see also: ALPHA, THETA

version 1.1.0      last change 01.09.1995
```

FIGURE J.4: Global seasonal distribution of Case-1 and Case-2 waters in 2003 (Matsushita et al., 2012)



Bibliography

- ABCMoorings (2014). “MooringSystems”. In: *ABCMoorings*. URL: <https://www.abc-moorings.weebly.com/>.
- Acevado, D. et al. (2017). “Barranquilla Feasibility Study”. In: p. 83.
- Andrade Amaya, Carlos Alberto, Óscar Eduardo Rangel Parra, and Émerson Herrera Vásquez (2015). “Atlas de los Datos Oceanográficos de Colombia 1922-2013. Temperatura, Salinidad, Densidad, Velocidad Geostroica”. In: ISSN: 9585897806.
- API, American Petroleum Institute (2005). *Design and Analysis of Stationkeeping Systems for Floating Structures*. Tech. rep.
- BMT Argoss (2017). “Wave Climate”. In: ed. by BMT Argoss. Amersfoort, The Netherlands.
- Bosboom, J and M Stive (2013). *Coastal Dynamics 1: Delft*. Delft Academic Press, v. 0.4.
- DNV, Det Norske Veritas (2017). *DNV-OS-E301 Position Mooring*. Tech. rep.
- Fenton, John D and WD McKee (1990). “On calculating the lengths of water waves”. In: *Coastal Engineering* 14.6, pp. 499–513. ISSN: 0378-3839.
- Fofonoff, Nicholas Paul and RC Millard Jr (1983). “Algorithms for the computation of fundamental properties of seawater”. In:
- Groenewoud, Peter (2017). *Tropical Storm Analysis for an Area off Columbia*. Report A870.
- Guerrero Galán, T (2017). “Concept Design of a 10 MW Ship-Shaped OTEC Plant”. In:
- IMO (1975). “Recommendation on dissemination of information, charting and manning of drilling rigs; production platforms and other similar structures”. In: *IMO resolutions*.
- (2014). *Implications of the united nations convention on the law of the sea for the international maritime organisation*. Report. International Maritime Organisation.
- IMO, International Maritime Organization (2009). *Code on Intact Stability*. Tech. rep.
- J.M.J. Journée, W.W. Massie (2001). “Offshore Hydromechanics”. In:
- Joanna Gyory Arthur J. Mariano, Edward H. Ryan (2013). *The Caribbean Current*. Report. URL: <http://oceancurrents.rsmas.miami.edu/caribbean/caribbean.html>.
- Kirkenier, J. A. (2014). “Techno-economic optimization of Organic Rankine Cycles using working fluid mixtures for 10 to 25 MW OTEC power plants.” In: URL: www.bluerise.nl.
- Kjerfve, Björn (1981). “Tides of the Caribbean sea”. In: *Journal of Geophysical Research: Oceans* 86.C5, pp. 4243–4247. ISSN: 2156-2202.
- Lee, ZhongPing and Chuanmin Hu (2006). “Global distribution of Case-1 waters: An analysis from SeaWiFS measurements”. In: *Remote Sensing of Environment* 101.2, pp. 270–276. ISSN: 0034-4257.
- Lee, ZhongPing et al. (2007). “Euphotic zone depth: Its derivation and implication to ocean-color remote sensing”. In: *Journal of Geophysical Research: Oceans* 112.C3. ISSN: 2156-2202.
- M. Bozorgmehrian M. Terwad, V. Aparna Peri (2013). “Mooring systems for offshore installations, trends and technology”. In: *Offshore Magazine*.
- MarineTraffic (2017). “Marine Traffic Density Map”. In: *MarineTraffic*. URL: <https://www.marinetraffic.com/>.
- Matsushita, Bunkei et al. (2012). “A simple method for distinguishing global Case-1 and Case-2 waters using SeaWiFS measurements”. In: *ISPRS journal of photogrammetry and remote sensing* 69, pp. 74–87. ISSN: 0924-2716.
- Phillystran. *Phillystran® Large Diameter Offshore Ropes - Spectra® / Dyneema® (High Modulus Polyethylene) Rope*. Tech. rep.
- *Product Catalog Phillystran® Large Diameter Offshore Ropes - Polyester*. Tech. rep.

- Preisendorfer, Rudolph W (1976). *Hydrologic Optics. Volume 5. Properties*. Report. Honolulu: US Dept. of Commerce, National Oceanic and Atmospheric Administration, Environmental Research Laboratories, Pacific Marine Environmental Laboratory.
- Rotterdam Maritime Group (2012). *Plan Maestro Puerto de Barranquilla*. Report. Rotterdam Maritime Group.
- Scripps Institution of Oceanography (2017). “Scripps Institution of Oceanography matlab toolbox”. In: *Scripps Institution of Oceanography*. URL: http://mooring.ucsd.edu/index.html?/software/matlab/matlab_ocean.html.
- Vega, Luis A (2013). “Ocean Thermal Energy Conversion”. In: *Renewable Energy Systems*. Springer, pp. 1273–1305.
- Vicinay. *The Future of Mooring*. Tech. rep.